

Covariant density functional theory: applications in exotic nuclei

Madrid, 18./19.12. 2007

Peter Ring

Technical University Munich
Universidad Autónoma de Madrid

Content

- **The Nuclear Density Functional**
- Nuclear Response Theory
- Exotic rotational excitations
- Methods beyond mean field
- Outlook

Density functional theory in nuclei

D.Brink
D.Vauterin

Skyrme

$$E[\hat{\rho}] = \langle \Psi | H | \Psi \rangle \approx \langle \Phi | H_{eff}(\rho) | \Phi \rangle$$

$|\Phi\rangle$ Slater determinant $\Leftrightarrow \hat{\rho}$ density matrix

$$|\Phi\rangle = \mathbf{A}(\varphi_1(\mathbf{r}_1) \cdots \varphi_A(\mathbf{r}_A)) \quad \hat{\rho}(\mathbf{r}, \mathbf{r}') = \sum_{i=1}^A |\varphi_i(\mathbf{r})\rangle \langle \varphi_i(\mathbf{r}')|$$

Mean field:

$$\hat{h} = \frac{\delta E}{\delta \hat{\rho}}$$

Eigenfunctions:

$$\hat{h}|\varphi_i\rangle = \varepsilon_i|\varphi_i\rangle$$

Interaction:

$$\hat{V} = \frac{\delta^2 E}{\delta \hat{\rho} \delta \hat{\rho}}$$

Extensions: Pairing correlations, Covariance
Relativistic Hartree Bogoliubov (RHB)

Hohenberg-Kohn theorem

Many-body system with Hamiltonian $\hat{H} = \hat{T} + \hat{V}$

We consider a realistic manybody system with the kinetic energy \hat{T} and two-body interaction $\hat{V}(\mathbf{r}_i, \mathbf{r}_k)$ in an external field $\hat{U}(\mathbf{r})$.
In this case the expectation value of the exact energy

$$E_{HK}[\rho(\mathbf{r})] = \langle \hat{T} + \hat{V} \rangle$$

is given by a **universal functional** $E[\rho(\mathbf{r})]$, which depends only on the **local density** $\rho(\mathbf{r})$, and not on the external potential $U(\mathbf{r})$.

The ground state is determined by minimizing $E[\rho]$ with respect to ρ

P. Hohenberg, W. Kohn, Phys.Rev. 136B (1964) 864

Some basic thermodynamics:

$T=1/\beta$: We consider a many-body system in a finite Volume V

Hamiltonian:

$$\hat{H} = H_0 + W$$

partition function:

$$Z(T, V) = \text{Tr}(e^{-\beta\hat{H}})$$

free energy:

$$F(T, V) = -T \ln Z$$

expectation values:

$$S = -\frac{\partial F}{\partial T}, \quad P = -\frac{\partial F}{\partial V},$$

differential form:

$$dF = -SdT - PdV$$

Legendre Transformation: (P↔V)

P is a monotonic function of V:

$$P = P(V) = -\frac{\partial F}{\partial V}$$

it can be inverted:

$$V = V(P)$$

Gibbs potential:

$$G = F + PV$$

$$G(T, P) = F(T, V(T, P)) + PV(T, P)$$

$$dG = -SdT + VdP$$

derivative:

$$V = \frac{\partial G}{\partial P}$$

Now we replace the volume V by an external potential
and the pressure P by the density

$$\begin{array}{l} V \rightarrow -U(\mathbf{r}) \\ P \rightarrow \rho(\mathbf{r}) \end{array}$$

Many-body system in an external field $U(\mathbf{r})$

We consider now a realistic manybody system in an external field $U(\mathbf{r})$ and a two-body interaction $V(r_i, r_k)$. The free energy depends now on $U(\mathbf{r})$ instead of the volume V , i.e. the energy is a **functional** of $U(\mathbf{r})$:

$$Z[T, U(\mathbf{r})] = \text{Tr} \left[e^{-\beta(\hat{T} + \hat{V} + \int \hat{\rho}(\mathbf{r}) U(\mathbf{r}) d^3r} \right]$$

Considering that

$$F[T, U(\mathbf{r})] = -T \ln Z[T, U(\mathbf{r})]$$

the functional derivative of F with respect to $U(\mathbf{r})$ is the density:

$$\rho(\mathbf{r}) = \frac{\delta F[T, U]}{\delta U(\mathbf{r})} \quad \Longrightarrow \quad U = U[\rho(\mathbf{r})]$$

Inverting this relation we can introduce a **Legendre transformation** replacing the independent function $U(\mathbf{r})$ by the density $\rho(\mathbf{r})$

Hohenberg-Kohn theorem

We find the potential $G(T, U[\rho(r)])$ (neglecting for simplicity T)

$$G[\rho] = F[U[\rho]] - \int \rho U[\rho] d^3 r$$

where the independent variable is $\rho(r)$. The potential G , which we call in the following E_{HK} , equation does not depend on $U(r)$.

It is a **universal functional** of $\rho(r)$ alone:

$$\begin{aligned} E_{HK}[\rho(r)] &= F[\rho(r)] - \int \rho(r) U(r) d^3 r \\ &= \langle \hat{T} + \hat{V} + \hat{U} \rangle - \langle \hat{U} \rangle = \langle \hat{T} + \hat{V} \rangle \end{aligned}$$

This is the **Hohenberg-Kohn theorem.**

The derivative of G with respect to $\rho(r)$ is $U(r)$:

$$U(\mathbf{r}) = - \frac{\delta E_{HK}}{\delta \rho(\mathbf{r})}$$

Decomposition of KH-functional

In practical applications the functional $E_{HK}[\rho(\mathbf{r})]$ is decomposed into three parts:

$$E_{HK}[\rho] = E_{ni}[\rho] + E_H[\rho] + E_{xc}[\rho]$$

The Hartree E_H is simple:
$$E_H[\rho] = \frac{1}{2} \int \rho(\mathbf{r}) V(\mathbf{r}, \mathbf{r}') \rho(\mathbf{r}') d^3 r d^3 r'$$

The non interacting part:
$$E_{ni}[\rho] = E_{HK}[\rho] \Big|_{V=0}$$

The exchange-correlation part is the rest:
$$E_{xc}[\rho] = E_{HK}[\rho] - E_{ni}[\rho] - E_H[\rho]$$

E_{xc} is less important and often approximated, but for modern calculations it plays an essential role.

Thomas Fermi approximation:

Thomas and Fermi used the **local density approximation (LDA)** in order to get an analytical expression for the non-interacting term. They calculated the kinetic energy density of a homogeneous system with constant density ρ

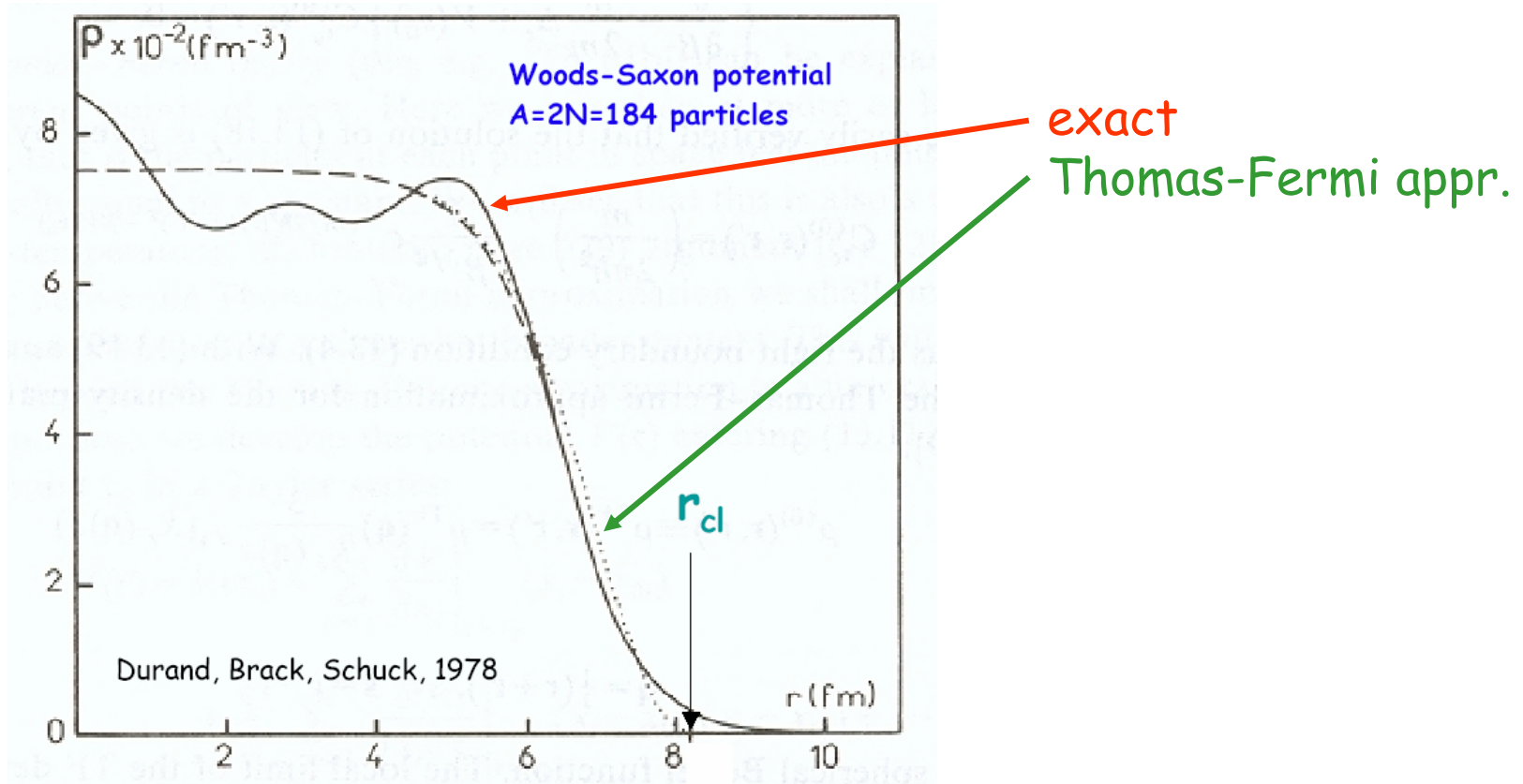
$$\frac{E}{V} = \gamma \int_{k < k_F} \frac{d^3 k}{(2\pi)^3} \frac{(\hbar k)^2}{2m} = \frac{\hbar^2}{2m} \frac{3}{5} \left(\frac{6\pi^2}{\gamma} \right)^{\frac{2}{3}} \rho^{\frac{5}{3}}$$

where γ is the spin/isospin degeneracy. Using this expression at the local density they find:

$$E_{TF} = \frac{\hbar^2}{2m} \frac{3}{5} \left(\frac{6\pi^2}{\gamma} \right)^{\frac{2}{3}} \int \rho^{\frac{5}{3}}(\mathbf{r}) d^3 r$$

This is not very good (molecules are never bound) and therefore one added later on gradient terms containing $\nabla\rho$ and $\Delta\rho$. This method is called **Extended Thomas Fermi (ETF)** theory. However, these are all asymptotic expansions and one always ends up with semi-classical approximations. **Shell effects** are never included.

Example for Thomas-Fermi approximation:



Kohn-Sham theory:

In order to reproduce shell structure Kohn and Sham introduced a single particle potential $V_{eff}(\mathbf{r})$, which is defined by the condition, that after the solution of the single particle eigenvalue problem

$$\left\{ -\frac{\hbar^2}{2m} \Delta + V_{eff}(\mathbf{r}) \right\} \varphi_k(\mathbf{r}) = \varepsilon_k \varphi_k(\mathbf{r})$$

the density obtained as $\rho(\mathbf{r}) = \sum_{i=1}^A |\varphi_i(\mathbf{r})|^2$ is the exact density

Obviously to each density $\rho(\mathbf{r})$ there exist such a potential $V_{eff}(\mathbf{r})$.

The non interacting part of the energy functional is given by:

$$E_{ni}[\rho] = \int \frac{\hbar^2}{2m} \tau(\mathbf{r}) d^3r = \int \frac{\hbar^2}{2m} \sum_{i=1}^A |\nabla \varphi_i(\mathbf{r})|^2 d^3r = \sum_{i=1}^A \varepsilon_i - \int \rho(\mathbf{r}) V_{eff}(\mathbf{r}) d^3r$$

and obviously we have:

$$V_{eff}(\mathbf{r}) = -\frac{\delta}{\delta \rho} E_{ni}[\rho] = -\frac{\delta}{\delta \rho} (E_{HK} - E_H - E_{xc})$$

Determination of V_{eff} :

In principle we can find $V_{\text{eff}}(\mathbf{r})$ by calculating the functional derivative of

$$V_{\text{eff}}(\mathbf{r}) = -\frac{\delta}{\delta\rho} E_{HK}[\rho] + \frac{\delta}{\delta\rho} E_H[\rho] + \frac{\delta}{\delta\rho} E_{xc}[\rho]$$

$$V_{\text{eff}}(\mathbf{r}) = U(\mathbf{r}) + V_H(\mathbf{r}) + V_{xc}(\mathbf{r})$$

with the Hartree potential

$$V_H(\mathbf{r}) = \int V(\mathbf{r}, \mathbf{r}') \rho(\mathbf{r}') d^3 r'$$

and the exchange-correlation potential

$$V_{xc}(\mathbf{r}) := \frac{\delta}{\delta\rho(\mathbf{r})} E_{xc}[\rho]$$

of course it all depends on the knowledge or on the approximation of the functional for the **exchange-correlation energy**

Kohn-Sham functional:

$$E_{KS}[\rho, \tau] = \int \frac{\hbar^2}{2m} \tau(\mathbf{r}) d^3 r + E_H[\rho] + E_{xc}[\rho]$$

Practical Applications:

Summarizing the Kohn-Sham scheme has the following steps

- a) determine a good approximation for the functional $E_{xc}[\rho]$
- b) start with some initial guess for ρ_0
- c) calculate from this ρ_0 the potentials $V_H(r)$ and $V_{xc}(r)$ and $V_{eff}(r)$
- d) solve the single particle Schrödinger equation for $V_{eff}(r)$ and obtain the wave functions $\varphi_i(r)$
- e) use these single particle wave functions to calculate the density $\rho_1(r)$ in the next step of the iteration
- f) repeat this circle until convergence is achieved.

Remarks to Kohn-Sham method:

We have the following remarks to the Kohn-Sham method

- 1) The method is exact under the condition that $V_{xc}[\rho]$ is known.
- 2) The single particle wave functions $\varphi_i(\mathbf{r})$ and the single particle energies ε_i are only auxiliary quantities. They have nothing to do with experiment. We only obtain the exact total energy and for the density, i.e. quantities accessible by the density $\rho(\mathbf{r})$.
- 3) The method works rather well even for shell structures

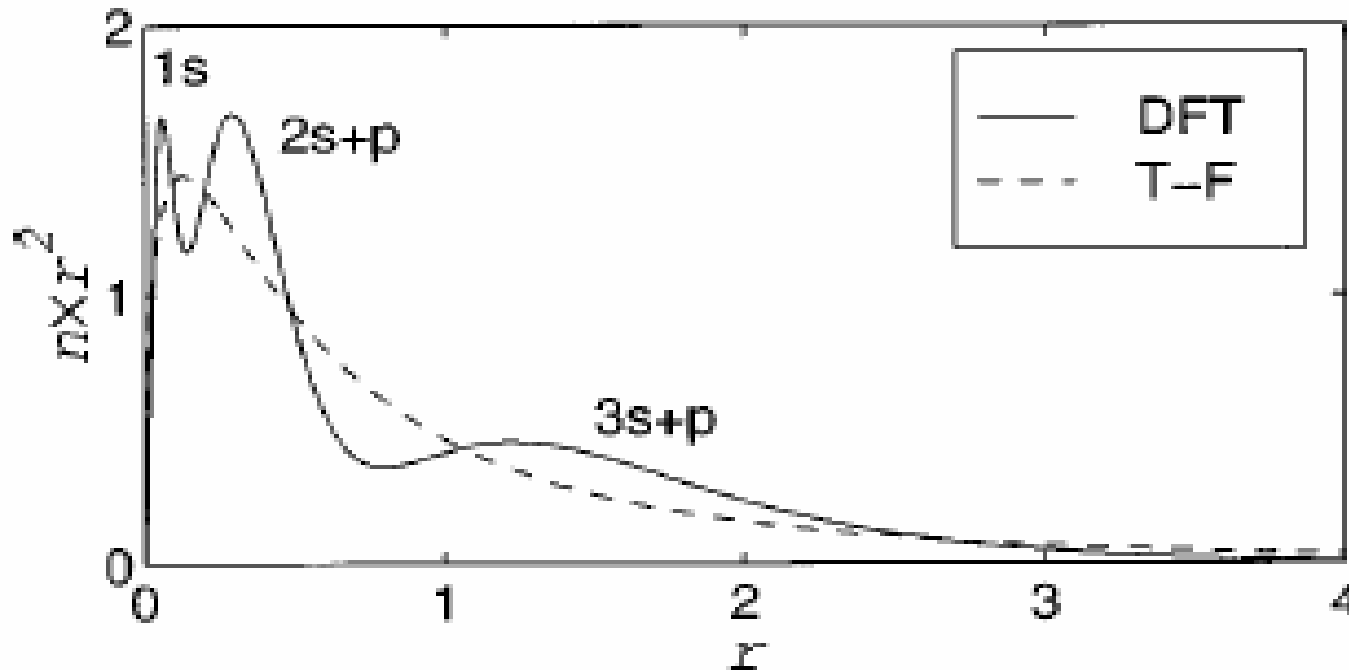
Methods to get a good approximation for the functional $E_{xc}[\rho]$

- 1) phenomenological formulas
- 2) in the local density approximation (LDA) the E_{xc} is calculated exactly by Monte-Carlo techniques for a homogeneous electron gas with density ρ . In the inhomogeneous system the LDA is used. An example: The binding energy of the Ar-atom is reproduced by the Thomas Fermi method with an accuracy of 20 %, by Kohn-Sham method with LDA approximation of 0.5 %.
- 3) there exist many more sophisticated techniques nowadays

DFT: density of Ar-atom

Ar Z=18

N.Argaman, G. Makov,
Am. J. Phys. 68, 69 (2000)



units: radius: Bohr radii
densities $\times r^2$ in inverse Bohr radii

limitations of exact density functionals:

formally exact

in practice

Kohn-Hohenberg: $E[\rho(\mathbf{r})]$

Kohn-Sham: $E[\rho(\mathbf{r}), \tau(\mathbf{r})]$

Skyrme: $E[\rho(\mathbf{r}), \tau(\mathbf{r}), J(\mathbf{r})]$

Gogny: $E[\rho(\mathbf{r}), \tau(\mathbf{r}), J(\mathbf{r}), \kappa(\mathbf{r})]$

no shell effects

no l·s,

no pairing

no config. mixing

generalized mean field: no configuration mixing,
no two-body correlations

local density: $\rho(\mathbf{r}) = \langle a^\dagger(\mathbf{r})a(\mathbf{r}) \rangle = \sum_i^A |\varphi_i(\mathbf{r})\rangle\langle\varphi_i(\mathbf{r})|$

kinetic energy density: $\tau(\mathbf{r}) = \sum_i^A |\nabla\varphi_i(\mathbf{r})\rangle\langle\nabla\varphi_i(\mathbf{r})|$

pairing density: $\kappa(\mathbf{r}) = \langle a^\dagger(\mathbf{r}, s)a^\dagger(\mathbf{r}, -s) \rangle$

twobody density: $\rho(\mathbf{r}, \mathbf{r}') = \langle a^\dagger(\mathbf{r})a(\mathbf{r})a^\dagger(\mathbf{r}')a(\mathbf{r}') \rangle$

Non-relativistic density functional theory in nuclei:

The building blocks of the nuclear energy density functional are various densities and currents:

For $\vec{x} = (\vec{r}, \sigma, \tau)$ we have the density matrix:

$$\begin{aligned}\rho(\vec{x}, \vec{x}') &= \sum_i |\varphi_i(\vec{x})\rangle\langle\varphi_i(\vec{x}')| \\ &= \frac{1}{4} \left\{ \rho_{00}(\vec{r}, \vec{r}') + \rho_{0i}(\vec{r}, \vec{r}')\sigma_i + \left[\rho_{q0}(\vec{r}, \vec{r}') + \rho_{qi}(\vec{r}, \vec{r}')\sigma_i \right] \tau_q \right\}\end{aligned}$$

isoscalar

isovector

Local quantities:

$$\rho_0(\vec{r}) = \rho_{00}(\vec{r}, \vec{r}) = \sum_{\sigma\tau} \rho(\vec{r}\sigma\tau, \vec{r}\sigma\tau) \quad \text{isoscalar density: } \rho_0 = \rho_n + \rho_p$$

$$\rho_1(\vec{r}) = \rho_{30}(\vec{r}, \vec{r}) = \sum_{\sigma\tau} \rho(\vec{r}\sigma\tau, \vec{r}\sigma\tau)\tau \quad \text{isovector density: } \rho_1 = \rho_n - \rho_p$$

$$\vec{s}_0(\vec{r}) = \sum_{\sigma\sigma'\tau} \rho(\vec{r}\sigma\tau, \vec{r}\sigma'\tau)\vec{\sigma}_{\sigma\sigma'} \quad \text{isoscalar spin density}$$

$$\vec{s}_1(\vec{r}) = \sum_{\sigma\sigma'\tau} \rho(\vec{r}\sigma\tau, \vec{r}\sigma'\tau)\tau\vec{\sigma}_{\sigma\sigma'} \quad \text{isovector spin density}$$

$$\vec{j}_T(\vec{r}) = \frac{i}{2} (\nabla' - \nabla) \rho_T(\vec{r}, \vec{r}') \Big|_{\vec{r}=\vec{r}'} \quad \text{current density} \quad T=0,1$$

$$\vec{J}_T(\vec{r}) = \frac{i}{2} (\nabla' - \nabla) \times \vec{s}_T(\vec{r}, \vec{r}') \Big|_{\vec{r}=\vec{r}'} \quad \text{spin current density}$$

$$\tau_T(\vec{r}) = (\nabla \cdot \nabla') \rho_T(\vec{r}, \vec{r}') \Big|_{\vec{r}=\vec{r}'} \quad \text{kinetic energy density}$$

$$\vec{T}_T(\vec{r}) = (\nabla \cdot \nabla') \vec{s}_T(\vec{r}, \vec{r}') \Big|_{\vec{r}=\vec{r}'} \quad \text{kinetic spin density}$$

The Skyrme functional can be derived from a density dependent two-body force

$$\begin{aligned}
 V_{Sk}(1,2) = & t_0(1 + x_0 \hat{P}_\sigma) \delta(\vec{r}_{12}) \\
 & + \frac{1}{2} t_1(1 + x_1 \hat{P}_\sigma) \left[\hat{k}^{+2} \delta(\vec{r}_{12}) + \delta(\vec{r}_{12}) \hat{k}^2 \right] \\
 & + \frac{1}{2} t_2(1 + x_2 \hat{P}_\sigma) \left[\hat{k}^+ \delta(\vec{r}_{12}) \hat{k} \right] \\
 & + iW_0(\vec{\sigma}_1 + \vec{\sigma}_2) \cdot \hat{k}^+ \times \delta(\vec{r}_{12}) \hat{k} \\
 & + \frac{1}{6} t_3(1 + x_3 \hat{P}_\sigma) \delta(\vec{r}_{12}) \rho^\alpha \left(\frac{\vec{r}_1 + \vec{r}_2}{2} \right)
 \end{aligned}$$

zero-range limit of a finite-range force up to second order in derivatives (finite range = momentum dependence!)

two-body spin-orbit

density dependent term (3-body, ...)

$$\hat{P}_\sigma = \frac{1}{2}(1 + \vec{\sigma}_1 \cdot \vec{\sigma}_2), \quad \hat{k} = \frac{1}{2i}(\vec{\nabla}_1 - \vec{\nabla}_2)$$

Energy functional:

$$E_{tot} = \int \mathcal{H}(\vec{r}) d^3r$$

Energy functional for N=Z:

$$E_{tot} = \int \mathcal{H}(\vec{r}) d^3r$$

$$\begin{aligned} \mathcal{H}(\vec{r}) = & \frac{\hbar^2}{2m} \tau + \frac{3}{8} t_0 \rho^2 + \frac{1}{16} t_3 \rho^{\alpha+2} + \frac{1}{16} (3t_1 + 5t_2) \rho \tau \\ & + \frac{1}{64} (9t_1 - 5t_2) (\vec{\nabla} \rho)^2 - \frac{3}{4} W_0 \rho \vec{\nabla} \vec{J} + \frac{1}{16} (t_1 - t_2) \vec{J}^2 \end{aligned}$$

equation of state (EOS)

$$\frac{E_0}{A} = \frac{H}{\rho} = \frac{3}{5} \frac{\hbar^2}{2m^*} k_f^2 + \frac{3}{8} t_0 \rho + \frac{1}{16} t_3 \rho^{\alpha+1}$$

incompressibility $K_\infty = k_f^2 \frac{\partial^2 E}{\partial k_f^2} \frac{1}{A}$

$$\rho = \frac{2}{3\pi^2} k_f^3$$

effective mass $\frac{\hbar^2}{2m^*} = \frac{\hbar^2}{2m} + \frac{1}{16} (3t_1 + 5t_2) \rho,$

4 parameter

Variation of the Skyrme functional:

We start from the Skyrme functional $E[\rho(\mathbf{r}), \tau(\mathbf{r}), \vec{J}(\mathbf{r})]$ and obtain the equations of motion:

$$\frac{\delta}{\delta\varphi_k^*} \left[E[\rho, \tau, \vec{J}] - \sum_n \varepsilon_n \int d^3r |\varphi_n|^2 \right] = 0,$$

and find for **spin-saturated** nuclei:

$$\delta E[\rho, \tau, \vec{J}] = \int d^3r \left[\frac{\hbar^2}{2m^*(\mathbf{r})} \delta\tau + U(\mathbf{r})\delta\rho + \vec{W}\delta\vec{J} \right] = 0,$$

with:
effective mass:

$$\frac{\hbar^2}{2m^*(\mathbf{r})} = \frac{\hbar^2}{2m} + \frac{1}{16} (3t_1 + 5t_2)\rho(\mathbf{r}),$$

normal potential

$$U(\mathbf{r}) = \frac{3}{4} t_0 \rho + \frac{3}{16} t_3 \rho^2 + \frac{1}{16} (3t_1 + 5t_2) \tau - \frac{1}{32} (9t_1 - 5t_2) \Delta\rho - \frac{3}{4} W_0 \vec{\nabla} \vec{J},$$

spin-orbit potential

$$\vec{W}(\mathbf{r}) = \frac{3}{4} W_0 \vec{\nabla} \rho$$

with

$$\rho(\mathbf{r}) = \sum_{i=1}^A \varphi_i^* \varphi_i$$

$$\tau(\mathbf{r}) = \sum_{i=1}^A \vec{\nabla} \varphi_i^* \vec{\nabla} \varphi_i$$

$$\vec{J}(\mathbf{r}) = \sum_{i=1}^A \varphi_i^* (\vec{\nabla} \times \vec{\sigma}) \varphi_i$$

this yields

$$\delta E = \sum_{i=1}^A \int d^3r \delta \varphi_k^* \left[-\vec{\nabla} \frac{\hbar^2}{2m^*(\mathbf{r})} \vec{\nabla} + U(\mathbf{r}) + \frac{3}{2} W_0 \frac{1}{r} \frac{\partial \rho}{\partial r} \vec{l} \vec{s} \right] \varphi_k$$

and we find the **Schroedinger equation**:

$$\left[-\vec{\nabla} \frac{\hbar^2}{2m^*(\mathbf{r})} \vec{\nabla} + U(\mathbf{r}) + \frac{3}{2} W_0 \frac{1}{r} \frac{\partial \rho}{\partial r} \vec{l} \vec{s} \right] \varphi_k = \varepsilon_k \varphi_k$$

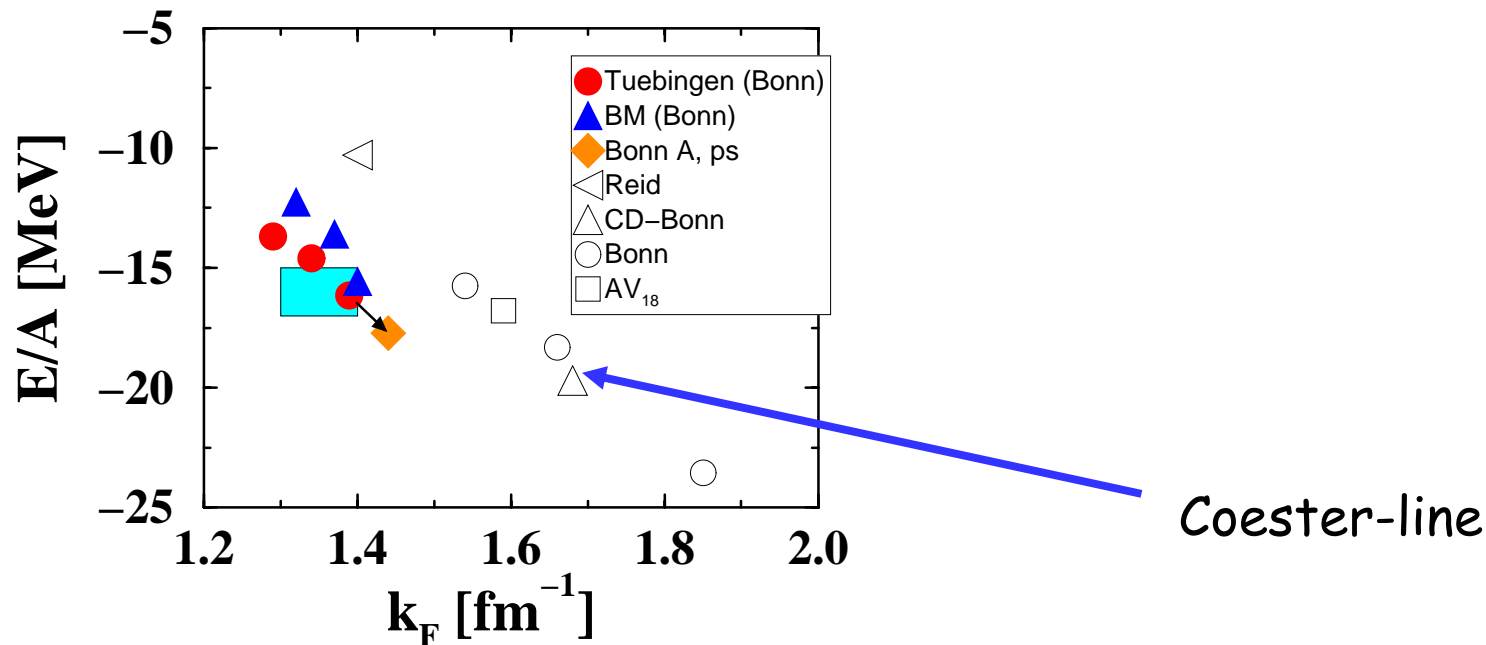
Covariant density functional theory:

Why covariant ?

- 1) no relativistic kinematic necessary: $\sqrt{p_F^2 + m_N^2} = m_N \sqrt{1 + 0.075}$
- 2) non-relativistic DFT works well
- 3) technical problems:
 - no harmonic oscillator
 - no exact soluble models
 - double dimension
 - huge cancellations V-S
 - no variational method
- 4) conceptual problems:
 - treatment of Dirac sea
 - no well defined many-body theory

Why covariant?

- 1) Large spin-orbit splitting in nuclei
- 2) Large fields $V \approx 350$ MeV, $S \approx -400$ MeV
- 3) Success of Relativistic Brueckner
- 4) Success of intermediate energy proton scatt.
- 5) relativistic saturation mechanism
- 6) consistent treatment of time-odd fields
- 7) Pseudo-spin Symmetry
- 8) Connection to underlying theories ?
- 9) As many symmetries as possible



Relativistic densities:

In the **relativistic treatment**, one has to deal with four-component Dirac spinor wave functions. Consequently, there are 16 independent bilinear covariants:

$$\bar{\psi}(\mathbf{r})\Gamma\psi(\mathbf{r})$$

This gives the following local densities:

$$\Gamma^s = 1$$

scalar density

$$\Gamma_{\mu}^v = \gamma_{\mu}$$

vector density

$$\Gamma_{\mu\nu}^t = (i/2)(\gamma_{\mu}\gamma_{\nu} - \gamma_{\nu}\gamma_{\mu})$$

tensor density

$$\Gamma^{\rho} = \gamma_5$$

pseudoscalar density

$$\Gamma_{\mu}^a = \gamma_{\mu}\gamma_5$$

axial density

(which have isoscalar and isovector components.) In most applications, only three densities are required:

$$\bar{\psi}\psi \quad (\sigma)$$

$$\bar{\psi}\gamma^{\mu}\psi \quad (\omega)$$

$$\bar{\psi}\gamma^{\mu}\vec{\tau}\psi \quad (\rho)$$

Dirac equation:

$$\begin{pmatrix} m + V - S & \vec{\sigma}(\vec{p} + \vec{V}) \\ \vec{\sigma}(\vec{p} + \vec{V}) & -m + V + S \end{pmatrix} \begin{pmatrix} g_i \\ f_i \end{pmatrix} = \epsilon_i \begin{pmatrix} g_i \\ f_i \end{pmatrix}$$

scalar potential

$S(\mathbf{r})$

vector potential (time-like)

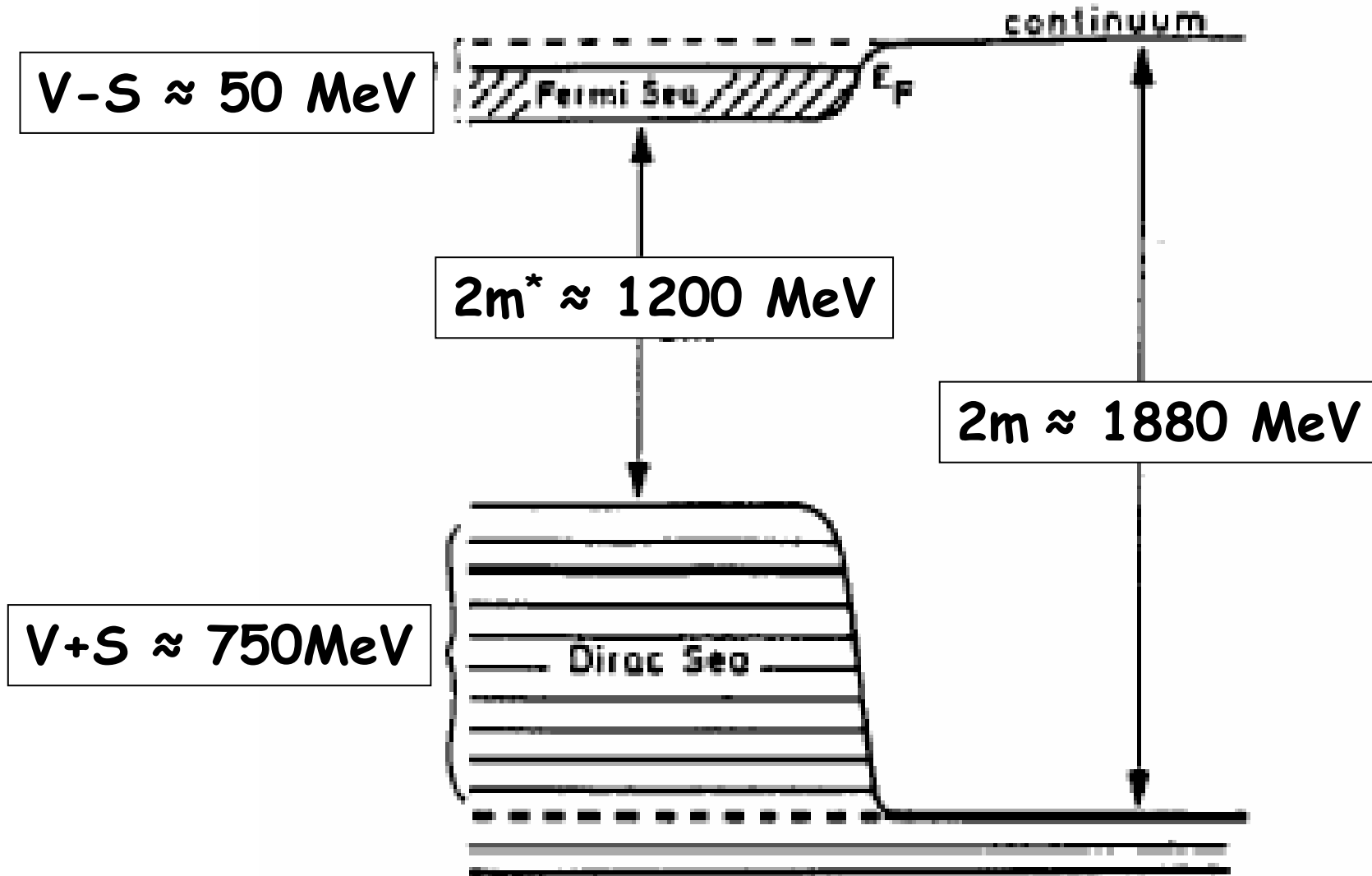
$V(\mathbf{r})$

vector potential (space-like)

$\vec{V}(\mathbf{r})$

vector space-like corresponds to magnetic potential (nuclear magnetism)
is time-odd and vanishes in the ground state of even-even systems

Relativistic potentials



Elimination of small components:

$(\varepsilon \rightarrow m+\varepsilon)$

$$f_i(\mathbf{r}) = \frac{1}{\varepsilon_i + 2m - W_+} \vec{\sigma} \vec{p} g_i(\mathbf{r})$$

$$W_{\pm} = V \pm S$$

$$\left\{ \vec{\sigma} \vec{p} \frac{1}{\varepsilon_i + 2\tilde{m}(\mathbf{r})} \vec{\sigma} \vec{p} + W_- \right\} g_i(\mathbf{r}) = \varepsilon_i g_i(\mathbf{r})$$

$$\tilde{m}(\mathbf{r}) = m - \frac{1}{2} W_+$$

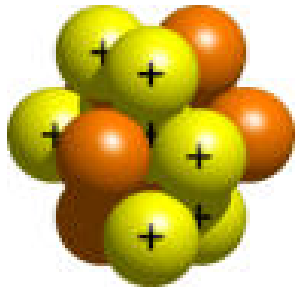
for $|\varepsilon_i| \ll 2\tilde{m}$

$$m^*(\mathbf{r}) = m - S$$

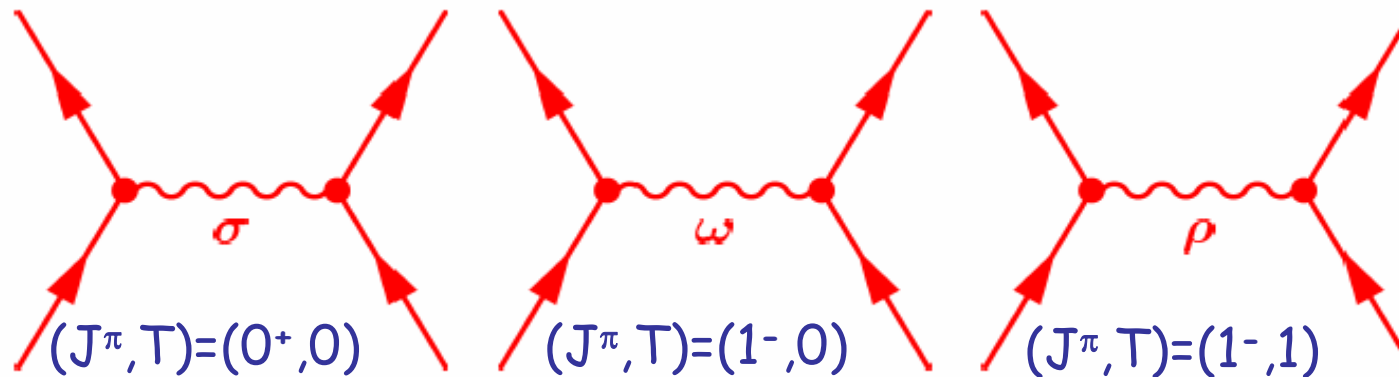
$$\left\{ \vec{p} \frac{1}{2\tilde{m}} \vec{p} + \frac{1}{4\tilde{m}^2} \frac{1}{r} \frac{\partial W_+}{\partial r} \vec{l} \vec{s} + W_- \right\} g_i(\mathbf{r}) \approx \varepsilon_i g_i(\mathbf{r})$$

Walecka model

$$E[\hat{\rho}]$$



Nucleons are coupled by exchange of mesons through an *effective Lagrangian* (EFT)



$$S(\mathbf{r}) = g_\sigma \sigma(\mathbf{r})$$

$$V(\mathbf{r}) = g_\omega \omega(\mathbf{r}) + g_\rho \vec{\tau} \vec{\rho}(\mathbf{r}) + eA(\mathbf{r})$$

Sigma-meson:
attractive scalar field

Omega-meson:
short-range repulsive

Rho-meson:
isovector field

Lagrangian density

free Dirac particle

free meson fields

free photon field

$$\begin{aligned} \mathcal{L} = & \bar{\psi} (i\gamma \cdot \partial - m) \psi + \frac{1}{2}(\partial\sigma)^2 - \frac{1}{2}m_\sigma^2\sigma^2 \\ & - \frac{1}{4}\Omega_{\mu\nu}\Omega^{\mu\nu} + \frac{1}{2}m_\omega^2\omega^2 - \frac{1}{4}\vec{R}_{\mu\nu}\vec{R}^{\mu\nu} + \frac{1}{2}m_\rho^2\vec{\rho}^2 - \frac{1}{4}F_{\mu\nu}F^{\mu\nu} \\ & - g_\sigma\bar{\psi}\sigma\psi - g_\omega\bar{\psi}\gamma \cdot \omega\psi - g_\rho\bar{\psi}\gamma \cdot \vec{\rho}\vec{\tau}\psi - e\bar{\psi}\gamma \cdot A\frac{(1-\tau_3)}{2}\psi \end{aligned}$$

Parameter:

meson masses: $m_\sigma, m_\omega, m_\rho$

meson couplings: $g_\sigma, g_\omega, g_\rho$

interaction terms

Equations of motion

$$\partial_\mu \frac{\partial L}{\partial(\partial_\mu q_k)} - \frac{\partial L}{\partial q_k} = 0.$$

for the nucleons we find the **Dirac equation**

$$(\gamma^\mu (i\partial_\mu - V_\mu) - m + S)\psi_i = 0.$$

No-sea approxim. !

for the mesons we find the **Klein-Gordon equation**

$$\begin{aligned} (\partial^\nu \partial_\nu + m_\sigma^2)\sigma &= -g_\sigma \rho_s \\ (\partial^\nu \partial_\nu + m_\omega^2)\omega_\mu &= g_\omega j_\mu \\ (\partial^\mu \partial_\mu + m_\rho^2)\vec{\rho}_\mu &= g_\rho \vec{j}_\mu \\ \partial^\nu \partial_\nu A_\mu &= e j_\mu^{(em)} \end{aligned}$$

$$\begin{aligned} \rho_s(x) &= \sum_{i=1}^A \bar{\psi}_i(x) \psi_i(x) \\ j_\mu(x) &= \sum_{i=1}^A \bar{\psi}_i(x) \gamma_\mu \psi_i(x) \\ \vec{j}_\mu(x) &= \sum_{i=1}^A \bar{\psi}_i(x) \vec{\tau} \gamma_\mu \psi_i(x) \\ j_\mu^{(em)}(x) &= \sum_{i=1}^A \bar{\psi}_i(x) \frac{1}{2} (1 - \tau_3) \gamma_\mu \psi_i(x) \end{aligned}$$

Static limit (with time reversal invariance)

for the nucleons we find the **static Dirac equation**

$$(\vec{\alpha}\vec{p} + V + \beta(m - S))\psi_i = \varepsilon_i\psi_i.$$

$$S = -g_s\sigma, \quad V = g_\omega\omega_0 + g_\rho\rho_0 + eA_0$$

for the mesons we find the **Helmholtz equations**

No-sea approxim. !

$$\begin{aligned}(-\Delta + m_\sigma^2)\sigma &= -g_\sigma\rho_s \\(-\Delta + m_\omega^2)\omega_0 &= g_\omega\rho_B \\(-\Delta + m_\rho^2)\rho_0^3 &= g_\rho\rho^3 \\-\Delta A_0 &= e\rho^{(em)}\end{aligned}$$

$$\begin{aligned}\rho_s &= \sum_{i=1}^A \bar{\psi}_i\psi_i \\ \rho_B &= \sum_{i=1}^A \psi_i^+\psi_i \\ \rho^3 &= \sum_{i=1}^A \psi_i^+\tau_3\psi_i \\ \rho^{(em)} &= \sum_{i=1}^A \psi_i^+\frac{1}{2}(1 - \tau_3)\psi_i\end{aligned}$$

Relativistic saturation mechanism:

We consider only the σ -field, the origin of attraction
its source is the scalar density

$$m_\sigma^2 \sigma = -g_\sigma \sum_{i=1}^A \bar{\Psi}_i \Psi_i = -g_\sigma \sum_{i=1}^A (g_i^+ g_i - f_i^+ f_i)$$

for **high densities**, when the collapse is close, the Dirac gap $\approx 2m^*$ decreases, the small components f_i of the wave functions increase and reduce the scalar density, i.e. the source of the σ -field, and therefore also scalar attraction.

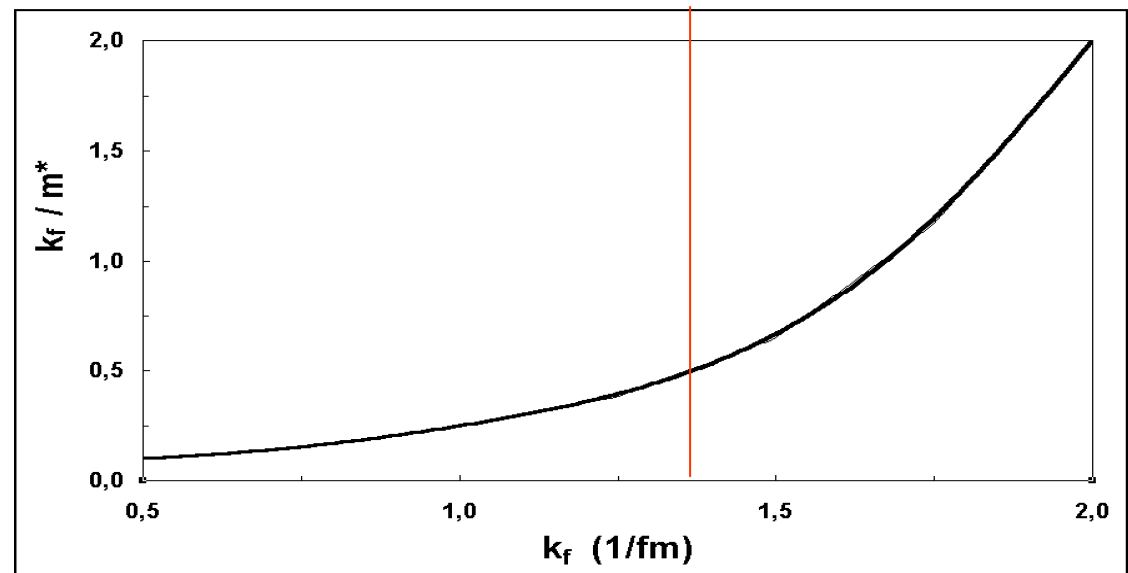
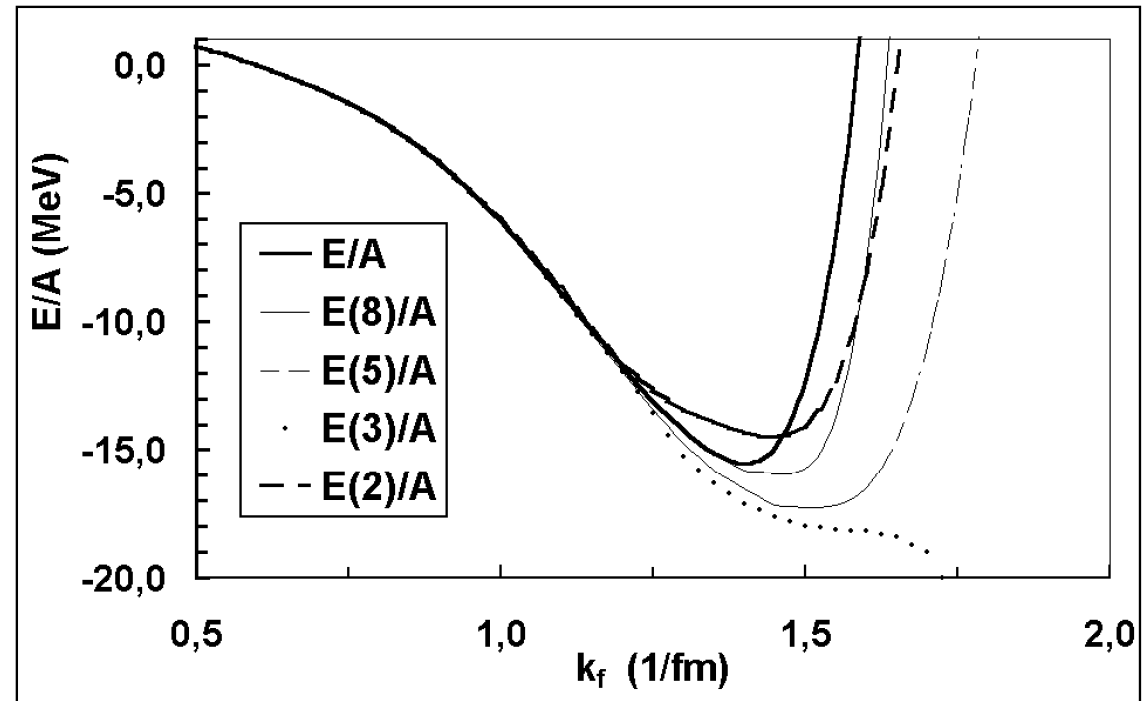
$$f_i(\mathbf{r}) = \frac{1}{\varepsilon_i + 2\tilde{m}} \vec{\sigma} \vec{k} g_i(\mathbf{r})$$

$$m_\sigma^2 \sigma \approx -g_\sigma \rho_B - 2 \sum_{i=1}^A f_i^+ f_i = -g_\sigma \rho_B + \frac{1}{\tilde{m}} \sum_{i=1}^A \nabla g_i^+ \nabla g_i$$

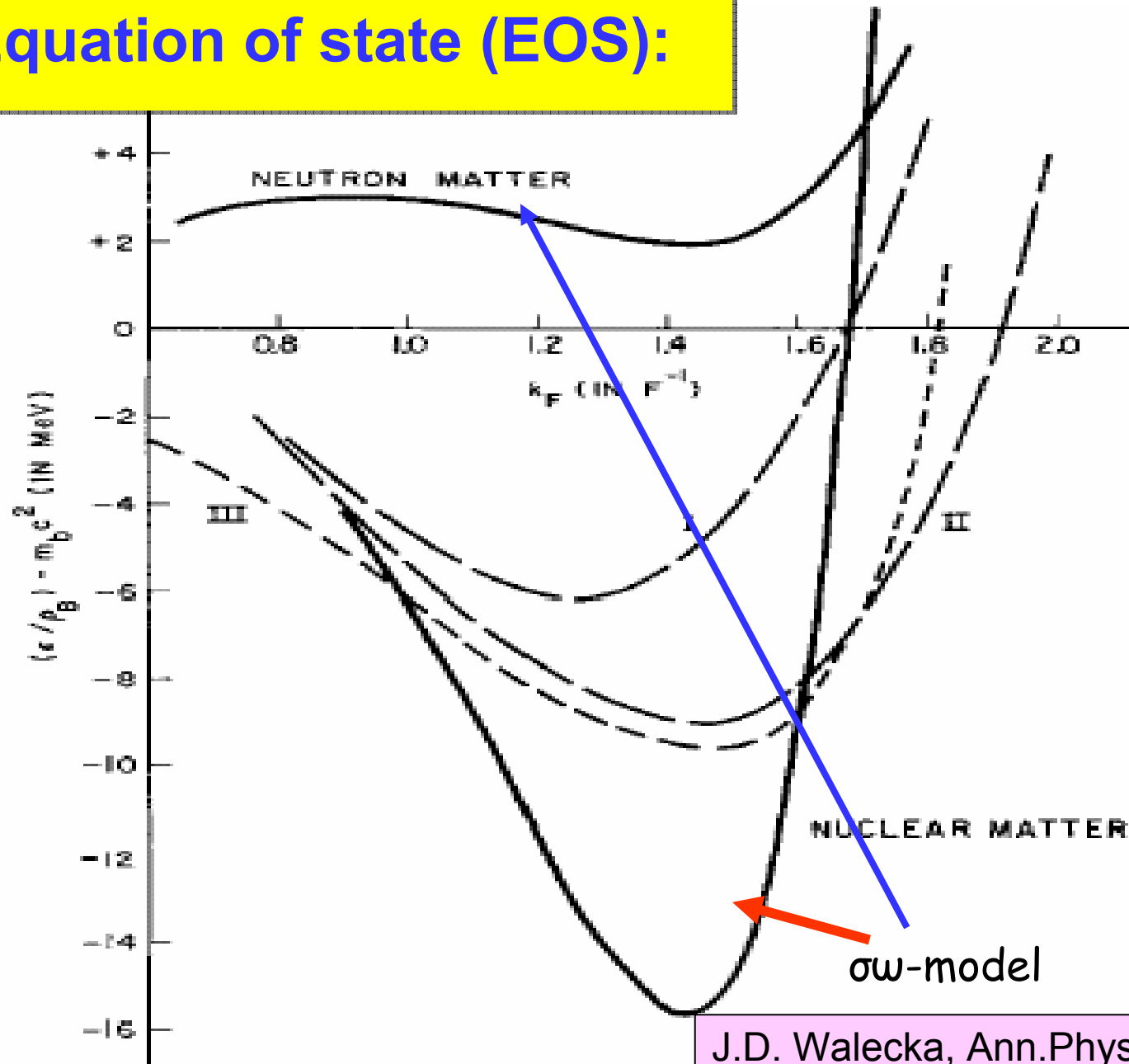
In the non-relativistic case, Hartree with Yukawa forces
would lead to collapse

Fouldy-Wouthousen:

2nd, 3th, 5th and 8th
order in k_f/m^*



Equation of state (EOS):



Effective density dependence:

non-linear potential:

Boguta and Bodmer, NPA 431, 3408 (1977)

NL1, NL3..

$$\frac{1}{2}m_{\sigma}^2\sigma^2 \Rightarrow U(\sigma) = \frac{1}{2}m_{\sigma}^2\sigma^2 + \frac{1}{3}g_2\sigma^3 + \frac{1}{4}g_3\sigma^4$$

density dependent coupling constants:

R.Brockmann and H.Toki, PRL 68, 3408 (1992)

S.Tygel and H.H.Wolter, NPA 656, 331 (1999)

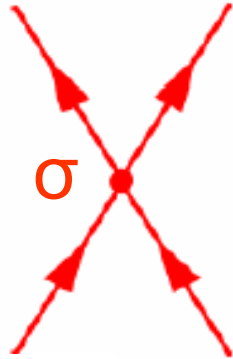
T. Niksic, D. Vretenar, P. Finelli, and P. Ring, PRC 56 (2002) 024306

$$g_{\sigma}, g_{\omega}, g_{\rho} \Rightarrow g_{\sigma}(\rho), g_{\omega}(\rho), g_{\rho}(\rho)$$

$$\mathbf{g} \rightarrow \mathbf{g}(\rho(\mathbf{r}))$$

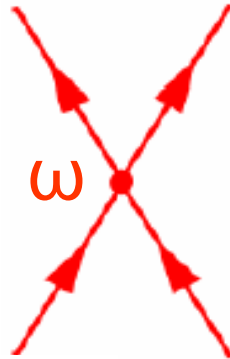
DD-ME1, DD-ME2

Point-Coupling Models



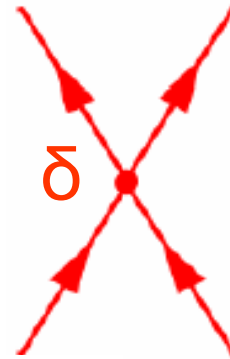
$$J=0, T=0$$

$$G_\sigma = \frac{g_\sigma^2}{m_\sigma^2}$$



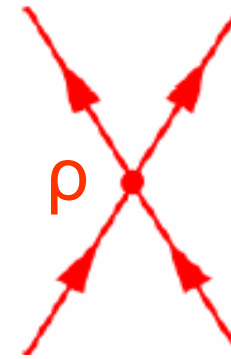
$$J=1, T=0$$

$$G_\omega = \frac{g_\omega^2}{m_\omega^2}$$



$$J=0, T=1$$

$$G_\delta = \frac{g_\delta^2}{m_\delta^2}$$



$$J=1, T=1$$

$$G_\rho = \frac{g_\rho^2}{m_\rho^2}$$

Manakos and Mannel, Z.Phys. **330**, 223 (1988)

Bürvenich, Madland, Maruhn, Reinhard, PRC **65**, 044308 (2002)

Lagrangian density for point coupling

free Dirac particle

$$\begin{aligned}
 \mathcal{L} = & \bar{\psi} (i\gamma \cdot \partial - m) \psi \\
 & + G_{\sigma} (\bar{\psi}\psi)(\bar{\psi}\psi) \quad + G_{\omega} (\bar{\psi}\gamma^{\mu}\psi)(\bar{\psi}\gamma_{\mu}\psi) \\
 & + G_{\delta} (\bar{\psi}\vec{\tau}\psi)(\bar{\psi}\vec{\tau}\psi) \quad + G_{\rho} (\bar{\psi}\gamma^{\mu}\vec{\tau}\psi)(\bar{\psi}\gamma_{\mu}\vec{\tau}\psi) \\
 & + D_{\sigma} (\bar{\psi}\partial^{\mu}\psi)(\bar{\psi}\partial_{\mu}\psi) \\
 & - \frac{1}{4} F_{\mu\nu} F^{\mu\nu} \quad + e^2 \bar{\psi} \gamma^{\mu} A_{\mu} \frac{(1 - \tau_3)}{2} \psi \quad (1)
 \end{aligned}$$

Parameter:

photon field

point couplings: $G_{\sigma}, G_{\omega}, G_{\delta}, G_{\rho}, \quad G_i = \left(\frac{g_i}{m_i}\right)^2$

derivative terms: D_{σ}

Three relativistic models:

Meson exchange with non-linear meson couplings:

Boguta and Bodmer, NPA. 431, 3408 (1977)

NL1, NL3, TM1, ...

Meson exchange with density dependent coupling constants:

R. Brockmann and H. Toki, PRL 68, 3408 (1992)

DD-ME1, DD-ME2

Point-coupling models with density dependent coupling constants:

Manakos and Mannel, Z.Phys. **330**, 223 (1988)

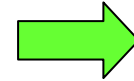
PC-F1,

How many parameters ?

7 parameters

symmetric nuclear matter:

$E/A, \rho_0$

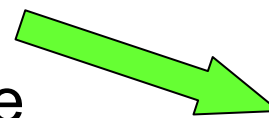


$$\frac{g_\sigma}{m_\sigma}$$

$$\frac{g_\omega}{m_\omega}$$

finite nuclei (N=Z):

$E/A,$ radii
spinorbit for free



$$m_\sigma$$

Coulomb (N≠Z):

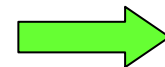
a_4



$$\frac{g_\rho}{m_\rho}$$

density dependence: T=0

K_∞

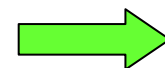


$$g_2$$

$$g_3$$

T=1

$r_n - r_p$



$$a_\rho$$

Nuclei used in the fit for DD-ME2

Nucleus	B.E (MeV)	r_c (fm)	$r_n - r_p$ (fm)	dE(%)	dr _c (%)	dr _{np}
¹⁶ O	127.801 (127.619)	2.727 (2.730)	-0.03	0.1	-0.1	
⁴⁰ Ca	342.741 (342.052)	3.464 (3.485)	-0.05	0.2	-0.6	
⁴⁸ Ca	414.770 (415.991)	3.481 (3.484)	0.18	-0.3	-0.1	
⁷² Ni	612.655 (613.173)	3.914	0.28	-0.1		
⁹⁰ Zr	783.155 (783.893)	4.275 (4.272)	0.07	-0.1	0.1	
¹¹⁶ Sn	986.928 (988.681)	4.615 (4.626)	0.12 (0.12)	-0.2	-0.2	3.8
¹²⁴ Sn	1048.859 (1049.962)	4.671 (4.674)	0.21 (0.19)	-0.1	-0.1	10.7
¹³² Sn	1103.469 (1102.860)	4.718	0.26	0.1		
²⁰⁴ Pb	1608.506 (1607.520)	5.500 (5.486)	0.17	0.1	0.3	
²⁰⁸ Pb	1639.826 (1636.446)	5.518 (5.505)	0.19 (0.20)	0.2	0.2	-4.7
²¹⁴ Pb	1661.182 (1663.298)	5.568 (5.562)	0.24	-0.1	0.1	
²¹⁰ Po	1649.695 (1645.228)	5.552	0.17	0.3		

Nuclear matter:

$E/A = -16$ MeV (5%), $\rho_0 = 1.53$ fm⁻³ (10%)

$K = 250$ MeV (10%), $a_4 = 33$ MeV (10%)

Parameterization of density dependence

MICROSCOPIC: Dirac-Brueckner calculations

saturation density

PHENOMENOLOGICAL:

$$g_i(\rho) = g_i(\rho_{\text{sat}}) f_i(x)$$

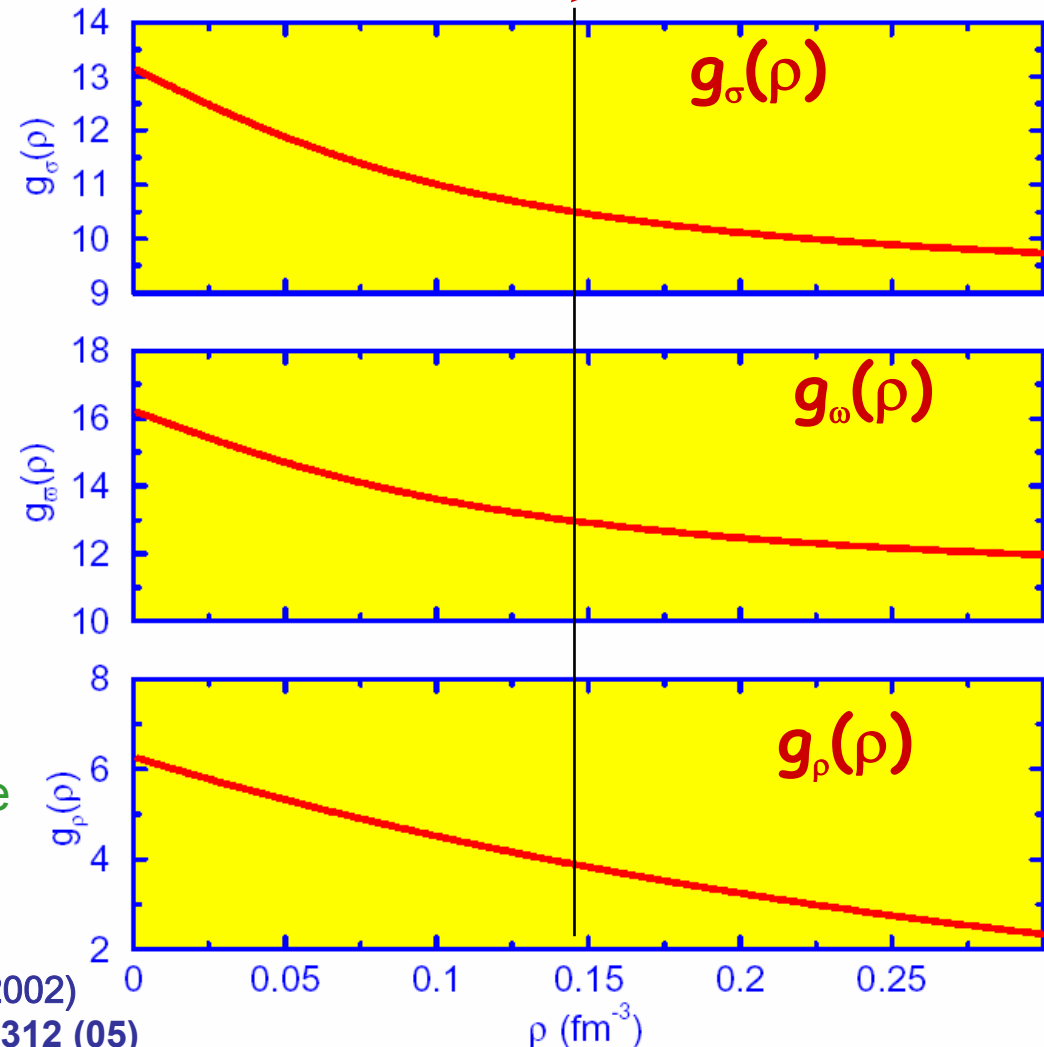
$$f_i(x) = a_i \frac{1+b_i(x+d_i)^2}{1+c_i(x+d_i)^2}$$

$$i = \sigma, \omega$$

$$g_\rho(\rho) = g_\rho(\rho_{\text{sat}}) e^{-a_\rho(x-1)}$$

$$x = \rho/\rho_{\text{sat}}$$

4 parameters for density dependence



Typel and Wolter, NPA 656, 331 (1999)

Niksic, Vretenar, Finelli, Ring, PRC 66, 024306 (2002)

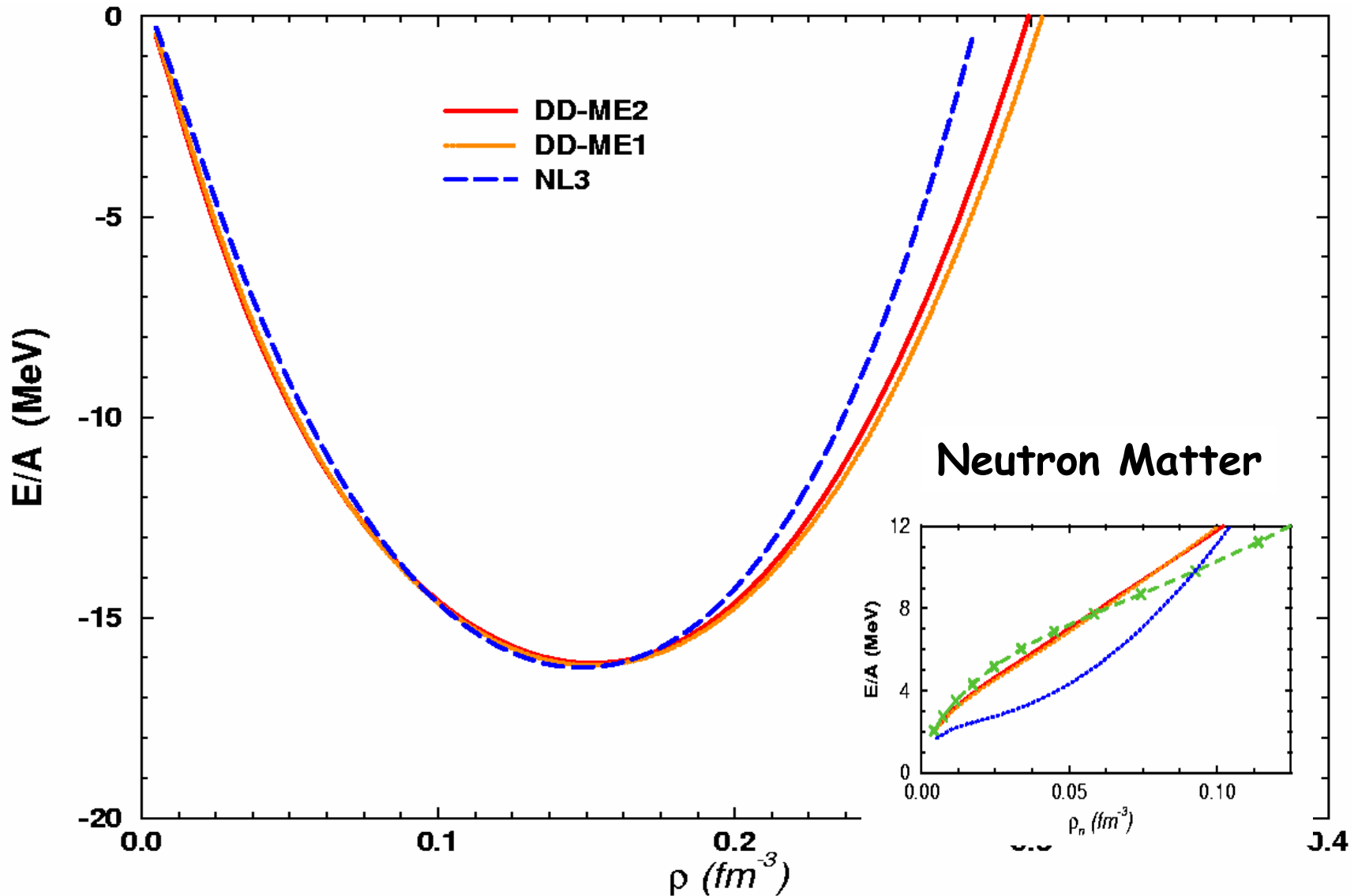
Lalazissis, Niksic, Vretenar, Ring, PRC 71, 024312 (05)

Nuclear matter properties:

	DD-ME2	DD-ME1	TW-99	NL3	NL3*
$\rho_0 [fm^{-3}]$	0.152	0.152	0.153	0.149	0.150
$a_v [MeV]$	-16.14	-16.20	-16.25	-16.25	-16.31
$K [MeV]$	250.89	244.5	240.0	271.8	258.5
$a_4 [MeV]$	32.3	33.1	32.5	37.9	38.3
$m^* [MeV]$	0.572	0.578	0.556	0.60	0.595

$$B(N, Z) = a_v A + a_s A^{2/3} + a_c \frac{Z^2}{A^{1/3}} + a_4 \frac{(N-Z)^2}{A}$$

Nuclear matter equation of state



Symmetry energy

$$E(\rho, \alpha) = E(\rho, 0) + S_2(\rho)\alpha^2 + S_4(\rho)\alpha^4 + \dots$$

$$S_2(\rho) = a_4 + \frac{p_0}{\rho_{\text{sat}}^2} (\rho - \rho_{\text{sat}}) + \frac{\Delta K_0}{18\rho_{\text{sat}}^2} (\rho - \rho_{\text{sat}})^2 + \dots$$

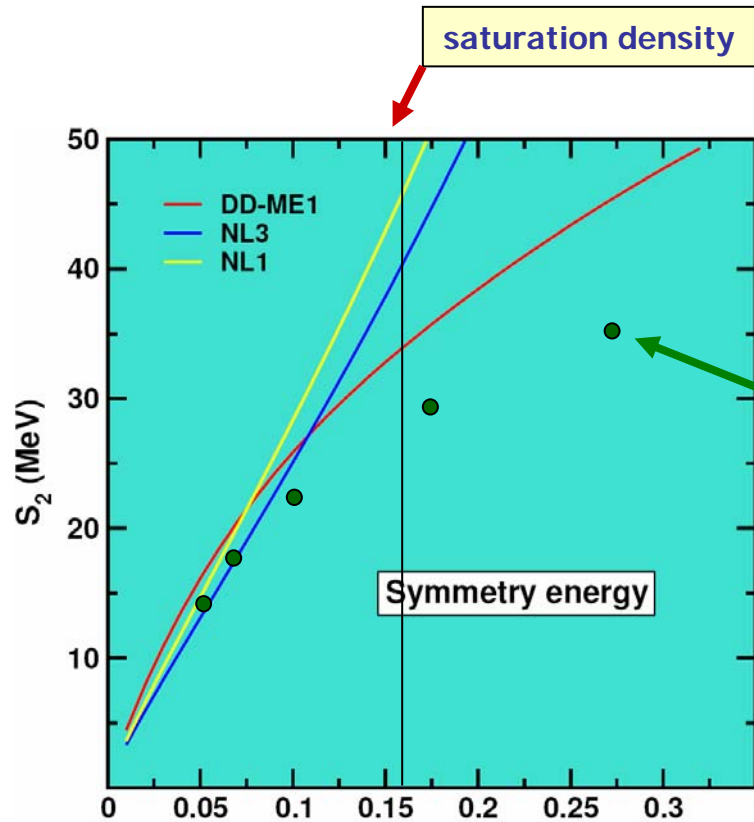
$$\alpha \equiv \frac{N-Z}{N+Z}$$

empirical values:

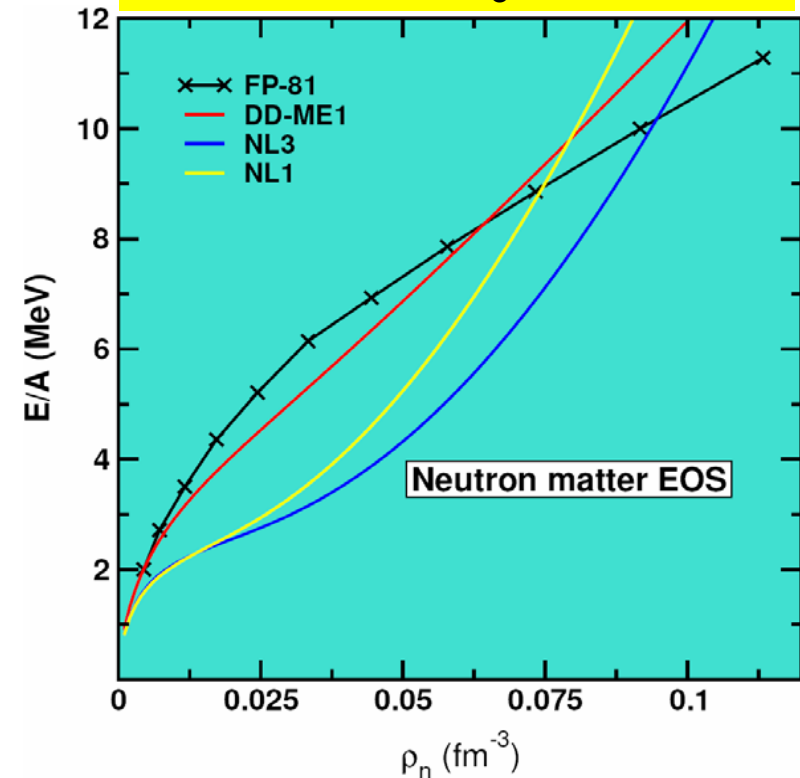
$$30 \text{ MeV} \leq a_4 \leq 34 \text{ MeV}$$

$$2 \text{ MeV/fm}^3 < p_0 < 4 \text{ MeV/fm}^3$$

$$-200 \text{ MeV} < \Delta K_0 < -50 \text{ MeV}$$



	DD-ME1	NL3	NL1
$a_4(\text{MeV})$	33.1	37.9	43.7
$p_0(\text{MeV/fm}^3)$	3.26	5.92	7.0
$\Delta K_0(\text{MeV})$	-128.5	52.1	67.3



General Remarks about Pairing:

- 1) There is plenty of **experimental evidence**
- 2) In principle pairing is a **small effect** ($\Delta \ll M$)
- 3) Most important close to the **Fermi surface**
- 4) Smearing of the Fermi surface (v^2)
- 5) Gap in the spectrum: $E_k = \sqrt{(\varepsilon_k - \lambda)^2 + \Delta^2}$
- 6) Influence on **response functions** (e.g. moments of inertia)

$$J^{(2)} = \sum_{\mathbf{v}} \frac{|\langle \mathbf{v} | J_x | 0 \rangle|^2}{E_{\mathbf{v}} - E_0} \approx \sum_{k < k'} \frac{|\langle k | J_x | k' \rangle|^2 (u_k v_{k'} - v_k u_{k'})}{E_k + E_{k'}}$$

- 7) Phase transition **normal fluid** \rightarrow **superfluid** (with λ, ω, T)
- 8) Few exp. data on **details** of pairing (one parameter Δ)
- 9) Crucial quantity: **pair-transfer matrix elements**

Seniority scheme:

$$\hat{V} = -G\hat{S}_+\hat{S}_-$$

$$\hat{S}_+ \sim [a_j^\dagger a_j^\dagger]_{J=0} \sim \sum a_m^\dagger a_{-m}^\dagger$$

S_+ creates a Cooper-pair

$$[\hat{S}_-, \hat{S}_+] = 1 - \frac{\hat{N}}{2j+1}$$

exact ground state:

$$|\Psi_0\rangle \sim (\hat{S}_+)^{N/2} |-\rangle \sim P^N e^{\eta \hat{S}_+} |-\rangle \quad \text{with} \quad \eta = \frac{v}{u}$$

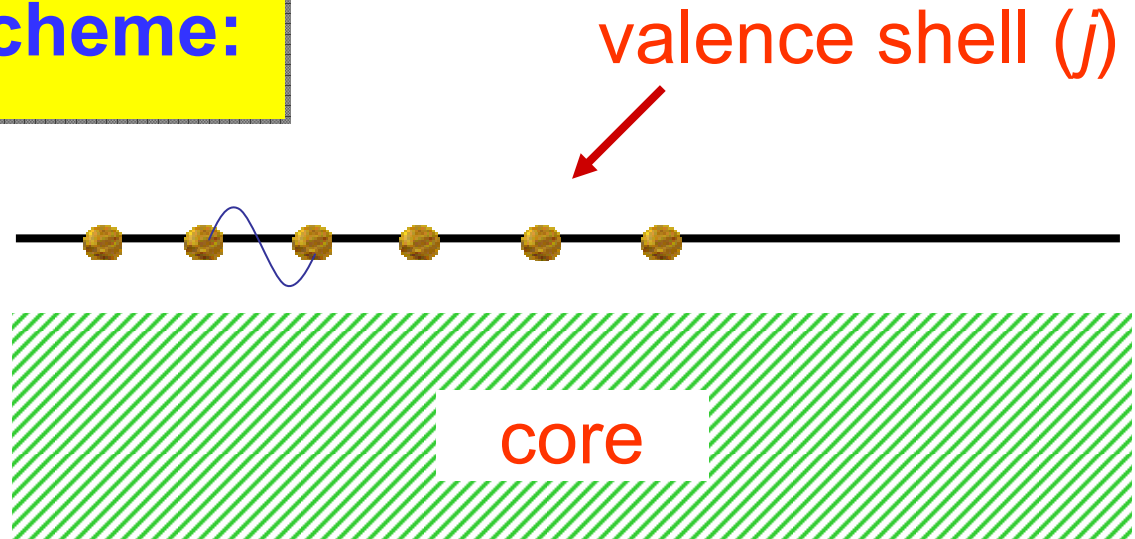
$$\sim P^N \prod (u + v a_m^\dagger a_{-m}^\dagger) |-\rangle = P^N |BCS\rangle$$

with the generalized product state:

$$|BCS\rangle = \prod \alpha_m |-\rangle$$

and the quasi-particles:

$$\alpha_m^\dagger = u a_m^\dagger + v a_{-m}$$



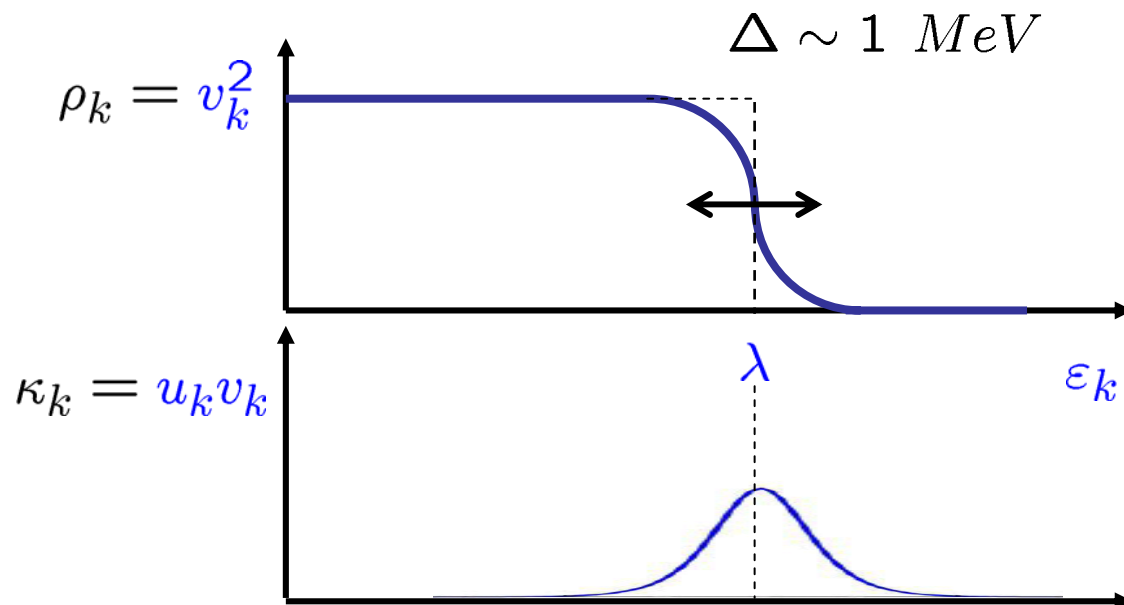
BCS-theory

$$|BCS\rangle = \prod_k (u_k + v_k a_k^\dagger a_{-k}^\dagger) |-\rangle$$

$$u_k^2 + v_k^2 = 1$$

$$\rho_k = \langle a_k^\dagger a_k \rangle = v_k^2 = \frac{1}{2} \left(1 - \frac{\varepsilon_k - \lambda}{\sqrt{(\varepsilon_k - \lambda)^2 + \Delta^2}} \right)$$

$$\kappa_k = \langle a_k^\dagger a_{-k}^\dagger \rangle = u_k v_k = \frac{\Delta}{2\sqrt{(\varepsilon_k - \lambda)^2 + \Delta^2}}$$



Hartree-Fock Bogoliubov Theory

This simple model can be generalized to the **full space** and to **arbitrary interactions**.

The HFB-wavefunction $|\text{HFB}\rangle = |\Phi\rangle$ is defined as the quasi-particle vacuum to the **quasiparticles**:

$$\alpha_k^+ = \sum_n U_{nk} c_n^+ + V_{nk} c_n \quad \alpha_k |\Phi\rangle = 0$$

with the normal density: $\rho_{nn'} = \langle \Phi | c_{n'}^+ c_n | \Phi \rangle = \sum_k V_{nk}^* V_{n'k}$

the pairing tensor: $\kappa_{nn'} = \langle \Phi | c_{n'} c_n | \Phi \rangle = \sum_k V_{nk}^* U_{n'k}$

The density functional depends on **two densities**:

$$E[\rho, \kappa] = E_{\text{RMF}}[\rho] + E_{\text{Gogny}}[\kappa]$$

Hartree-Fock Bogoliubov Equations

The variation of $E'[\rho, \kappa] = E[\rho, \kappa] - \lambda \text{Tr}(\rho)$ with respect to ρ and κ yields two coupled equations for the HFB wave functions $U_k(\mathbf{r})$ and $V_k(\mathbf{r})$

$$\begin{pmatrix} \hat{h} & \hat{\Delta} \\ -\Delta^* & -\hat{h}^* \end{pmatrix} \begin{pmatrix} U_k(\mathbf{r}) \\ V_k(\mathbf{r}) \end{pmatrix} = \begin{pmatrix} U_k(\mathbf{r}) \\ V_k(\mathbf{r}) \end{pmatrix} E_k$$

with two potentials: the normal mean field the pairing field

$$\hat{h} = \frac{\delta E'}{\delta \hat{\rho}}$$

$$\hat{\Delta} = \frac{\delta E}{\delta \hat{\kappa}}$$

we have no longer a sharp Fermi surface ($\rho^2 \neq \rho$)
but there is still a constraint: $\hat{\rho}^2 - \hat{\rho} = \hat{\kappa} \hat{\kappa}^*$

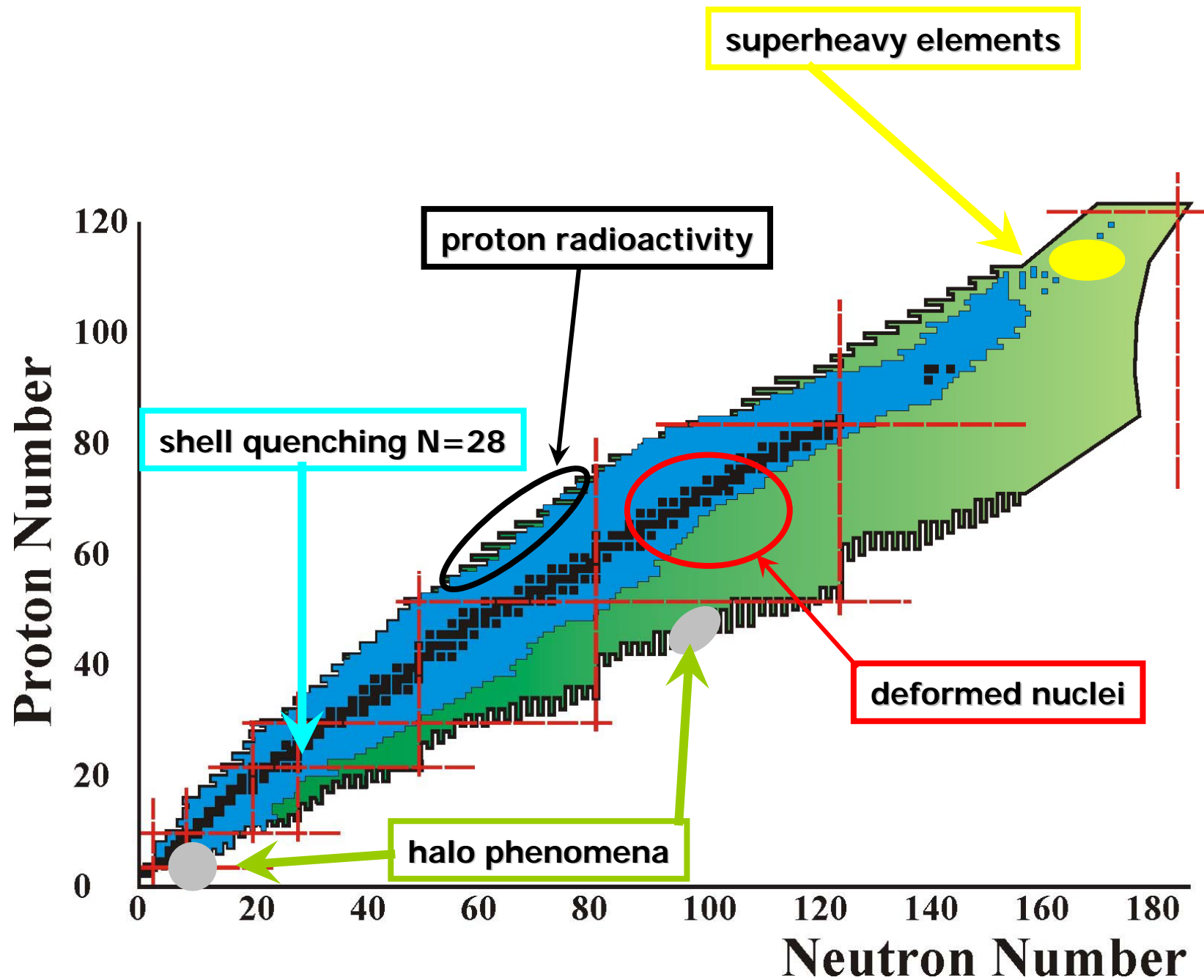
we have independent quasiparticles with the
occupation numbers 0 or 1

Conclusions part I:

- 1) density functional theory is in principle exact
- 2) microscopic derivation of $E(\rho)$ very difficult
- 3) Lorentz symmetry gives essential constraints
 - large spin orbit splitting
 - relativistic saturation
 - unified theory of time-odd fields
- 4) in realistic nuclei one needs a density dependence
 - non-linear coupling of mesons
 - density dependent coupling-parameters
- 5) modern parameter sets (7 parameter) provide excellent description of ground state properties
 - binding energies (1 ‰)
 - radii (1 %)
 - deformation parameters
- 6) pairing effects are non-relativistic

Content

- Density functional theory in nuclei
- Ground state properties
- Nuclear dynamics and excitations
- Methods beyond mean field
- Conclusions



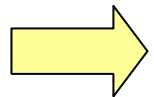
reduction of the spin-orbit potential

The **spin-orbit potential** originates from the addition of two large fields: the field of the vector mesons (short range repulsion), and the scalar field of the sigma meson (intermediate attraction).

$$V_{s.o.} \approx \frac{1}{r} \frac{\partial}{\partial r} V_{ls}(r)$$

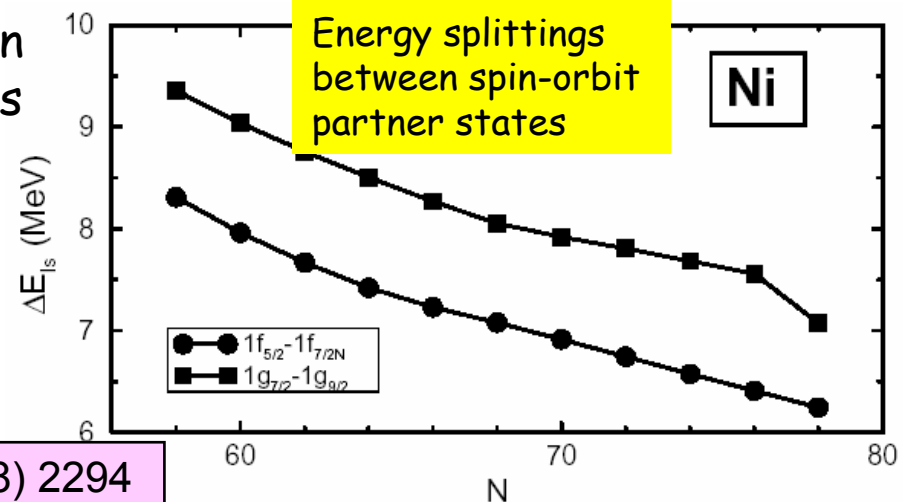
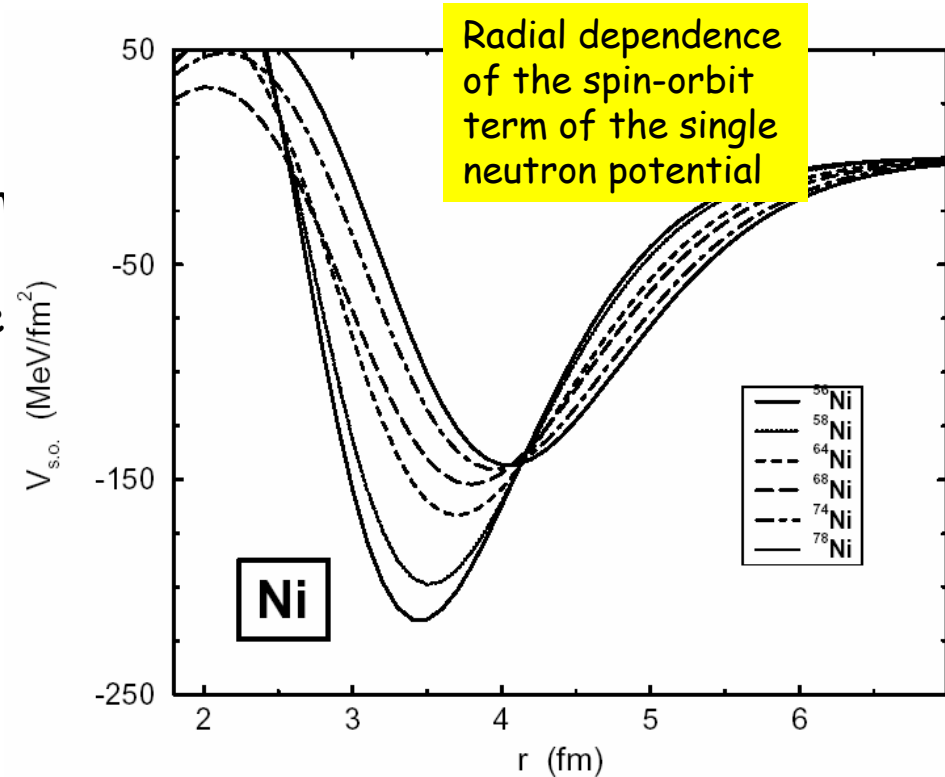
$$V_{ls} = \frac{m}{m_{eff}} (V + S)$$

weakening of the effective single-neutron spin-orbit potential in neutron-rich isotopes

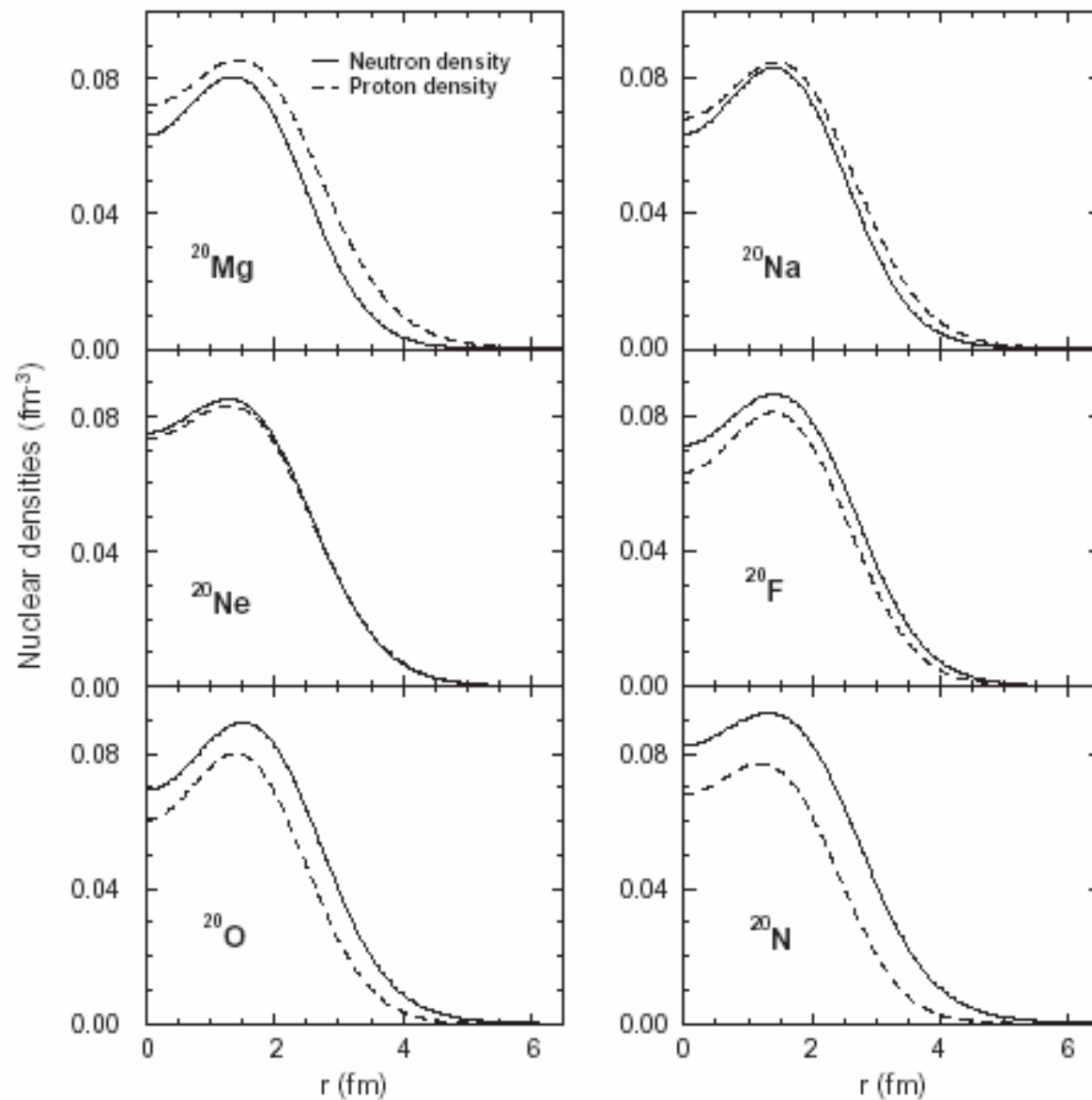


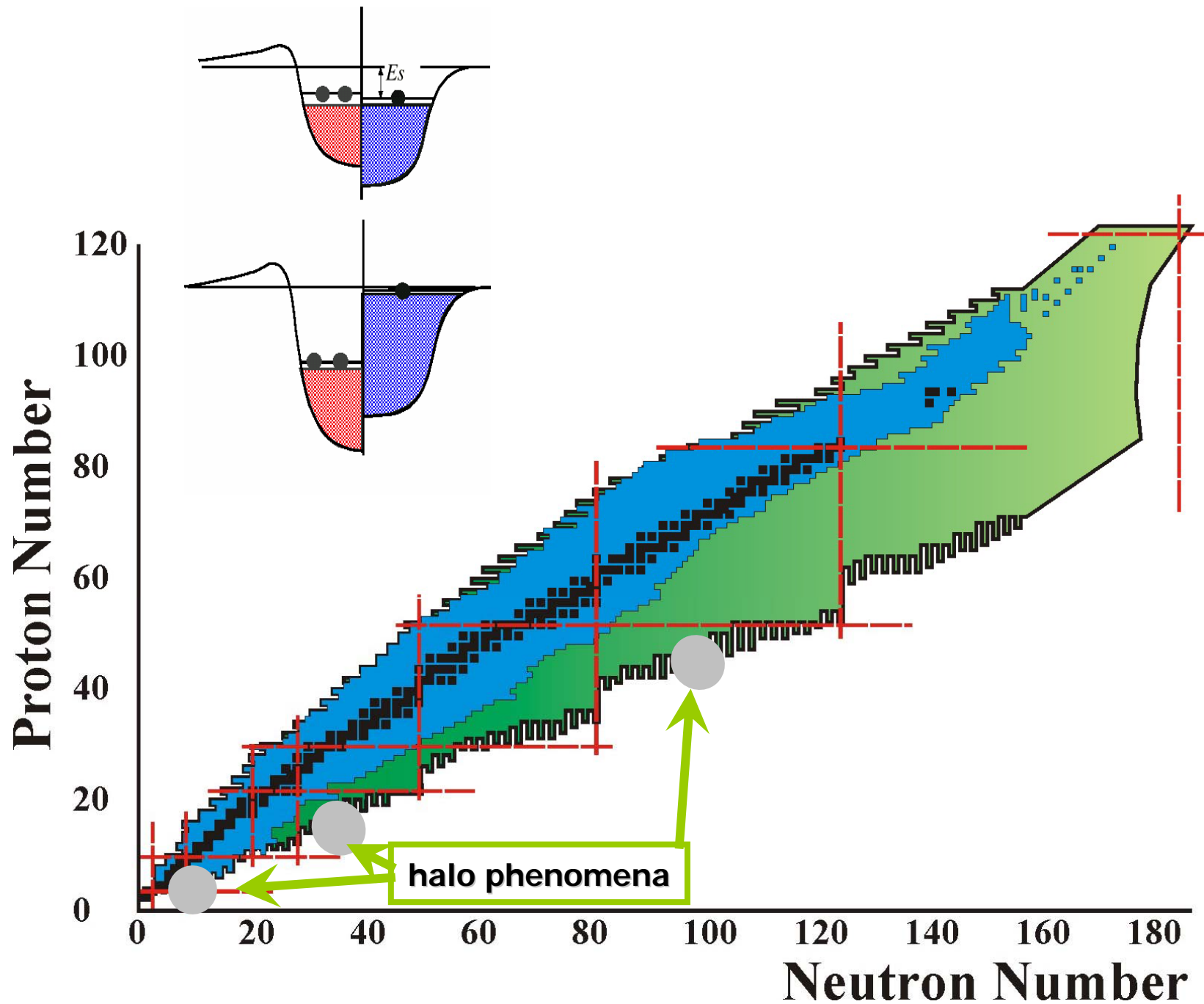
reduced energy spacings between spin-orbit partners

$$\Delta E_{ls} = E_{n,l,j=l-1/2} - E_{n,l,j=l+1/2}$$

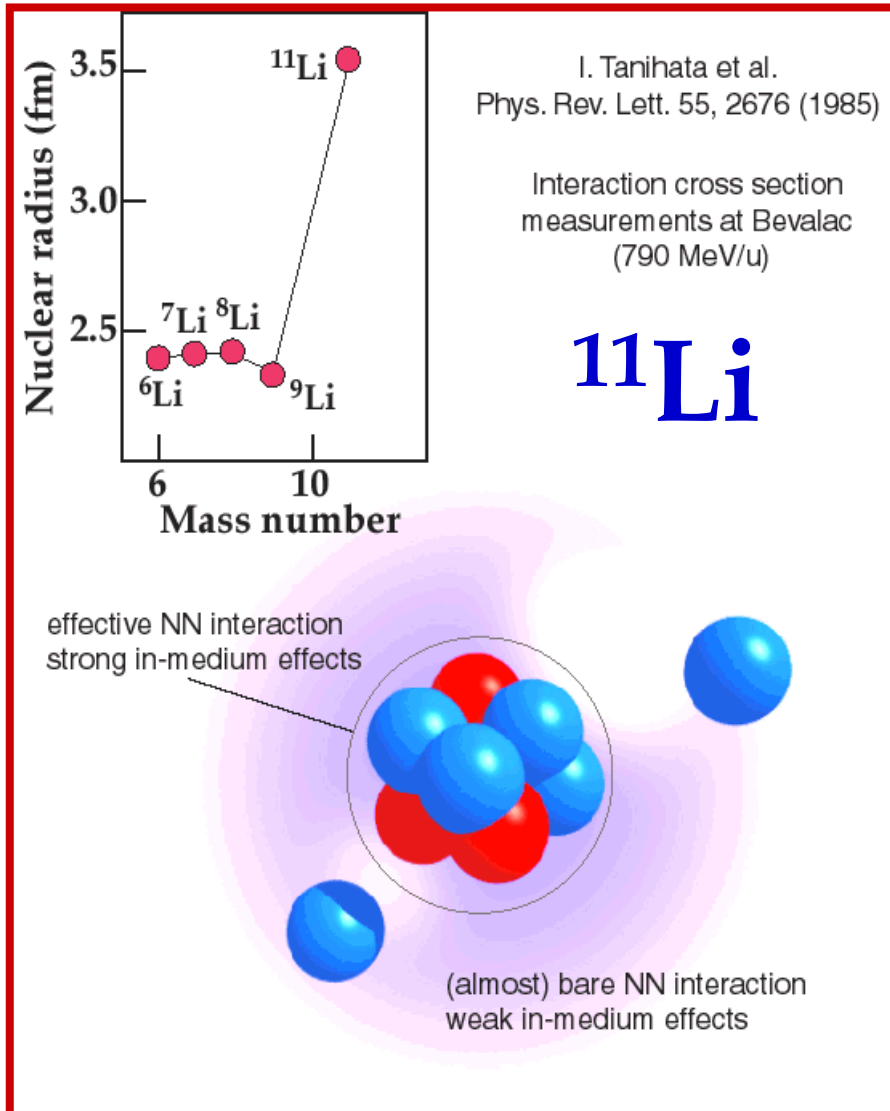


Neutron and Proton Skins





Neutron halo's



Mean field theory of halo's: (RHB in the continuum)

advantages:

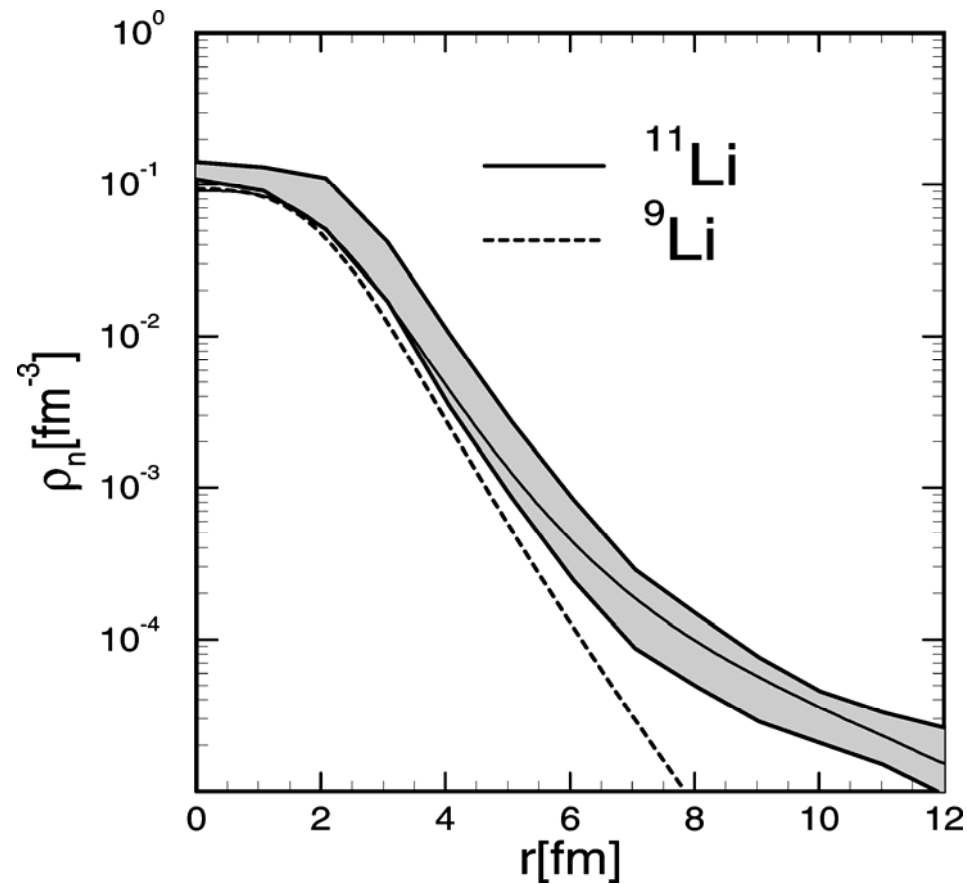
- * residual interaction by pairing
- * self-consistent description
- * universal parameters
- * polarization of the core
- * treatment of the continuum

problems:

- * center of mass motion
- * boundary conditions at infinity

Densities in Li-isotopes

J. Meng and P. Ring , PRL 77, 3963 (1996)
J. Meng and P. Ring , PRL 80, 460 (1998)



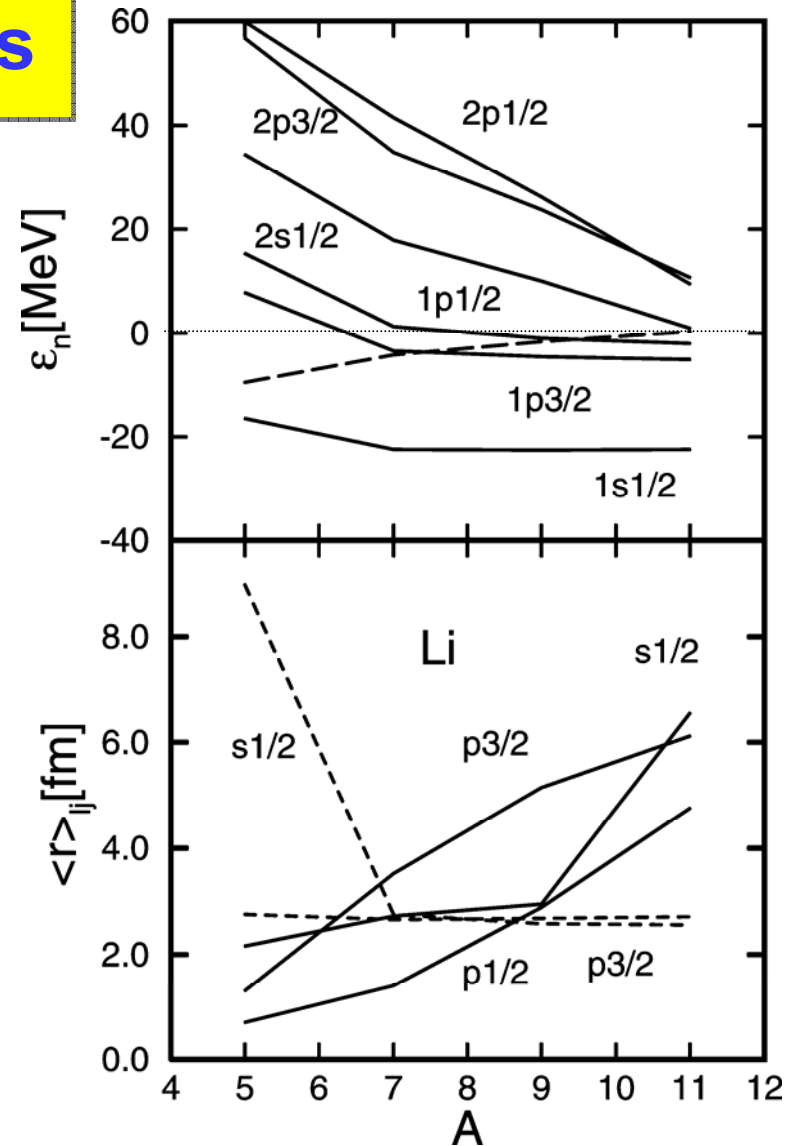
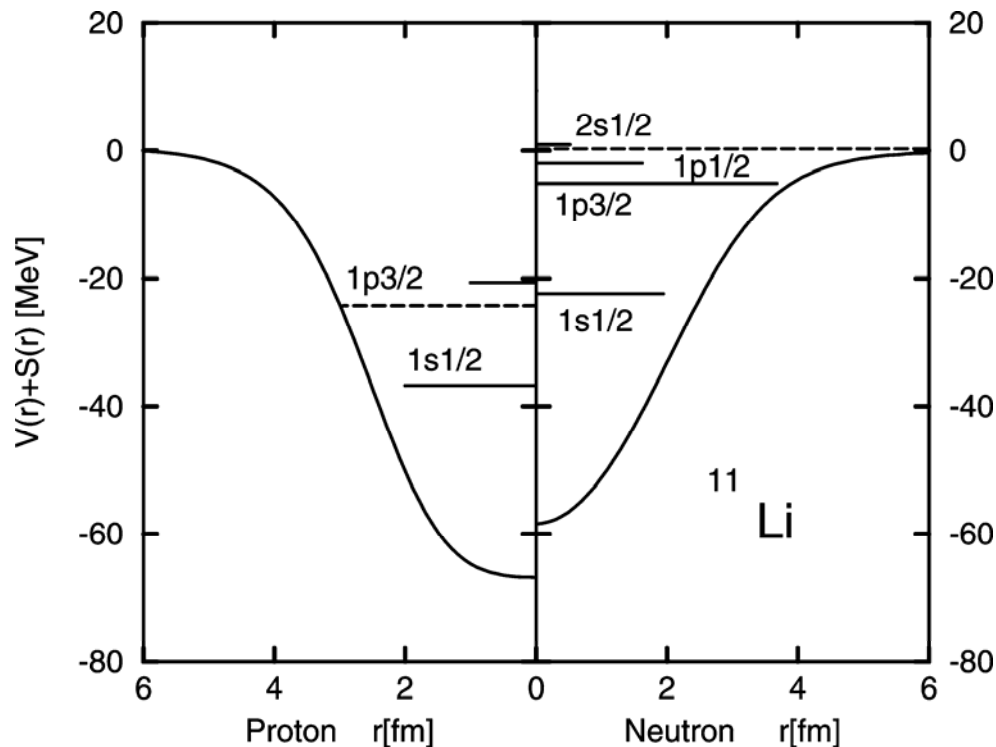
rel. Hartree-Bogoliubov
in the continuum
density dependent δ -pairing

canonical basis in Li-isotopes

- * eigenstates of the density matrix
- * wavefunction has BCS-type

$$|\Phi\rangle = \prod_n (u_n + v_n a_n^+ a_n^+) |-\rangle$$

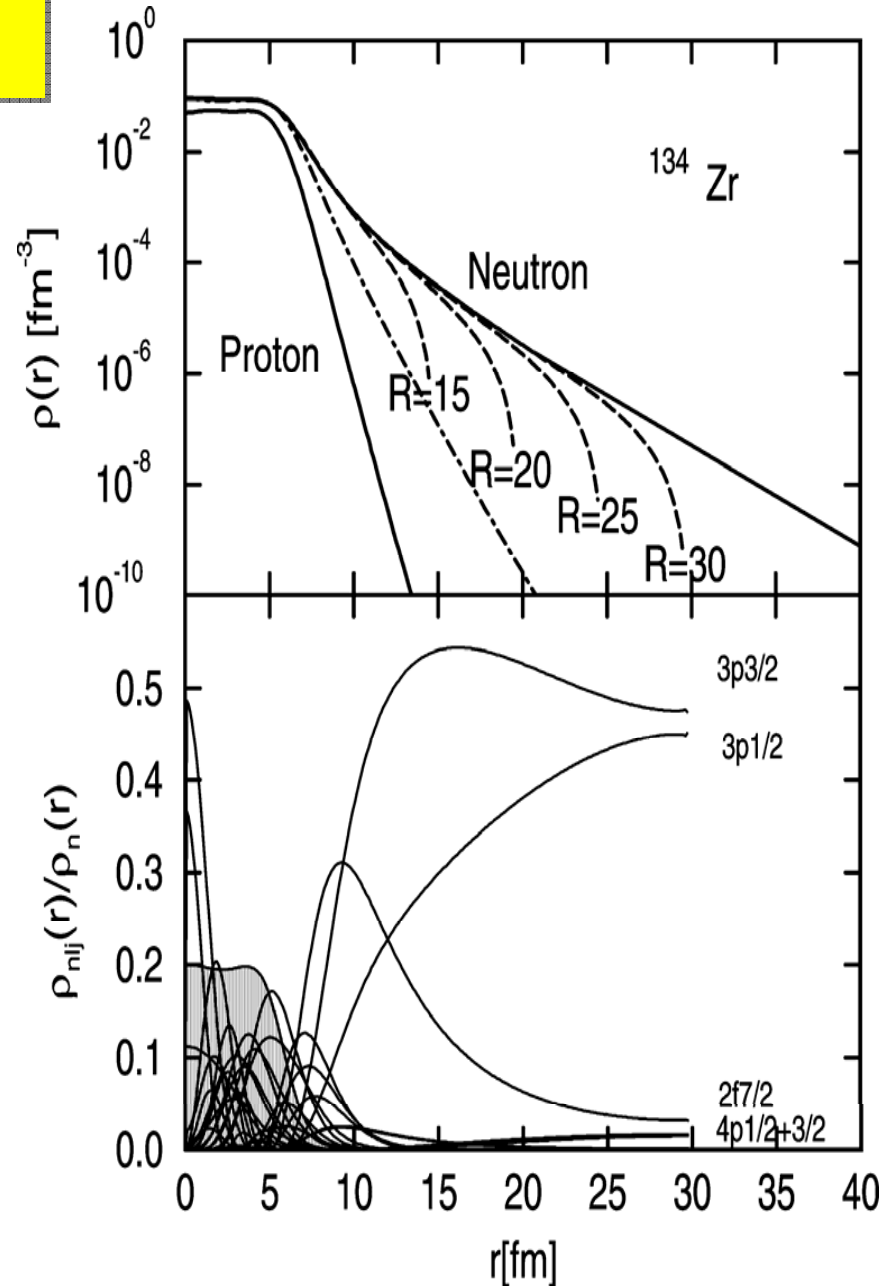
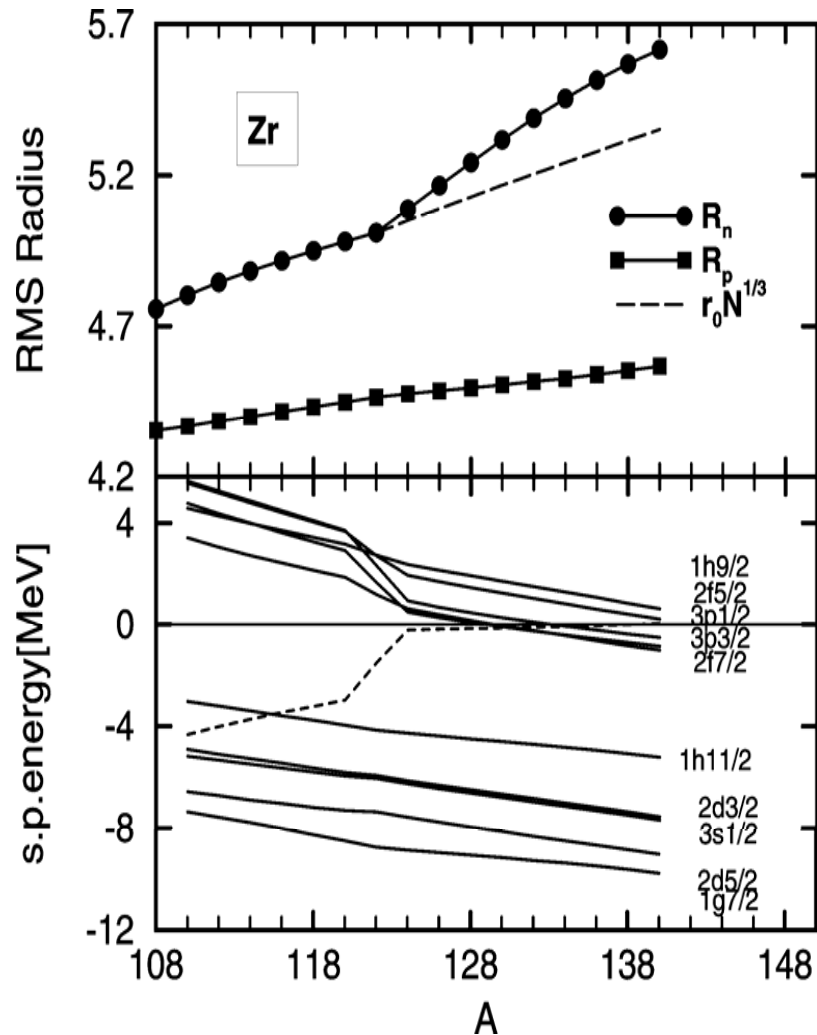
$$\varepsilon_n = \langle n|h|n\rangle, \quad \Delta_n = \langle n|\Delta|n\rangle$$

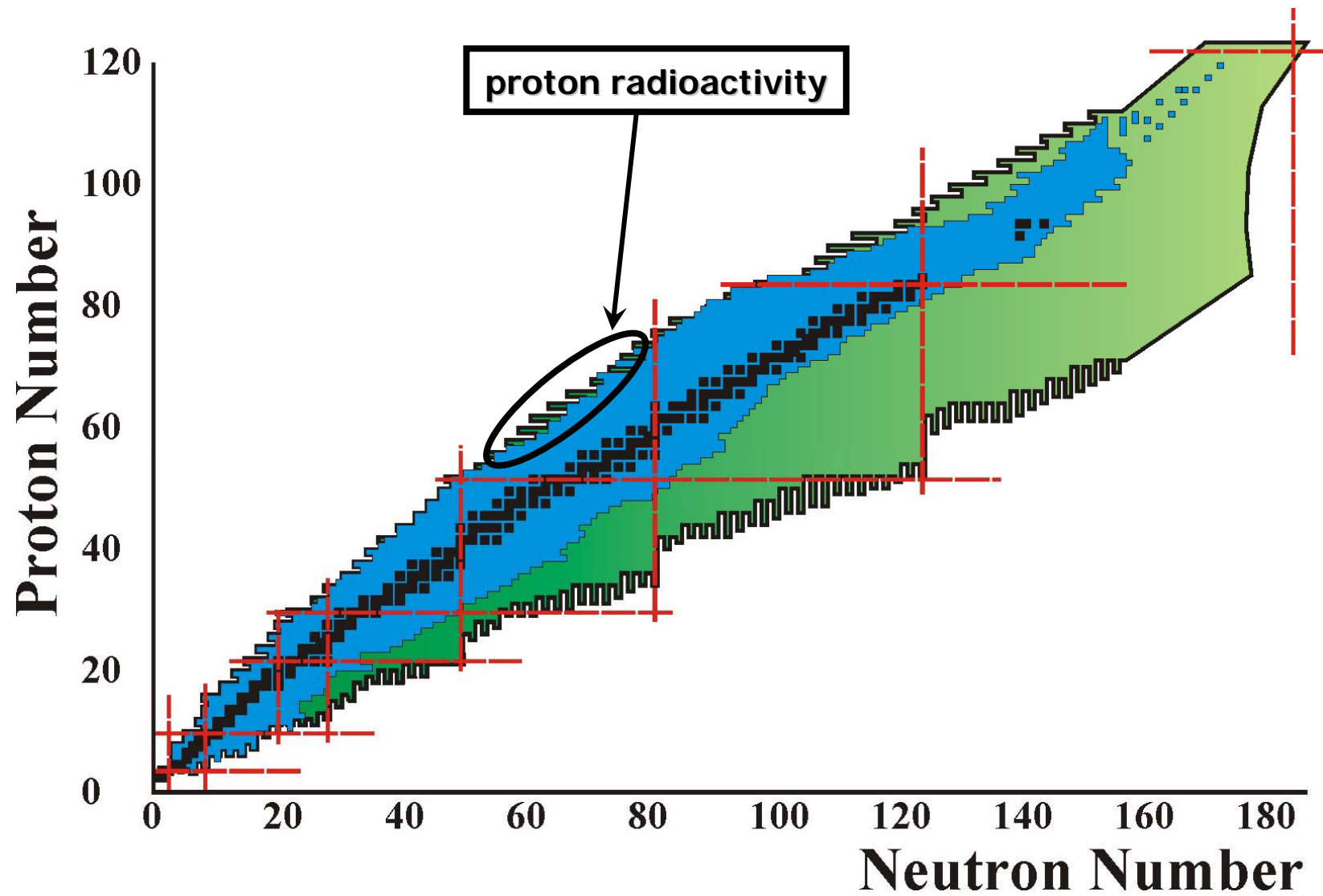


J. Meng and P. Ring, PRL 77, 3963 (1996)

Giant halo in the Zr region:

J. Meng and P. Ring, PRL 80, 460 (1998)

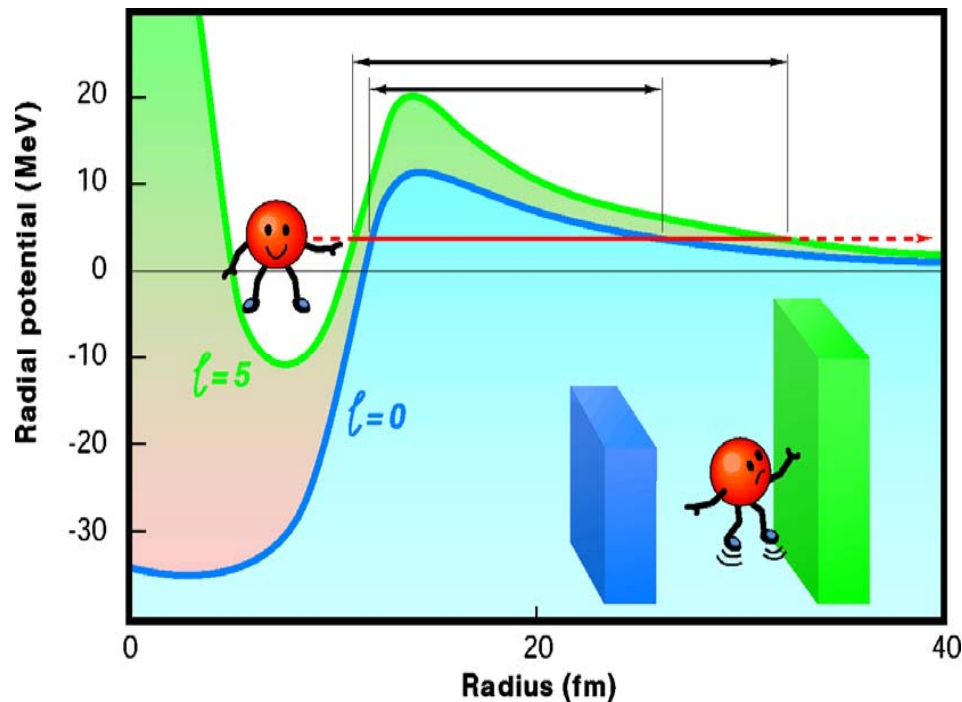




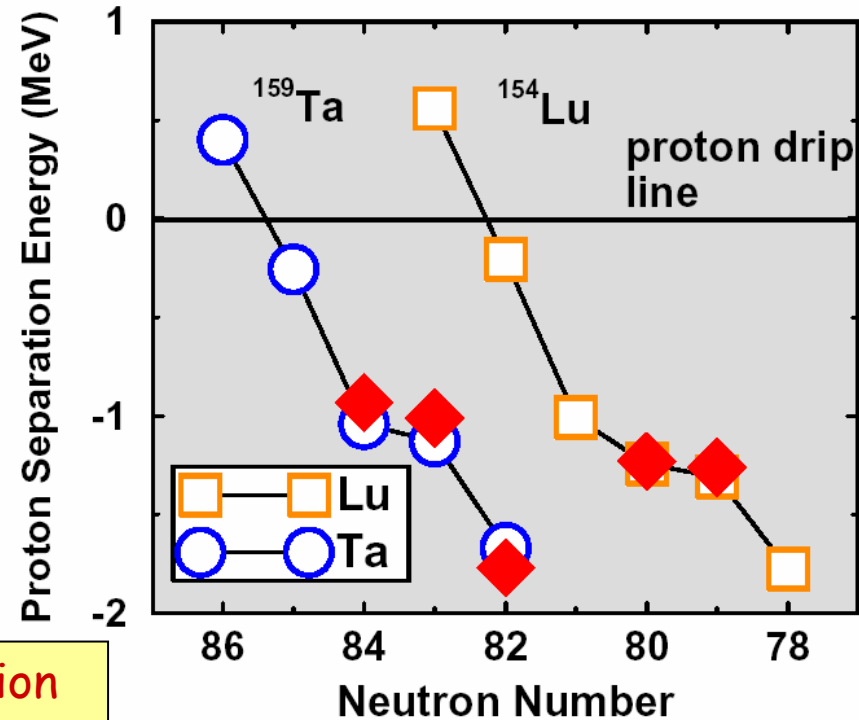
Nuclei at the proton drip line:

Vretenar, Lalazissis, Ring, Phys.Rev.Lett. 82, 4595 (1999)

characterized by exotic ground-state decay modes such as the direct emission of charged particles and β -decays with large Q-values.



Ground-state proton emitters

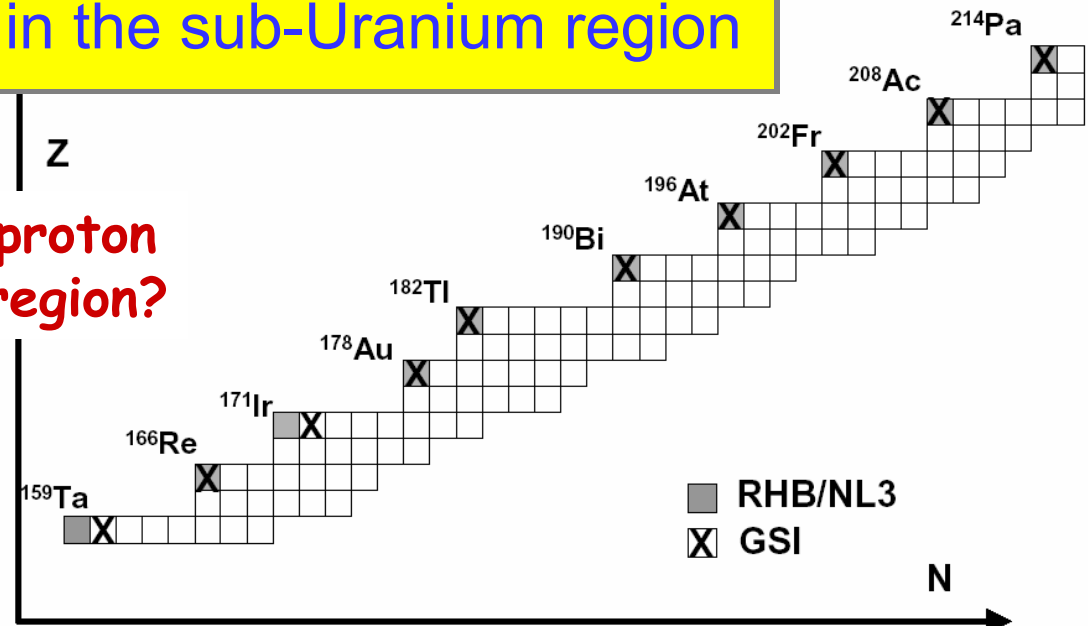


Self-consistent RHB calculations \rightarrow separation energies, quadrupole deformations, odd-proton orbitals, spectroscopic factors

Lalazissis, Vretenar, Ring
Phys.Rev. C60, 051302 (1999)

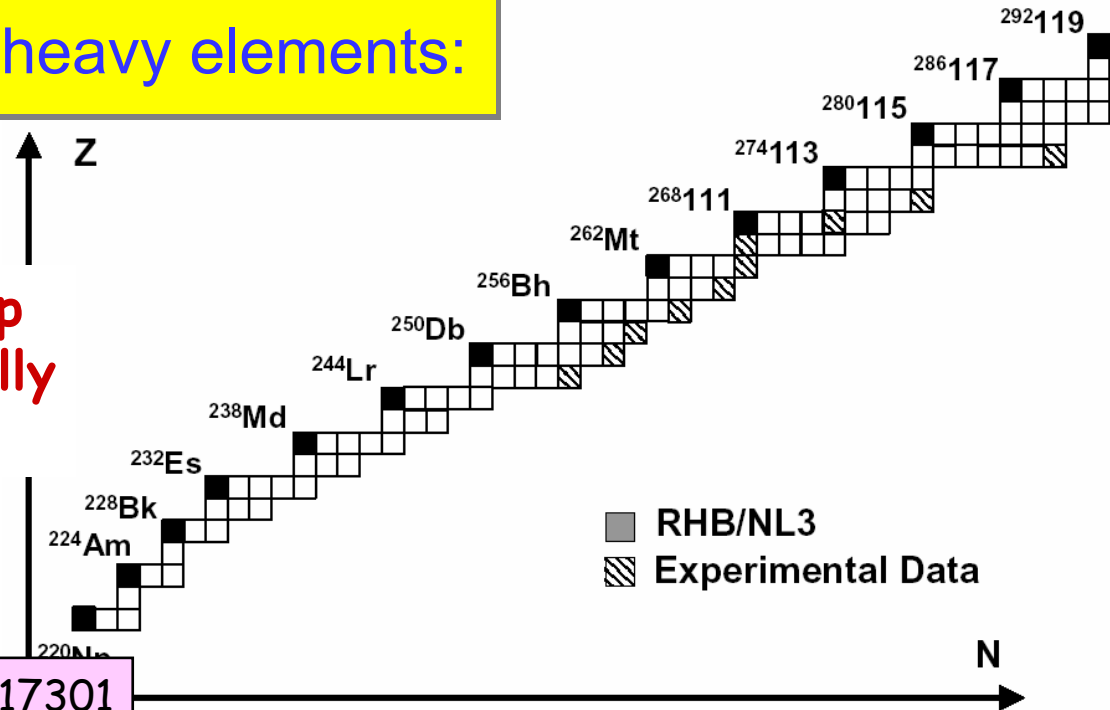
Proton drip-line in the sub-Uranium region

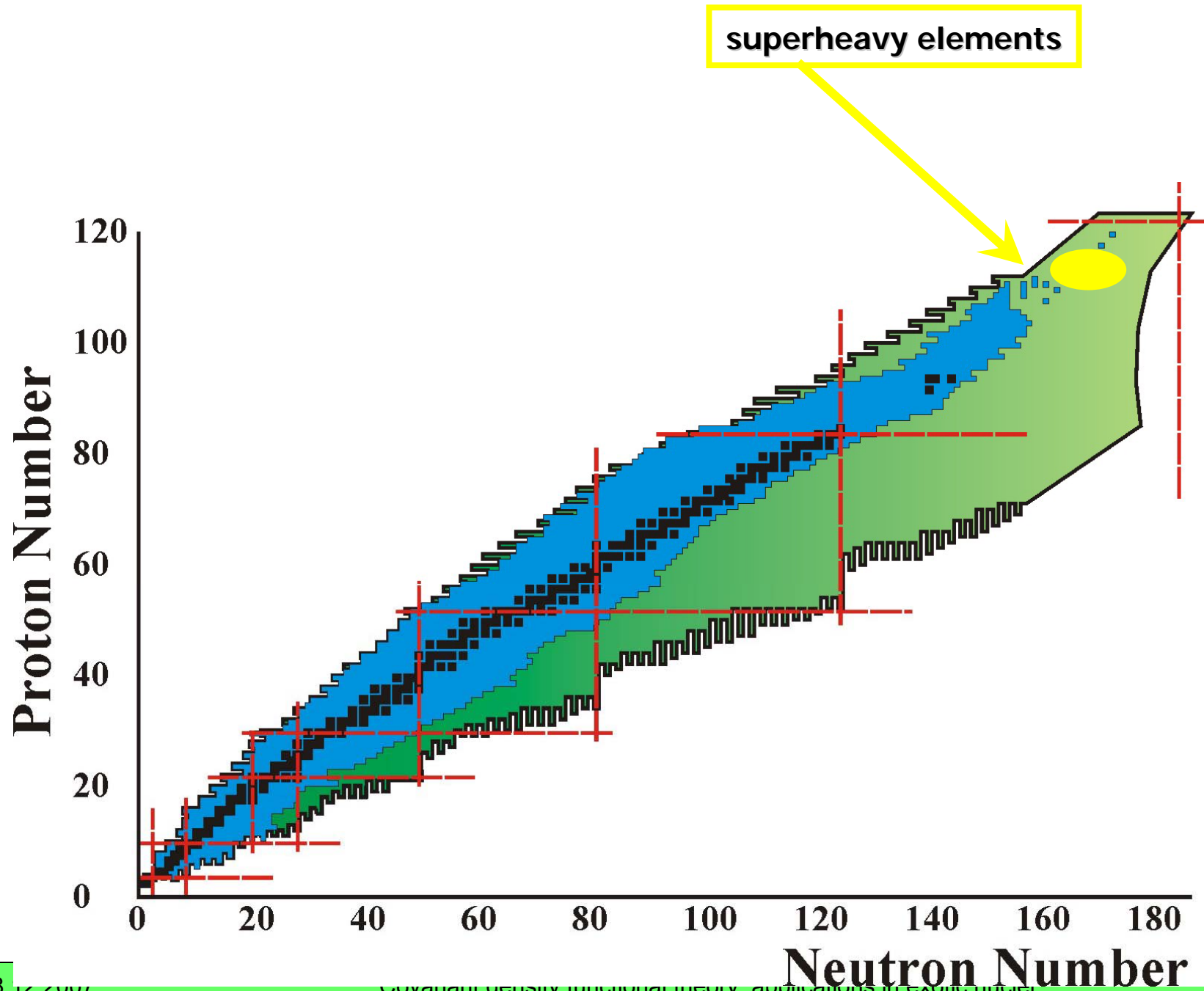
Possible ground-state proton emitters in this mass region?



Proton drip-line for super-heavy elements:

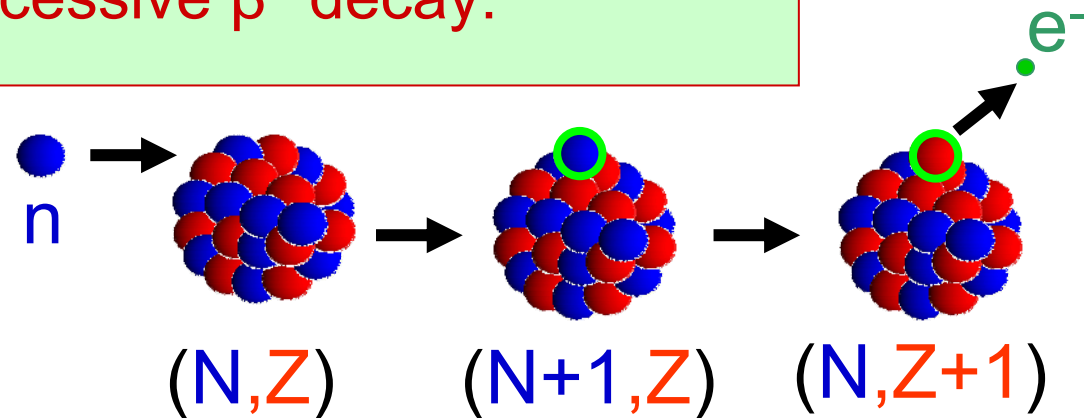
How far is the proton-drip line from the experimentally known superheavy nuclei?



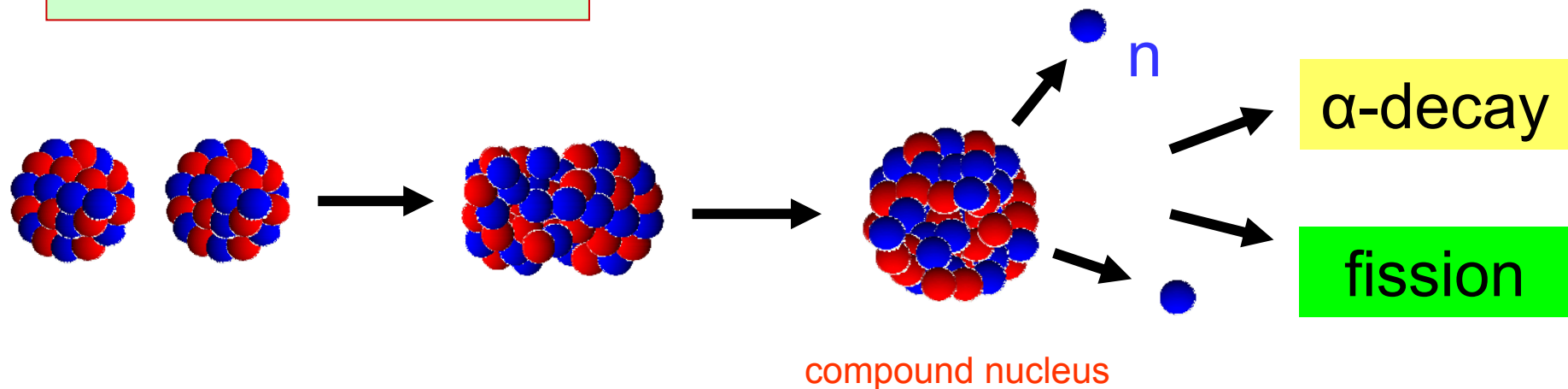


Synthesis of super-heavy elements

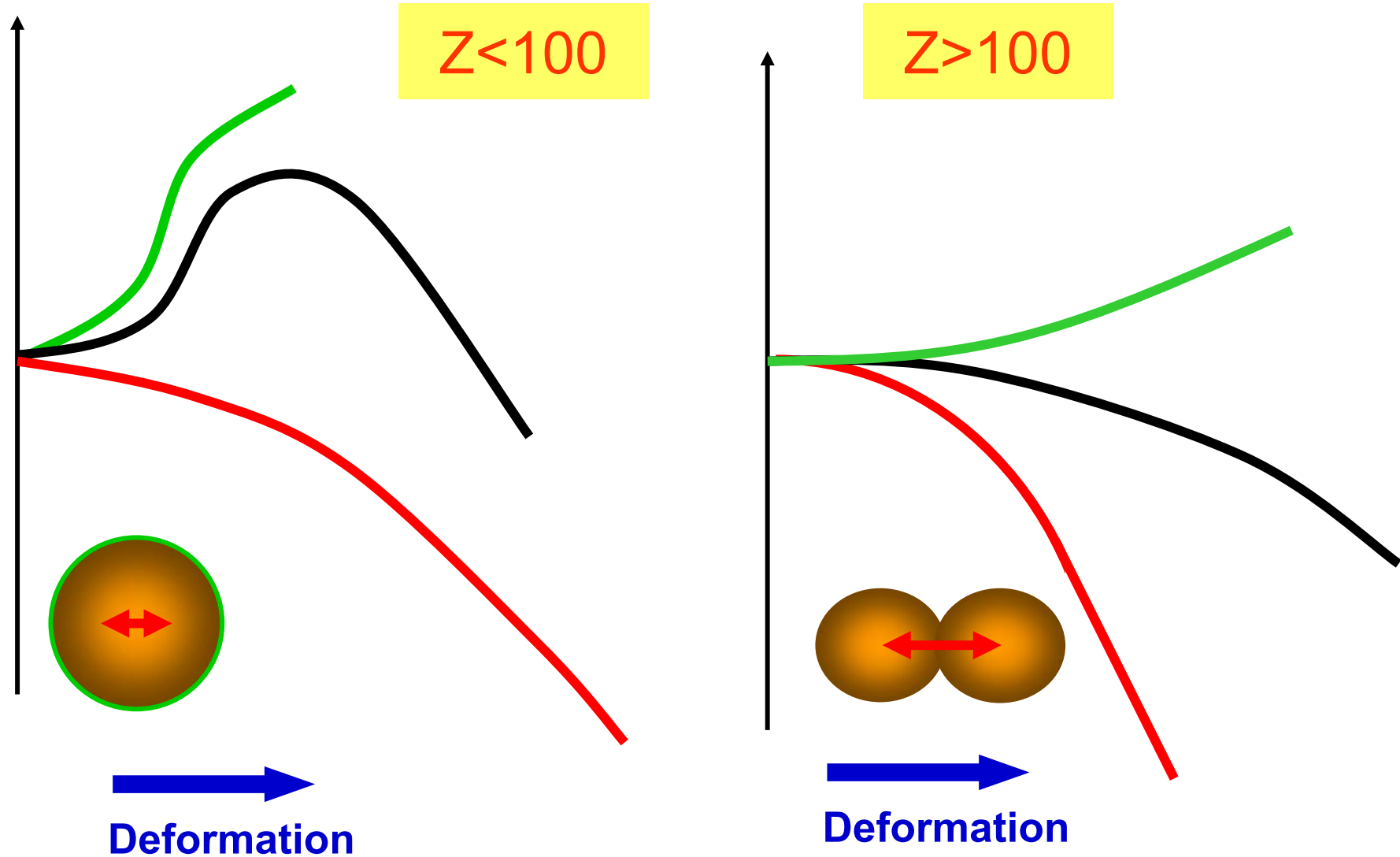
neutron capture and successive β^- -decay:



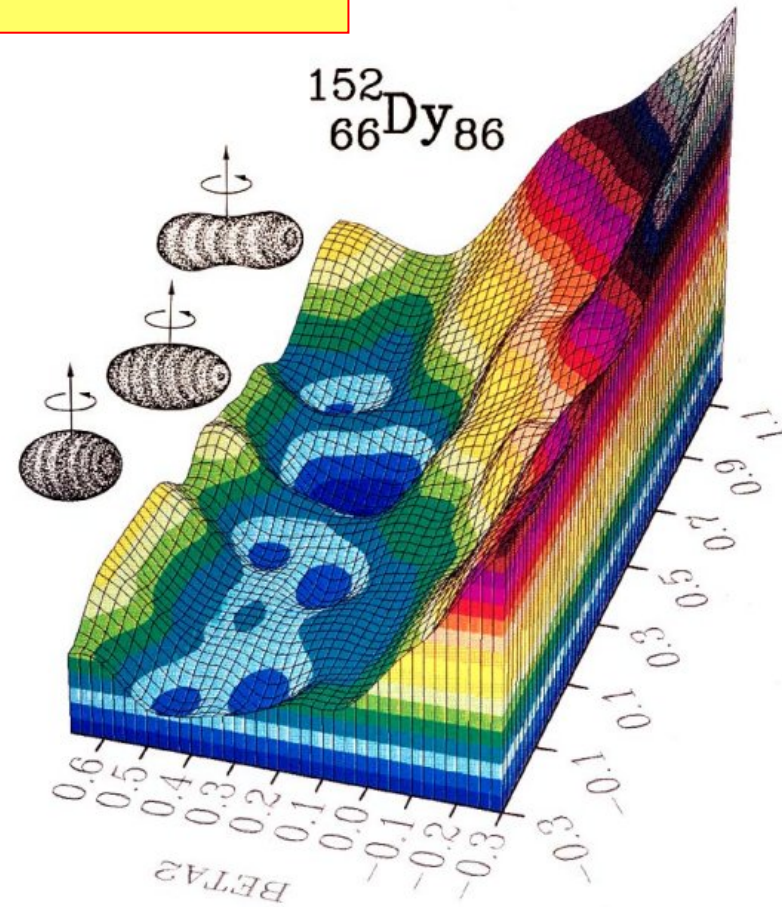
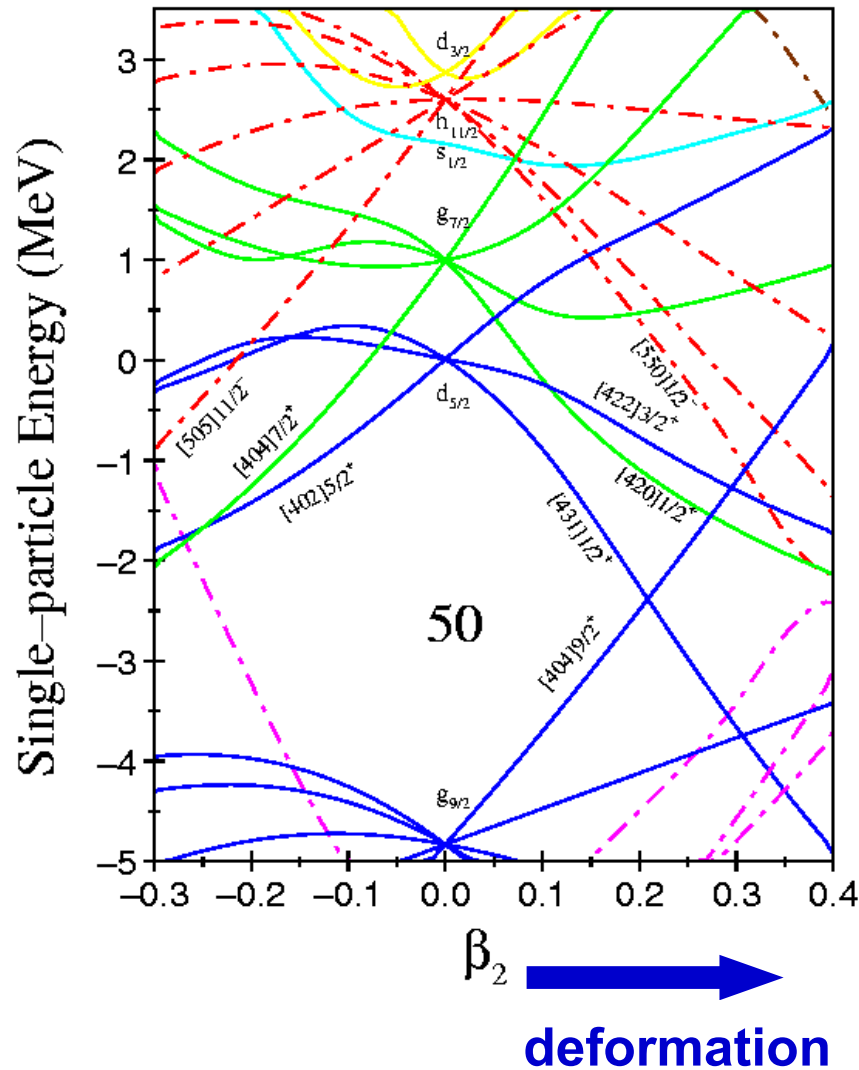
fusion of two nuclei:



Classical nuclear droplet

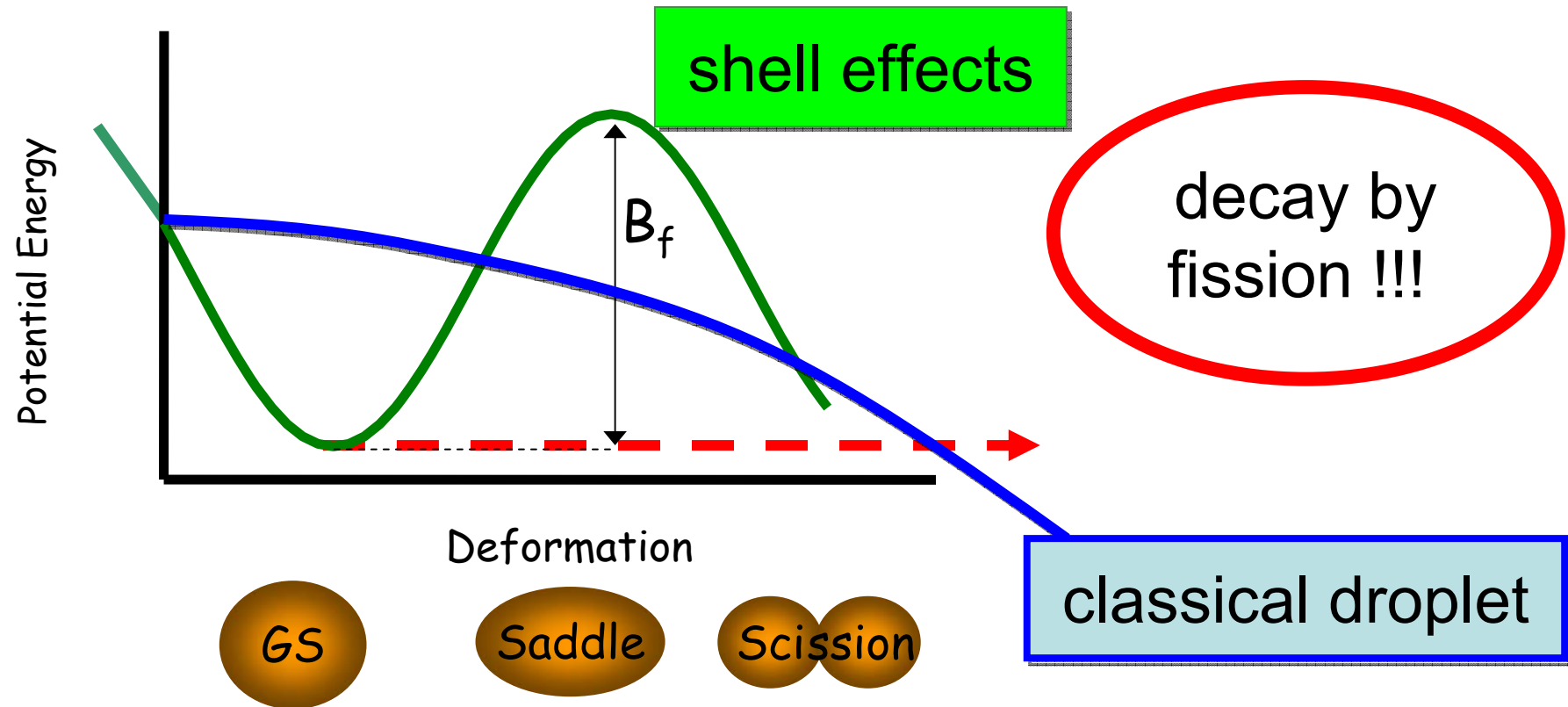


Quantum mechanical shell effects



Shell effects lead to enhanced stability at specific proton and neutron numbers (**magic numbers**)

Quantenmechanical shell effects

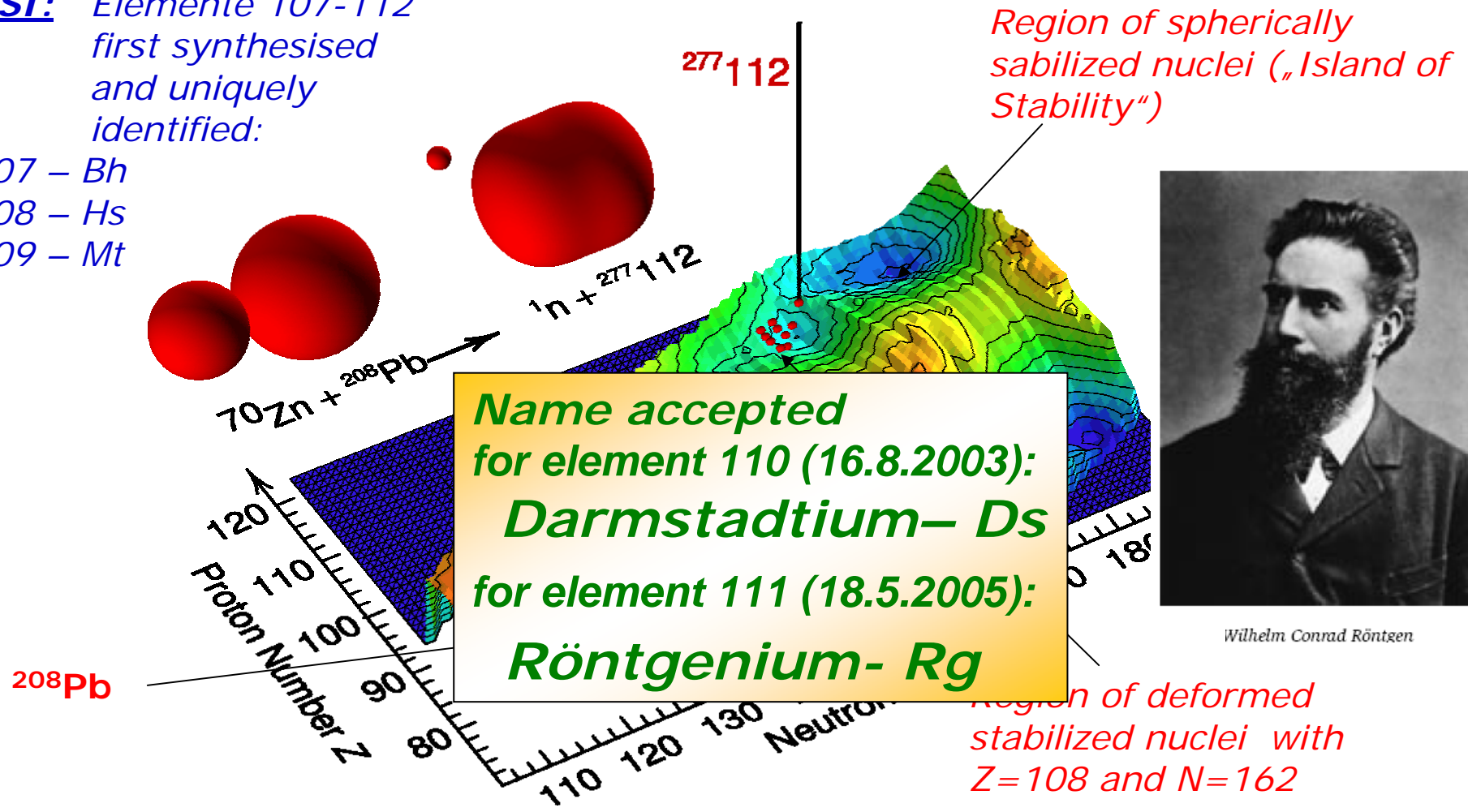


Elements with $Z > 100$ are stabilized by shell effects

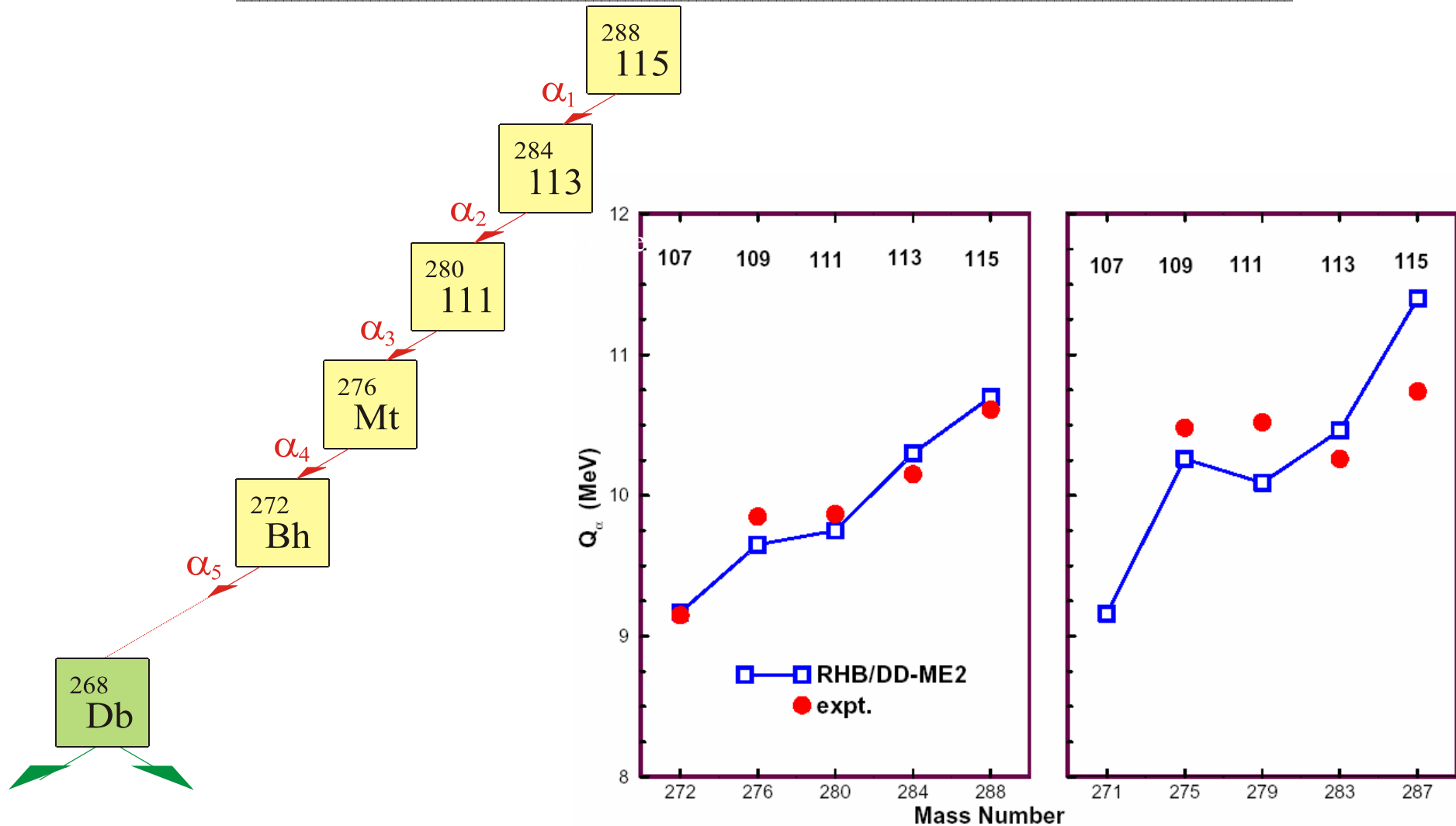
Shell correction E_{shell} in the region of superheavy elements
P. Möller et al.

GSI: Elemente 107-112 first synthesised and uniquely identified:

- 107 – Bh
- 108 – Hs
- 109 – Mt



Superheavy Elements: Q_α -values




● Exp: Yu.Ts.Oganessian *et al*, PRC 69, 021601(R) (2004)

Content

- Covariant density functional theory
- Ground state properties
- Nuclear dynamics and excitations
- Methods beyond mean field
- Conclusions

Time dependent mean field theory:

$$\int dt \{ \langle \Phi(t) | i\partial_t | \Phi(t) \rangle - E[\hat{\rho}(t)] \} = 0$$



$$i\partial_t \hat{\rho} = [\hat{h}(\hat{\rho}) + \hat{f}, \hat{\rho}]$$

$$i\partial_t \psi_i(t) = \left(\vec{\alpha} \left(\frac{1}{i} \vec{\nabla} - \vec{V} \right) + V + \beta(m - S) \right) \psi_i(t)$$

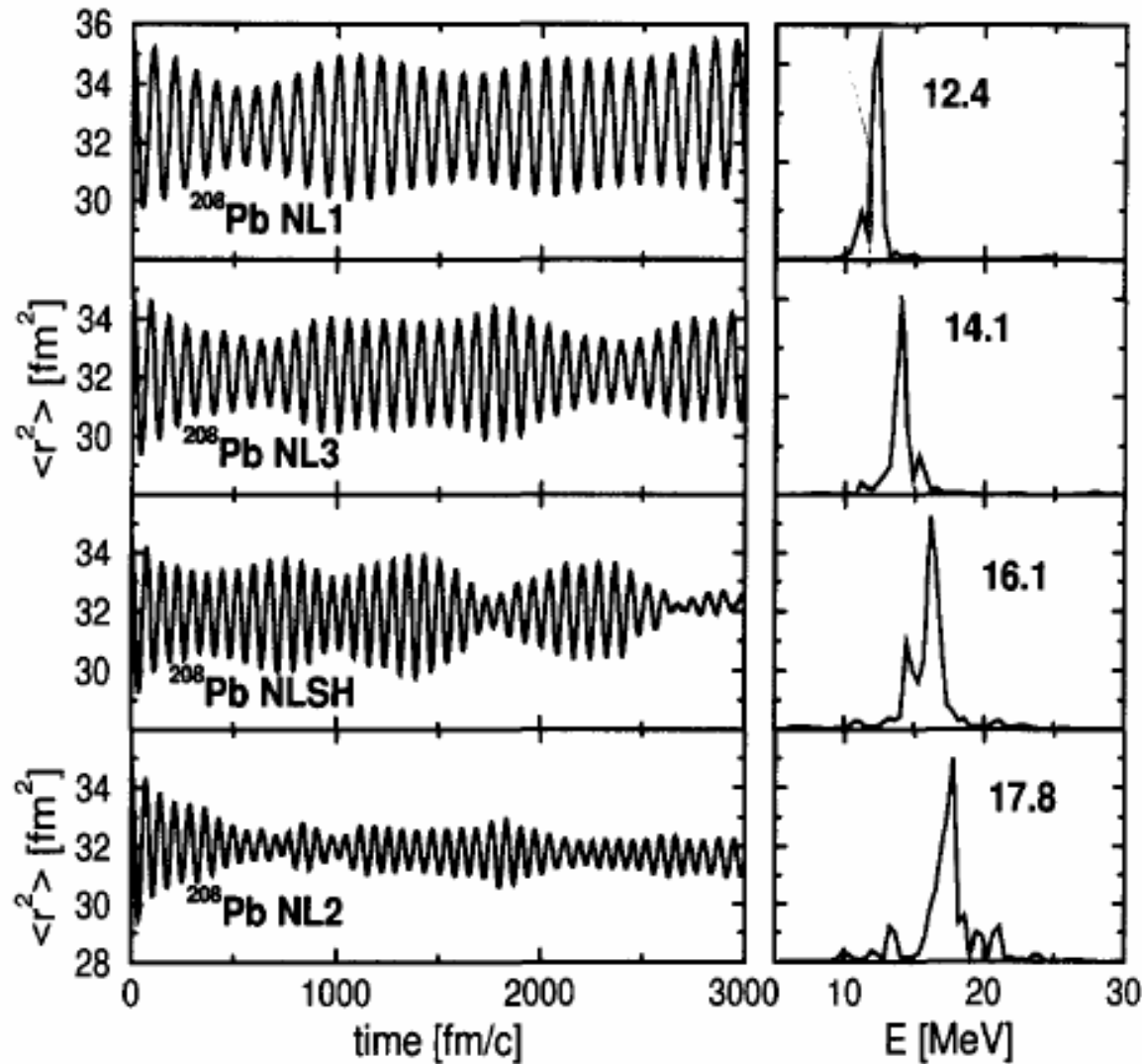
No-sea approxim. !

$$\begin{aligned} [-\Delta + m_\sigma^2] \sigma(t) &= -g_\sigma \rho_s(t) & \rho_s &= \sum_{i=1}^A \bar{\psi}_i \psi_i \\ [-\Delta + m_\omega^2] \omega_0(t) &= g_\omega \rho_B(t) & \rho_B &= \sum_{i=1}^A \psi_i^\dagger \psi_i \\ [-\Delta + m_\omega^2] \vec{\omega}(t) &= g_\omega \vec{j}_B(t) & \vec{j}_B &= \sum_{i=1}^A \bar{\psi}_i \vec{\alpha} \psi_i \end{aligned}$$

and similar equations for the ρ - and A -field

$$\langle \Phi(t) | r^2 | \Phi(t) \rangle$$

Breathing mode: ^{208}Pb



$$K_\infty = 211$$

$$K_\infty = 271$$

$$K_\infty = 355$$

Interaction:

$$\hat{V} = \frac{\delta^2 E}{\delta \hat{\rho} \delta \hat{\rho}}$$

Order and Chaos

GMR: $T=0$

GMR: $T=1$

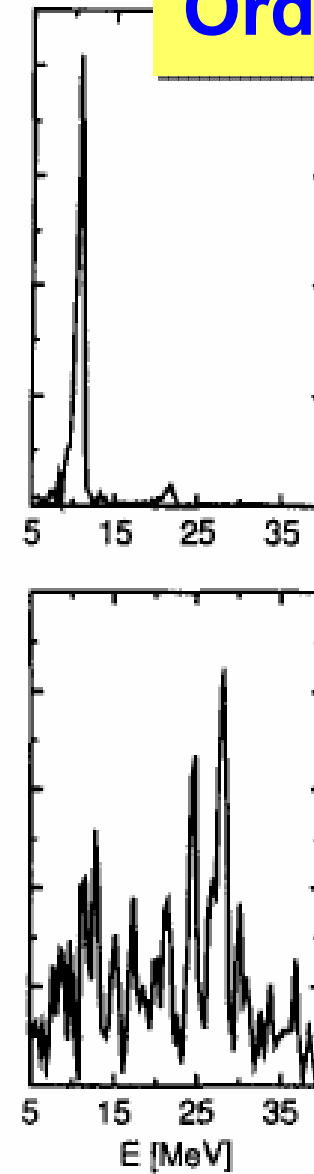
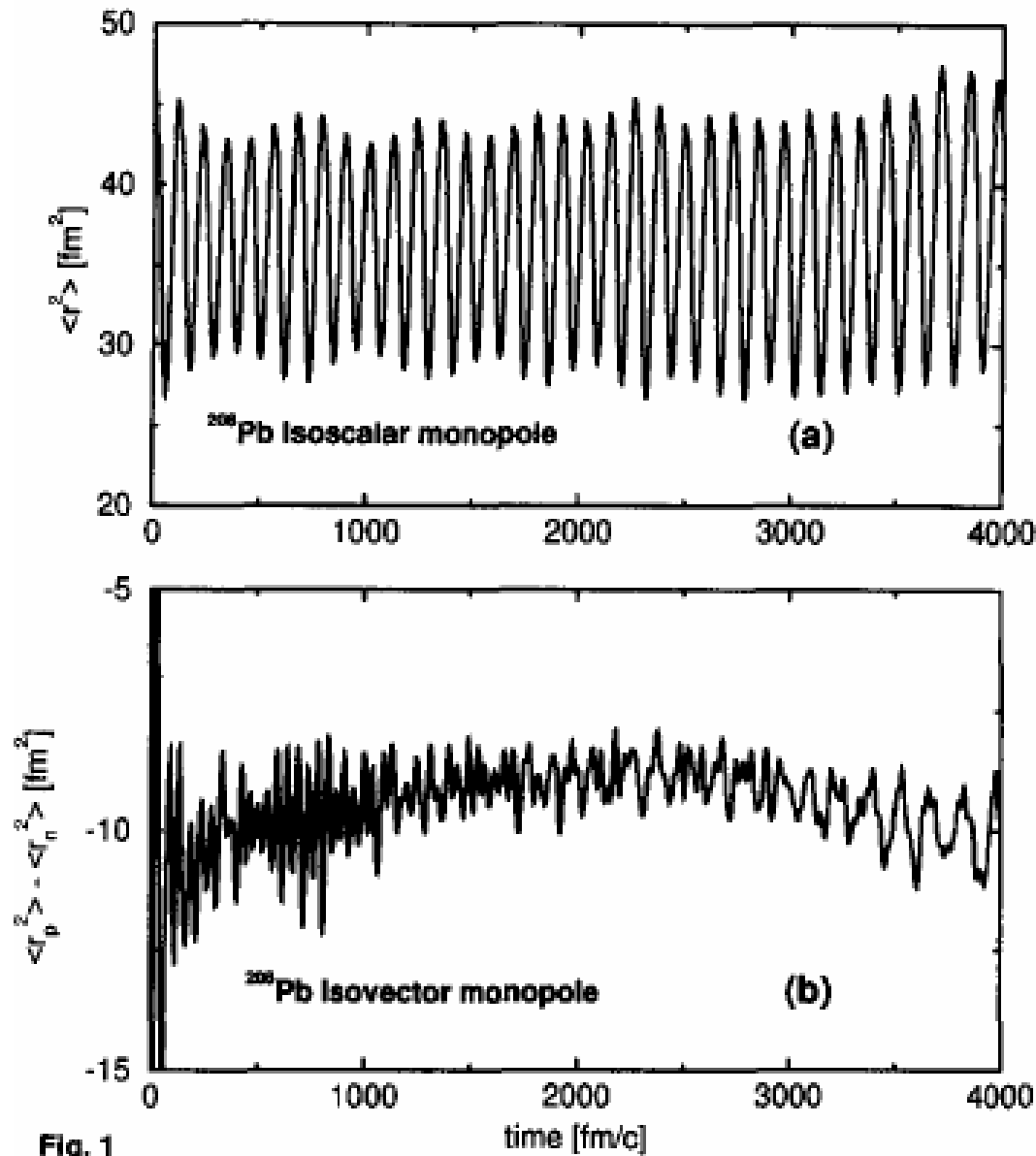


Fig. 1

D. Vretenar et al., PRE 56(1997) 6418

Relativistic RPA for excited states

Small amplitude limit:

$$\hat{\rho}(t) = \hat{\rho}^{(0)} + \delta\hat{\rho}(t)$$

ground-state density

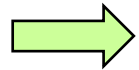
$$\begin{pmatrix} A & B \\ -B^* & -A^* \end{pmatrix} \begin{pmatrix} X \\ Y \end{pmatrix} = \hbar\omega \begin{pmatrix} X \\ Y \end{pmatrix}$$

$\delta\rho_{ph}, \delta\rho_{\alpha h}$

$\delta\rho_{hp}, \delta\rho_{h\alpha}$

RRPA matrices:

$$A_{minj} = (\epsilon_n - \epsilon_i)\delta_{mn}\delta_{ij} + \frac{\partial h_{mi}}{\partial \rho_{nj}}, \quad B_{minj} = \frac{\partial h_{mi}}{\partial \rho_{jn}}$$

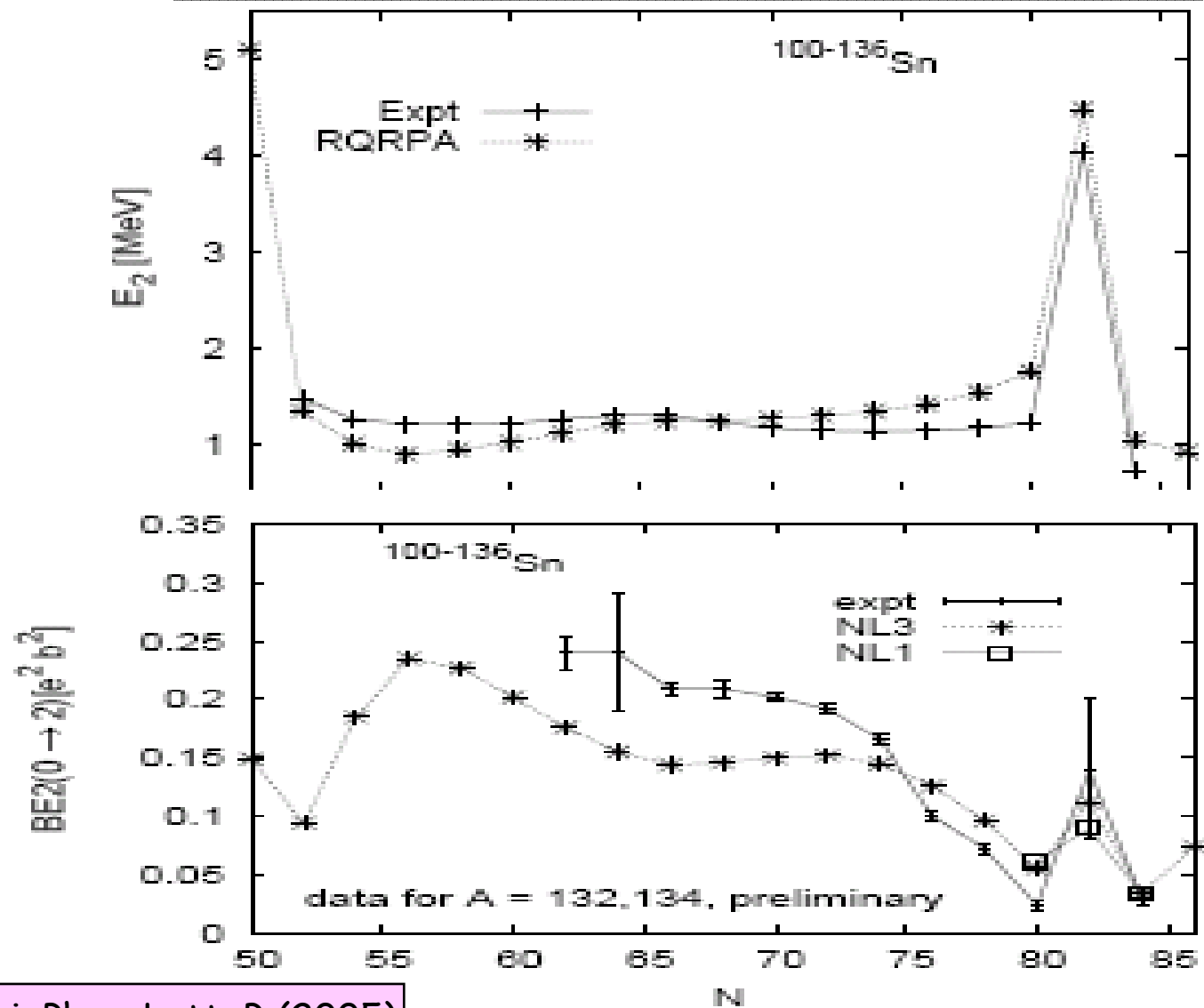


the same effective interaction determines the Dirac-Hartree single-particle spectrum and the residual interaction

Interaction:

$$\hat{V} = \frac{\delta^2 E}{\delta \hat{\rho} \delta \hat{\rho}}$$

2⁺-excitation in Sn-isotopes:

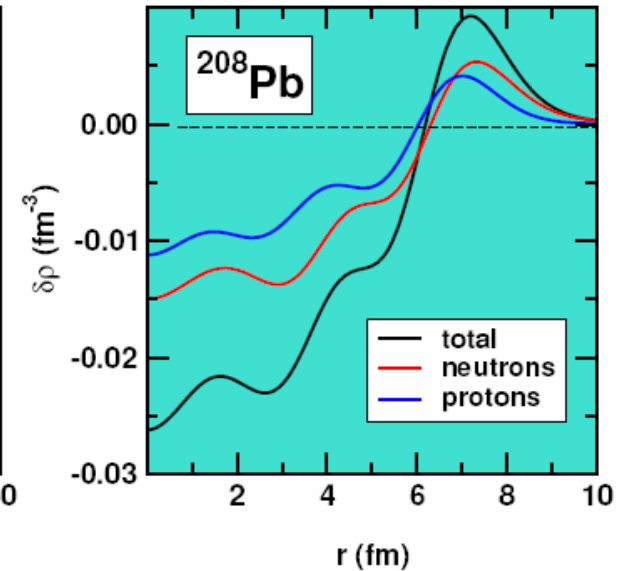
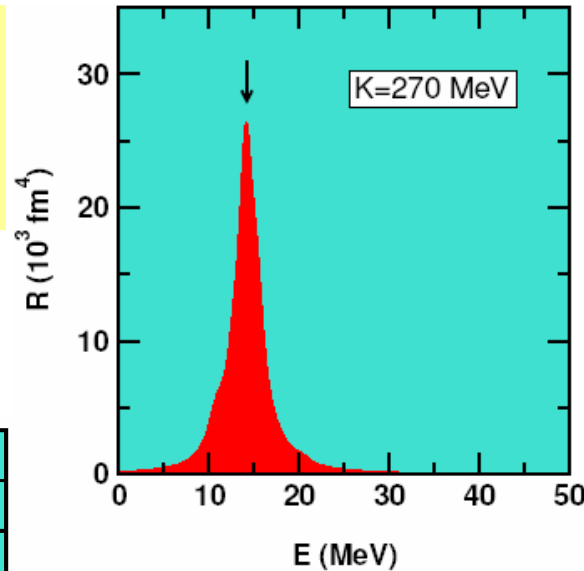
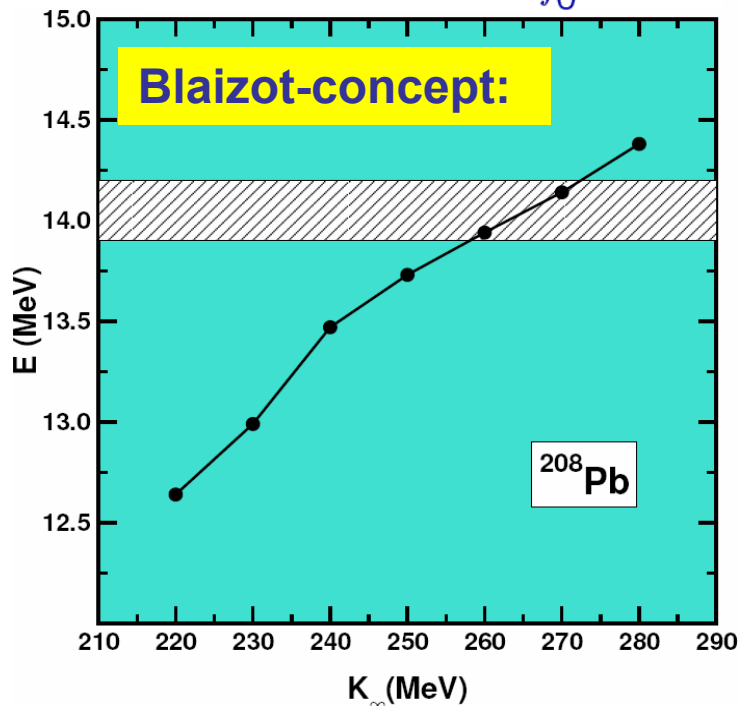


A. Ansari, Phys. Lett. B (2005)

Isoscalar Giant Monopole: IS-GMR

The ISGMR represents the essential source of experimental information on the nuclear incompressibility

$$K_0 = p_f^2 \left. \frac{d^2 E/A}{dp_f^2} \right|_{p_{f0}}$$



constraining the nuclear matter compressibility

$$\rho(t) = \rho_0 + \delta\rho(t)$$

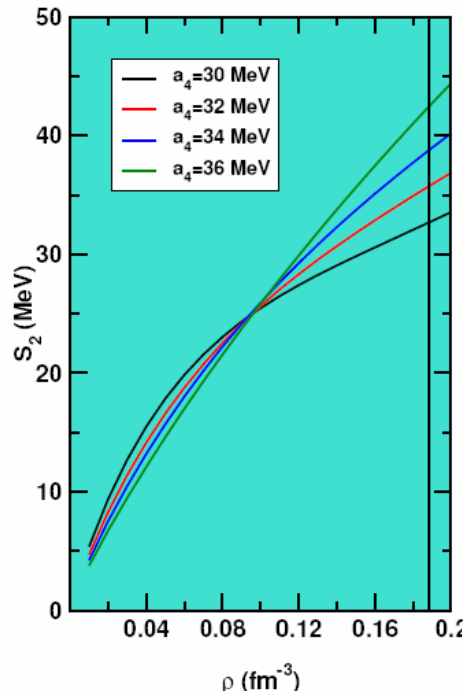
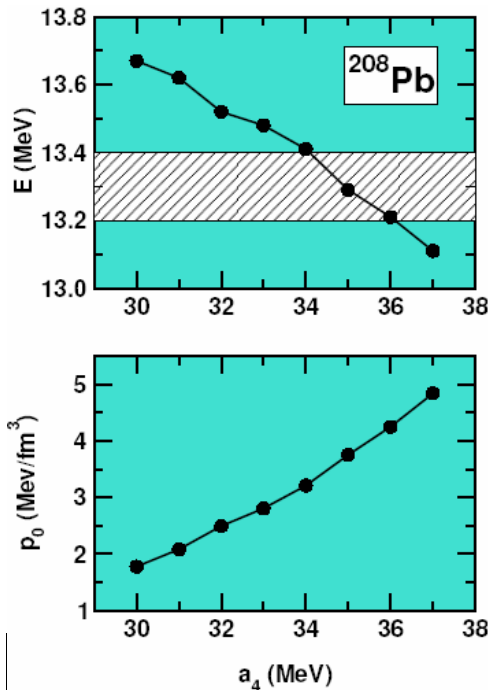
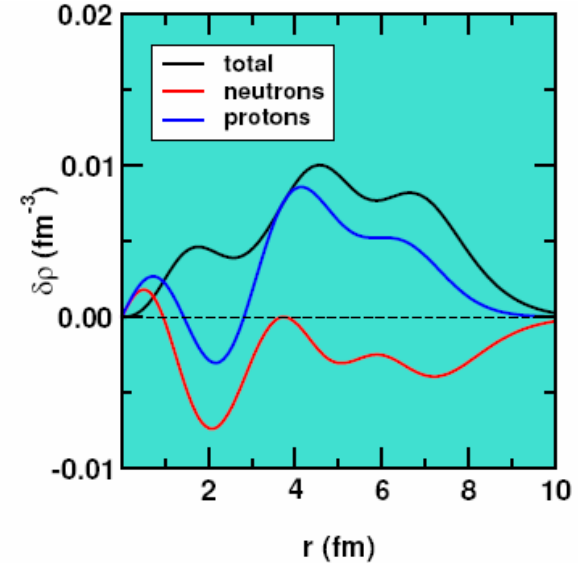
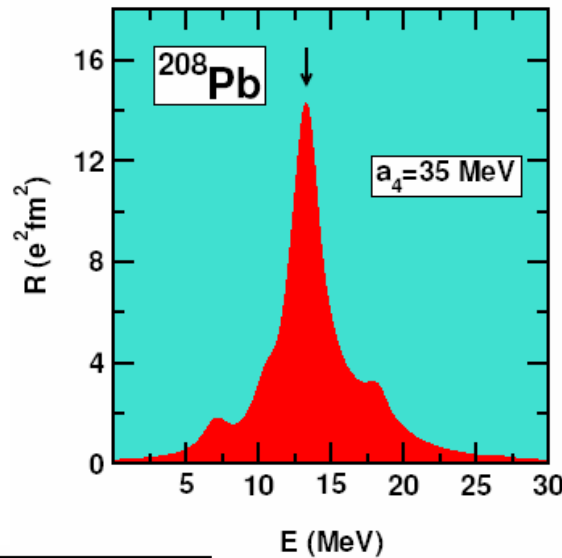
RMF models reproduce the experimental data only if

$$250 \text{ MeV} \leq K_0 \leq 270 \text{ MeV}$$

T. Niksic et al., PRC 66 (2002) 024306

Isovector Giant Dipole: IV-GDR

the IV-GDR represents one of the sources of experimental informations on the nuclear matter symmetry energy



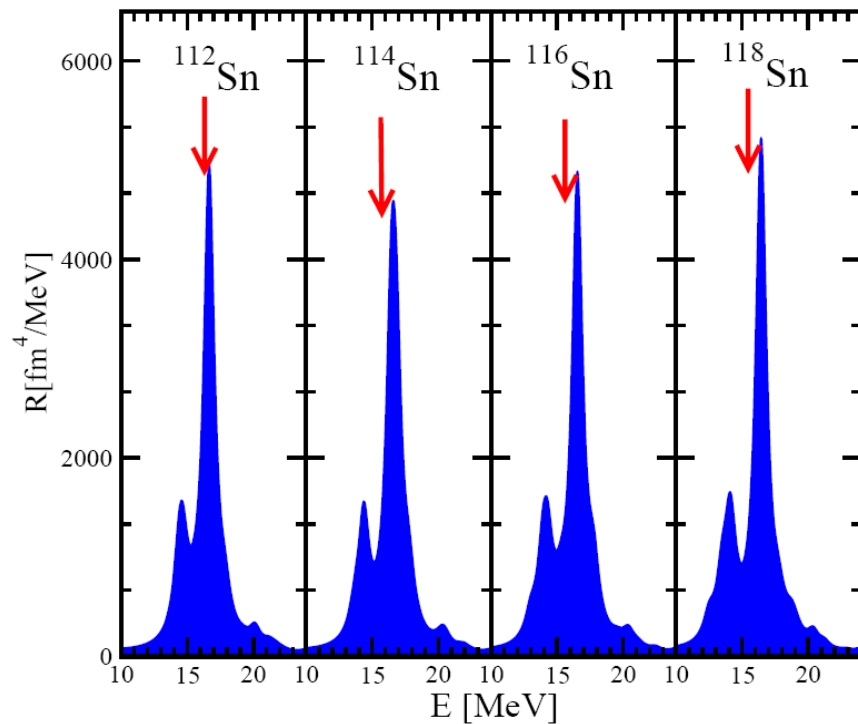
constraining the nuclear matter symmetry energy

the position of IV-GDR is reproduced if

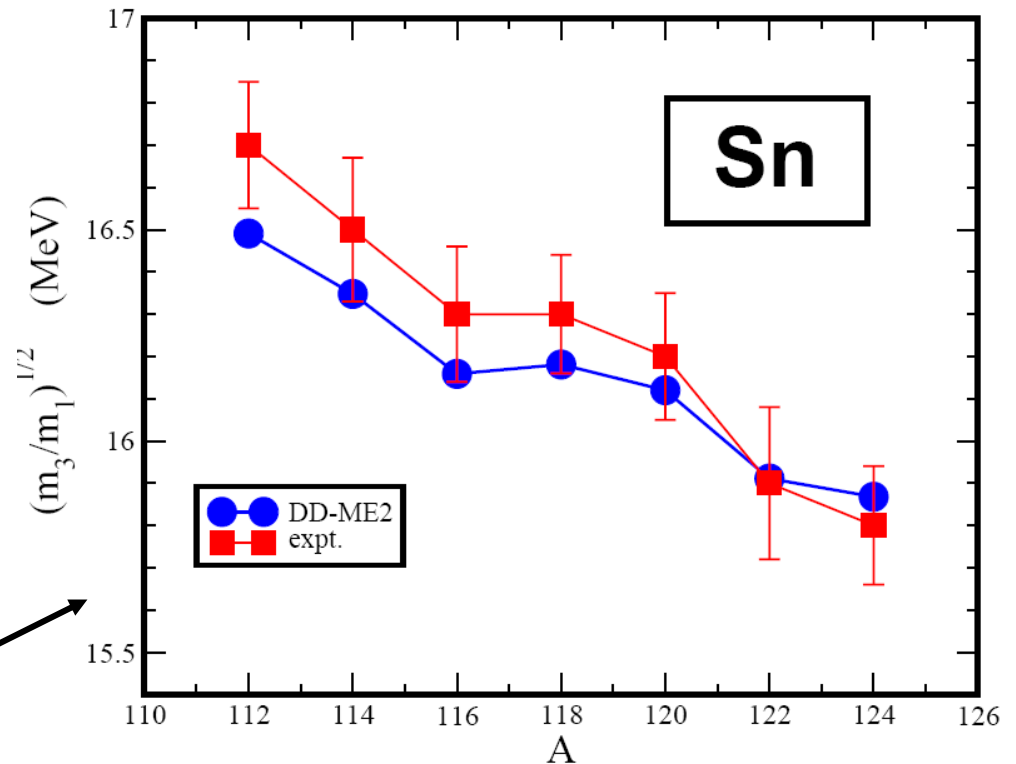
$$32 \text{ MeV} \leq a_4 \leq 36 \text{ MeV}$$

Isoscalar Giant Monopole in Sn-isotopes

Isoscalar GMR in spherical nuclei → nuclear matter compression modulus K_{nm} .

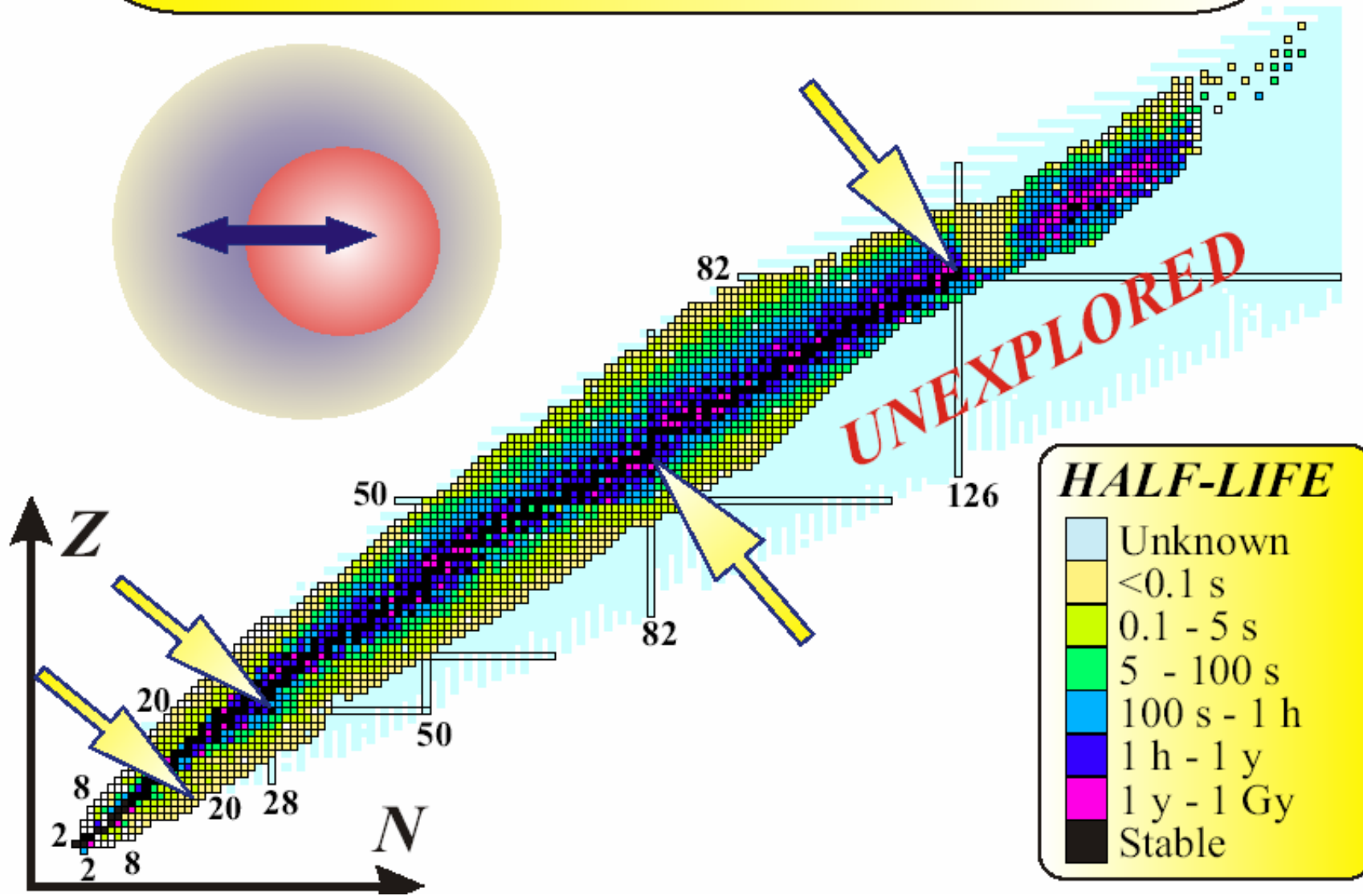


Sn isotopes:
DD-ME2 / Gogny pairing



Theory: Lalazissis et al
Exp: U. Garg, unpublished

Experimental indications of the soft dipole mode



Photoneutron Cross Sections for Unstable Neutron-Rich Oxygen Isotopes

A. Leistenschneider, T. Aumann, K. Boretzky, D. Cortina, J. Cub, U. Datta Pramanik, W. Dostal, Th. W. Elze, H. Emling, H. Geissel, A. Grünschloß, M. Hellstr, R. Holzmann, S. Ilievski, N. Iwasa, M. Kaspar, A. Kleinböhl, J. V. Kratz, R. Kulesa, Y. Leifels, E. Lubkiewicz, G. Münzenberg, P. Reiter, M. Rejmund, C. Scheidenberger, C. Schlegel, H. Simon, J. Stroth, K. Stümmerer, E. Wajda, W. Walus, and S. Wan

Institut für Kernphysik, Johann Wolfgang Goethe-Universität, D-60486 Frankfurt, Germany

Gesellschaft für Schwerionenforschung (GSI), D-64291 Darmstadt, Germany

Institut für Kernchemie, Johannes Gutenberg-Universität, D-55099 Mainz, Germany

Institut für Kernphysik, Technische Universität, D-64289 Darmstadt, Germany

Instytut Fizyki, Uniwersytet Jagelloński, PL-30-059 Kraków, Poland

Sektion Physik, Ludwig-Maximilians-Universität, D-85748 Garching, Germany

(Received 19 December 2000)

The dipole response of stable and unstable neutron-rich oxygen nuclei of masses $A=17$ to $A=22$ has been investigated experimentally utilizing electromagnetic excitation in heavy-ion collisions at beam energies about 600 MeV/nucleon. A kinematically complete measurement of the neutron decay channel in inelastic scattering of the secondary beam projectiles from a Pb target was performed. Differential electromagnetic excitation cross sections $d\sigma/dE$ were derived up to 30 MeV excitation energy. In contrast to stable nuclei, the deduced dipole strength distribution appears to be strongly fragmented and systematically exhibits a considerable fraction of low-lying strength.

DOI: 10.1103/PhysRevLett.86.245601

The study of the response of a nucleus to electromagnetic excitation is a central topic in nuclear physics. The properties of the nuclear dipole response at excitation energies above the particle emission threshold of stable nuclei is dominated by the giant resonance strength. In contrast to stable nuclei, the dipole strength of neutron-rich nuclei is distributed over a wide range of excitation energies. For neutron-rich nuclei, the dipole strength is shifted towards lower excitation energies. The dipole strength depends strongly on the effective dipole resonance. In turn, measurements of the dipole response of exotic nuclei can provide information on the isospin dependence of the nucleon-nucleon interaction [7]. Systematic experimental information on the dipole response of exotic nuclei, however, is scarce. For some light halo nuclei, low-lying dipole strength has been observed in electromagnetic excitation [8–11]. For the one-neutron halo nucleus ^{11}Li [11], the observed dipole strength at low excitation energies was interpreted as a threshold effect, involving the transition of a valence neutron into the continuum. For ^7He and ^6Li , a coherent dipole resonance of neutrons against the core was observed [12]. The appearance of a collective dipole resonance is general and was predicted for heavy nuclei [19,20], located at excitation energies around the dipole resonance (GDR) [19].

5442

0031-9007

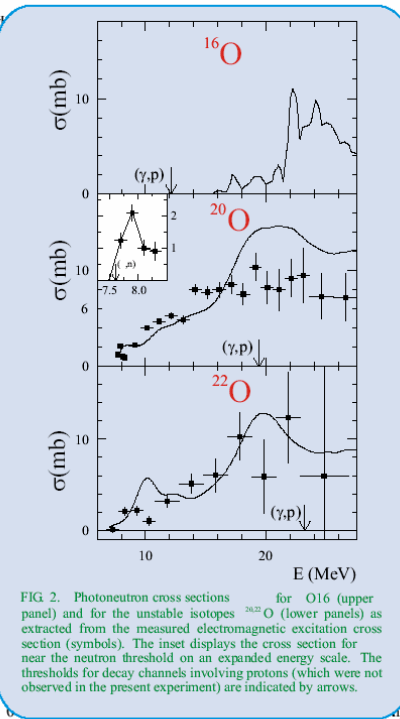
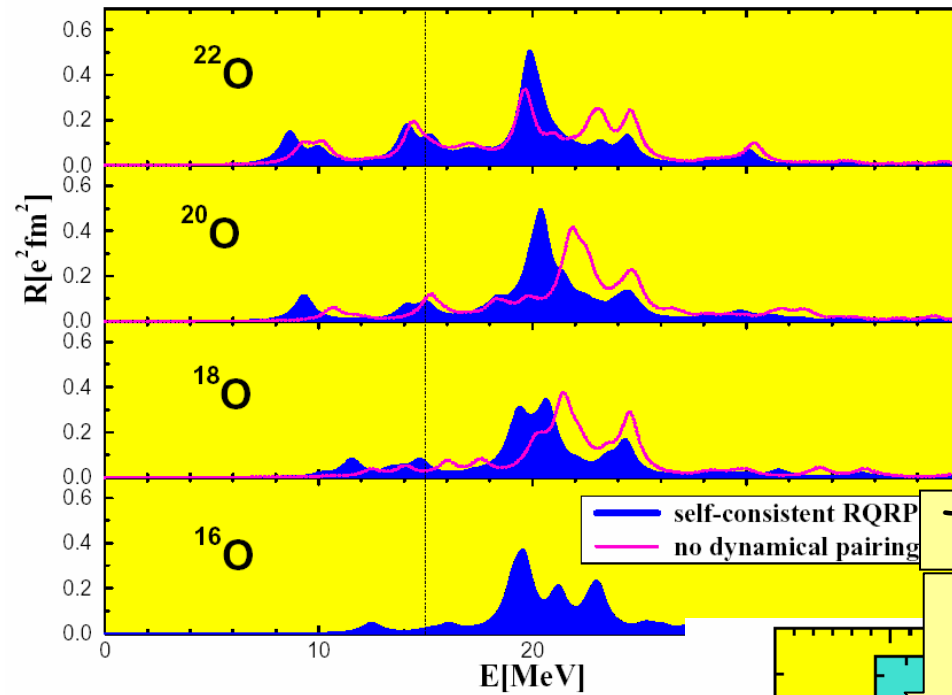


FIG. 2. Photoneutron cross sections for ^{16}O (upper panel) and for the unstable isotopes ^{20}O (lower panels) as extracted from the measured electromagnetic excitation cross section (symbols). The inset displays the cross section for near the neutron threshold on an expanded energy scale. The thresholds for decay channels involving protons (which were not observed in the present experiment) are indicated by arrows.

25.60.–t, 27.20.+n

my resonance, may arise from neutrons vibrating against the core. It is interesting to note that a systematic increase in dipole strength in neutron-rich nuclei has been observed from theoretical aspects, e.g., calculations in the γ -process of the γ -process [21]. Dipole resonances and lower lying strength have been investigated systematically for all neutron-rich oxygen isotopes. For doubly magic nuclei, one may expect a dipole resonance from the inert ^{16}O core. The dipole resonance of the last neutron is 7–8 MeV for ^{16}O and about 4 MeV for ^{20}O . Thus the dipole resonance might be good candidates for dipole resonance. We use the electromagnetic excitation of high targets. Similar to stable nuclei, the dipole strength is mostly sensitive to electric dipole (E1) contributions. For weighted sum rule for E1 dipole strength, we arbitrarily at an excitation energy of 10 MeV. The electromagnetic excitation cross section, respectively (calculated for a Pb target). It was demonstrated that the dipole strength can be determined qualitatively from a measurement of the electromagnetic dissociation cross section by applying the sum rule [24]. The high secondary beam energy of 600 MeV/nucleon allows for the

Physical Society



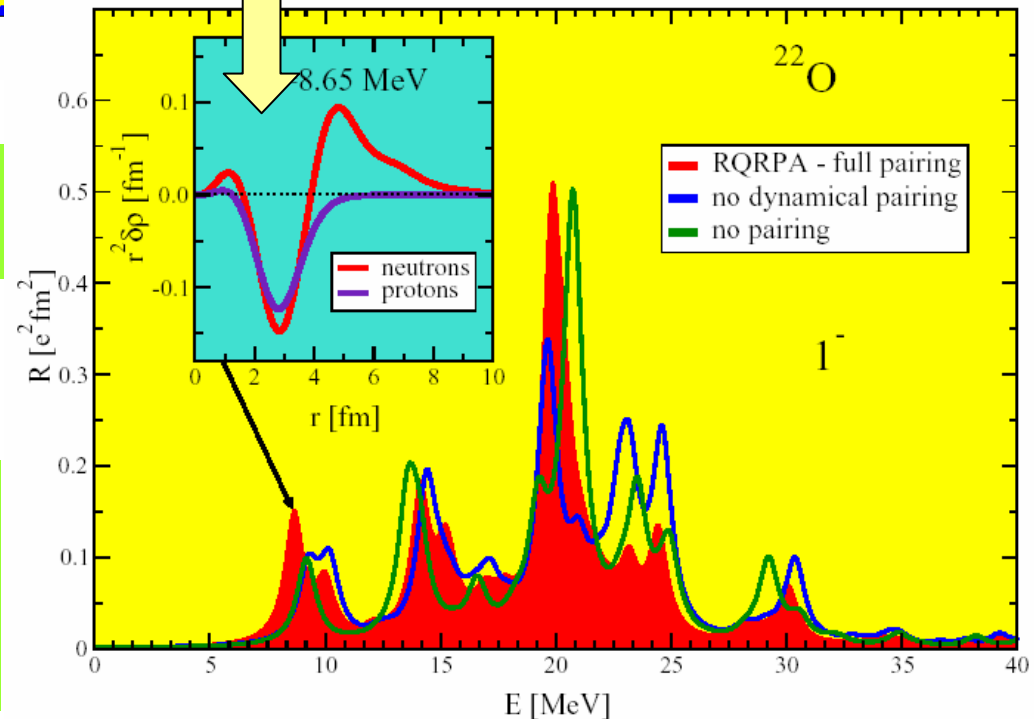
Evolution of IV dipole strength in Oxygen isotopes

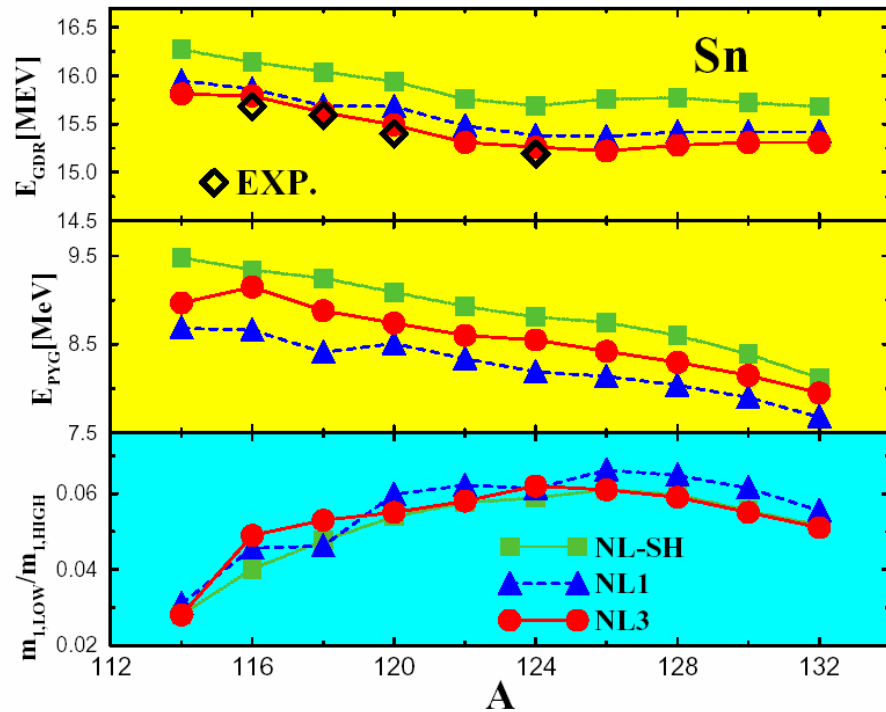
RHB + RQRPA calculations with the NL3 relativistic mean-field plus D1S Gogny pairing interaction.

Transition densities

What is the structure of low-lying strength below 15 MeV ?

Effect of pairing correlations on the dipole strength distribution

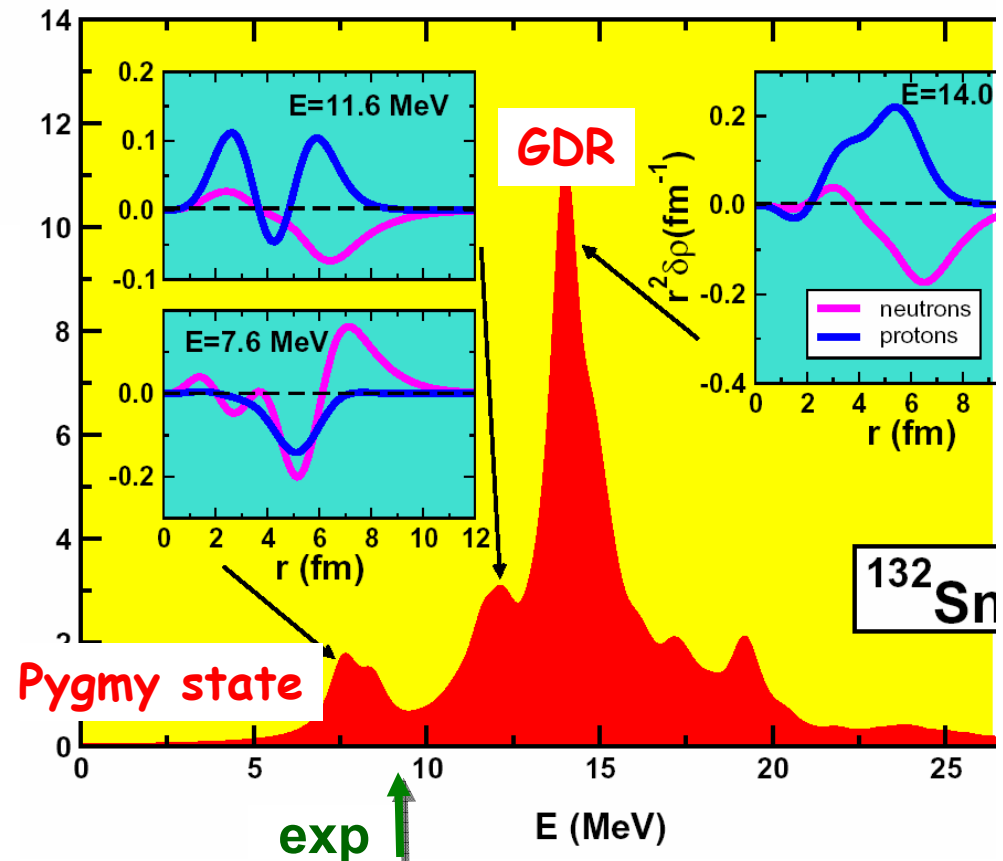




Mass dependence of GDR and Pygmy dipole states in Sn isotopes. Evolution of the low-lying strength.

Isvector dipole strength in ^{132}Sn .

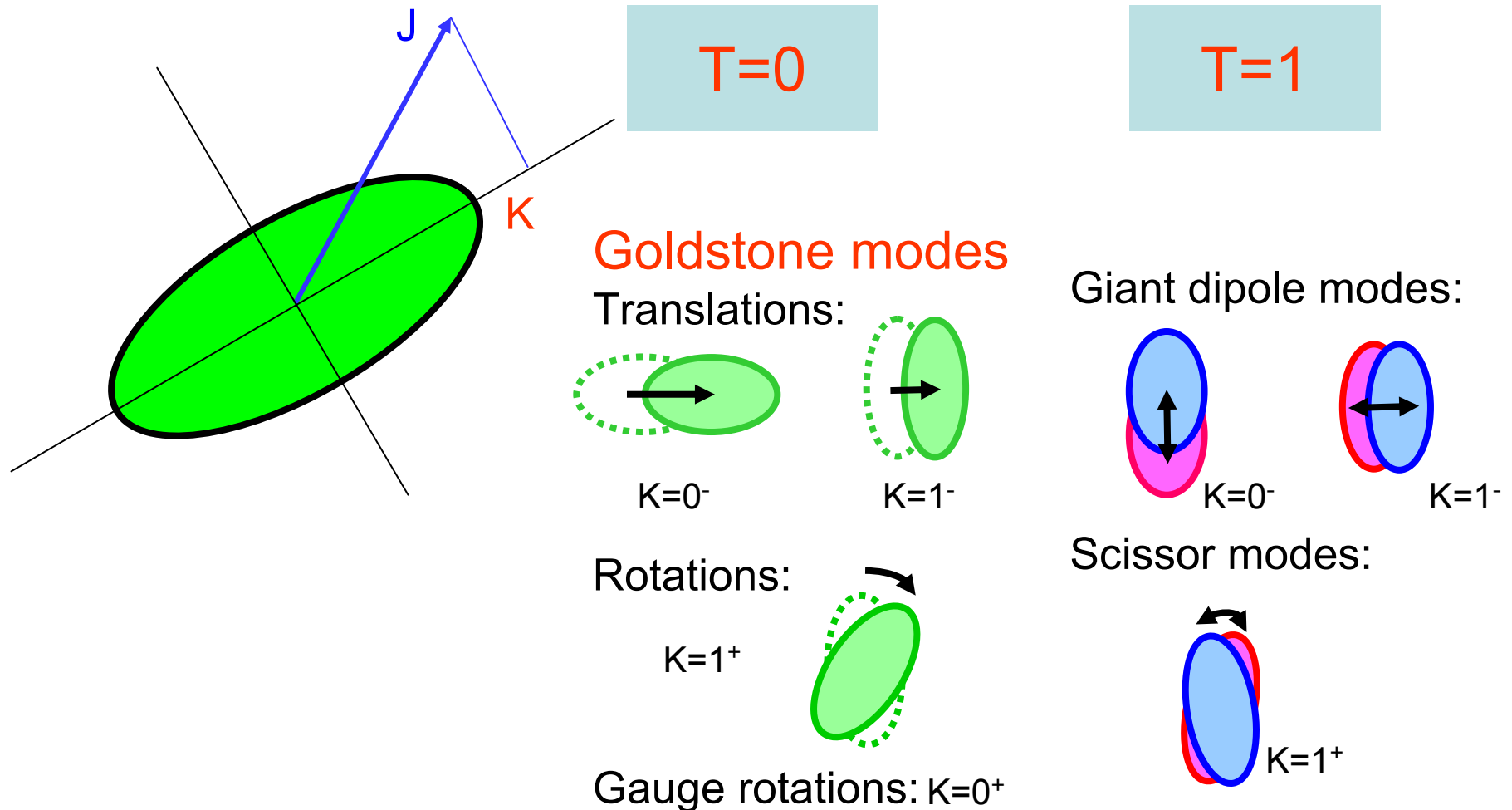
Nucl. Phys. A692, 496 (2001)



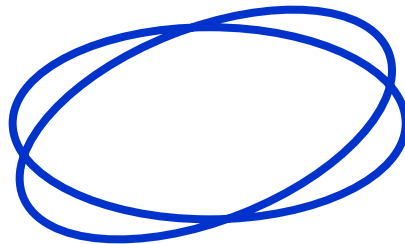
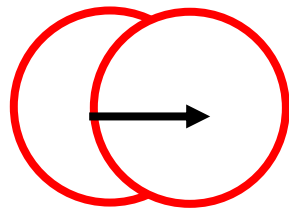
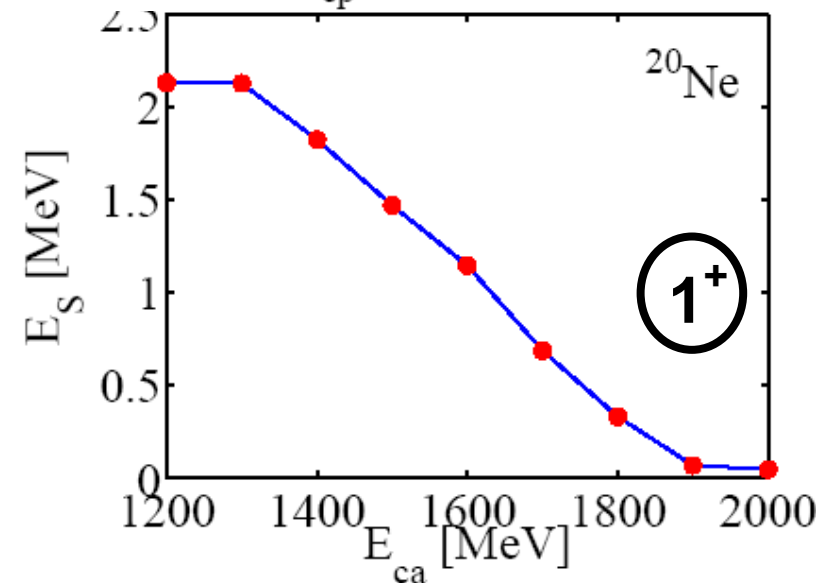
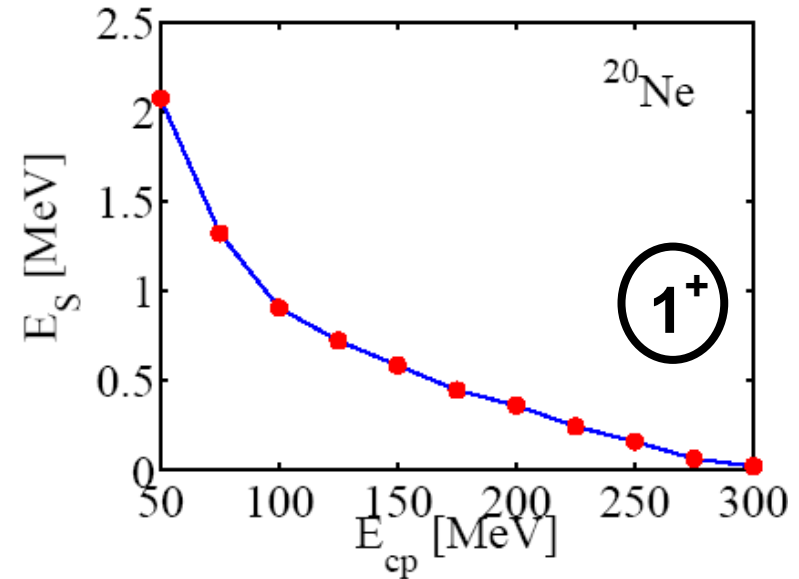
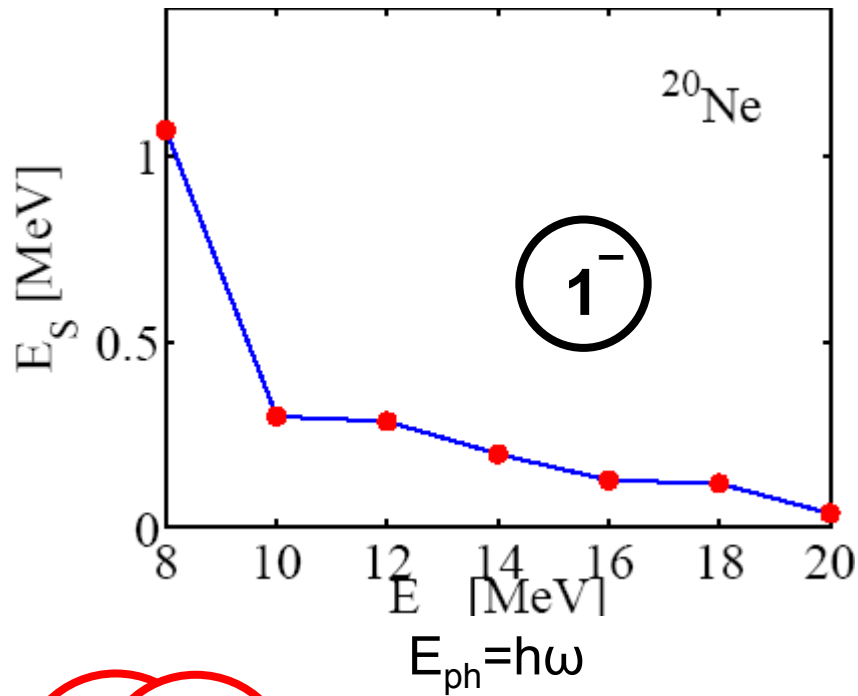
Distribution of the neutron particle-hole configurations for the peak at 7.6 MeV (1.4% of the EWSR)

^{132}Sn at 7.6 MeV	
28.2%	$2d_{3/2} \rightarrow 2f_{5/2}$
21.9%	$2d_{5/2} \rightarrow 2f_{7/2}$
19.7%	$2d_{3/2} \rightarrow 3p_{1/2}$
10.5%	$1h_{11/2} \rightarrow 1i_{13/2}$
3.5%	$2d_{5/2} \rightarrow 3p_{3/2}$
1.9%	$1g_{7/2} \rightarrow 2f_{5/2}$
1.5%	$1g_{7/2} \rightarrow 1h_{9/2}$
0.6%	$1g_{7/2} \rightarrow 2f_{7/2}$
0.6%	$2d_{3/2} \rightarrow 3p_{3/2}$

Vibrations in deformed nuclei

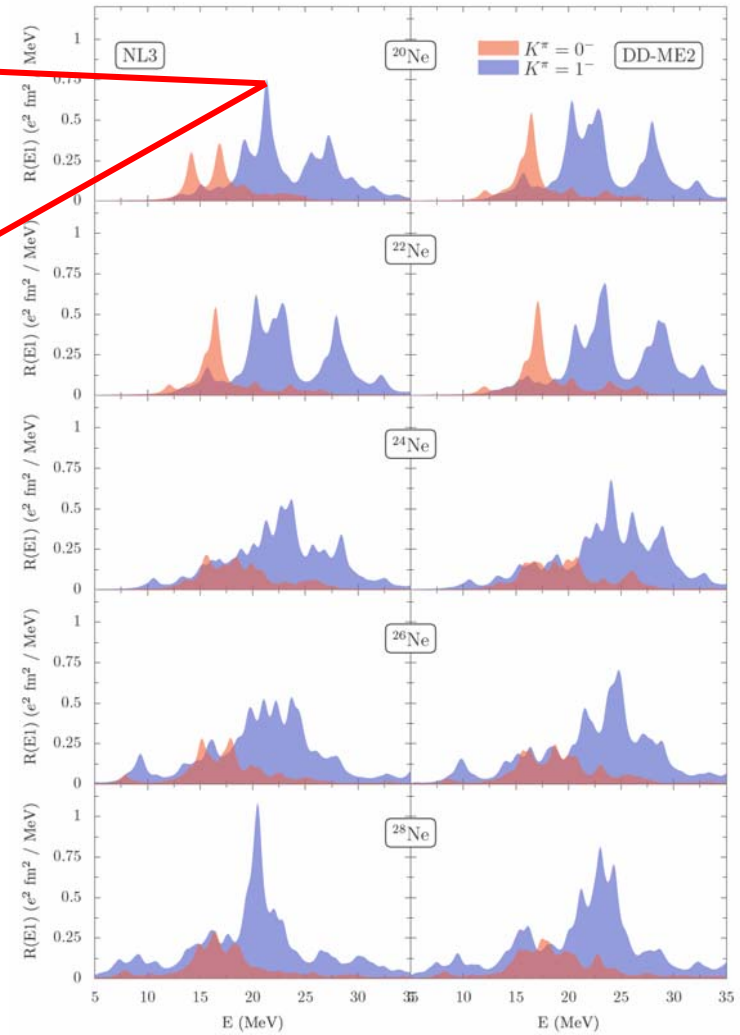
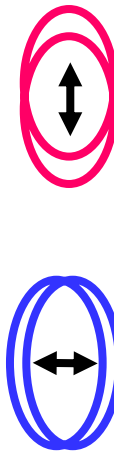
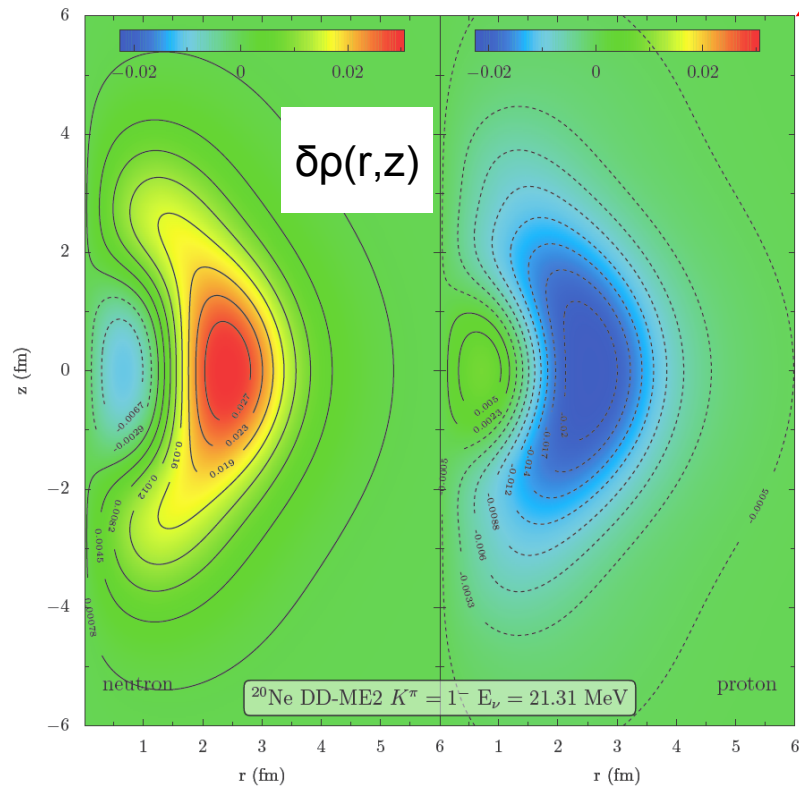
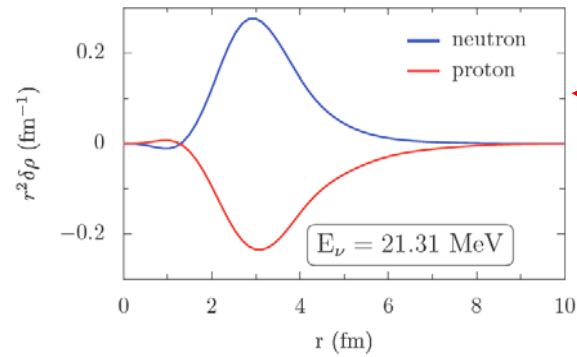


Goldstone modes in ^{20}Ne

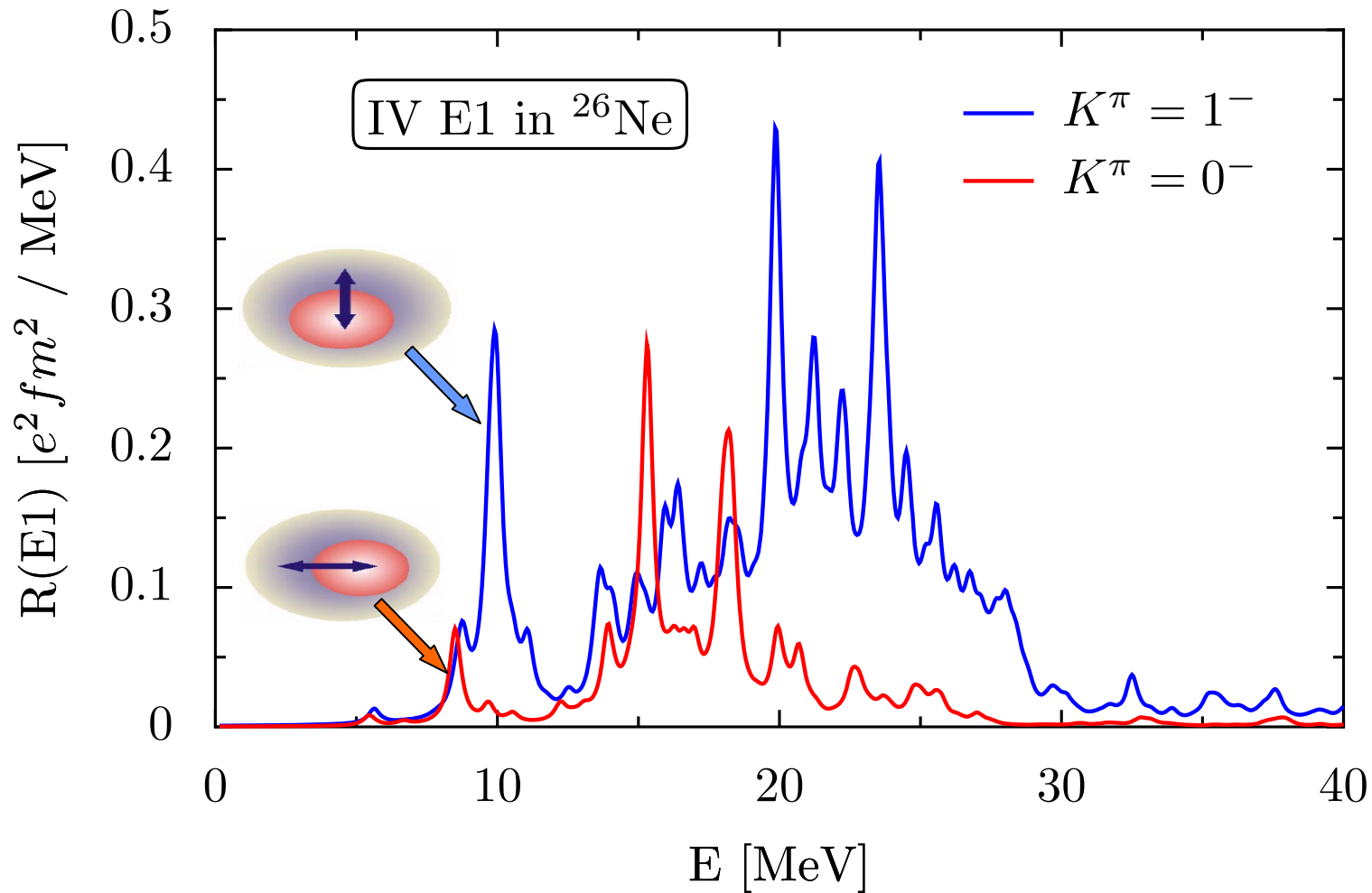


NL3

evolution of the GDR in deformed Ne isotopes



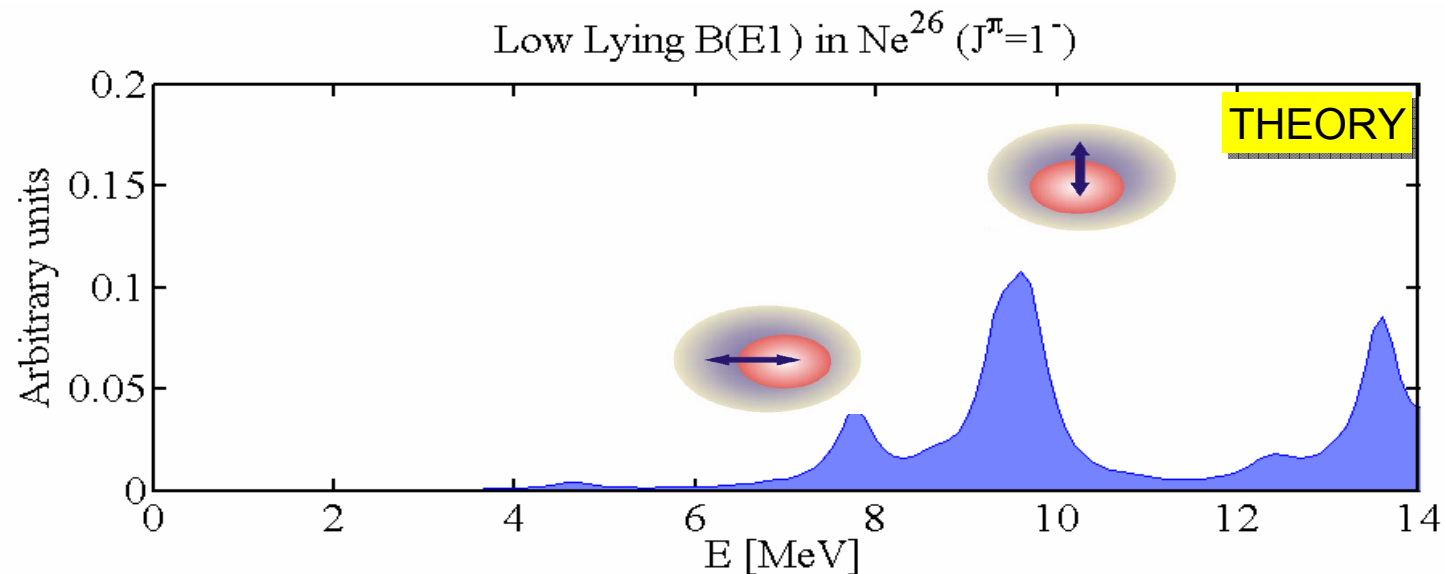
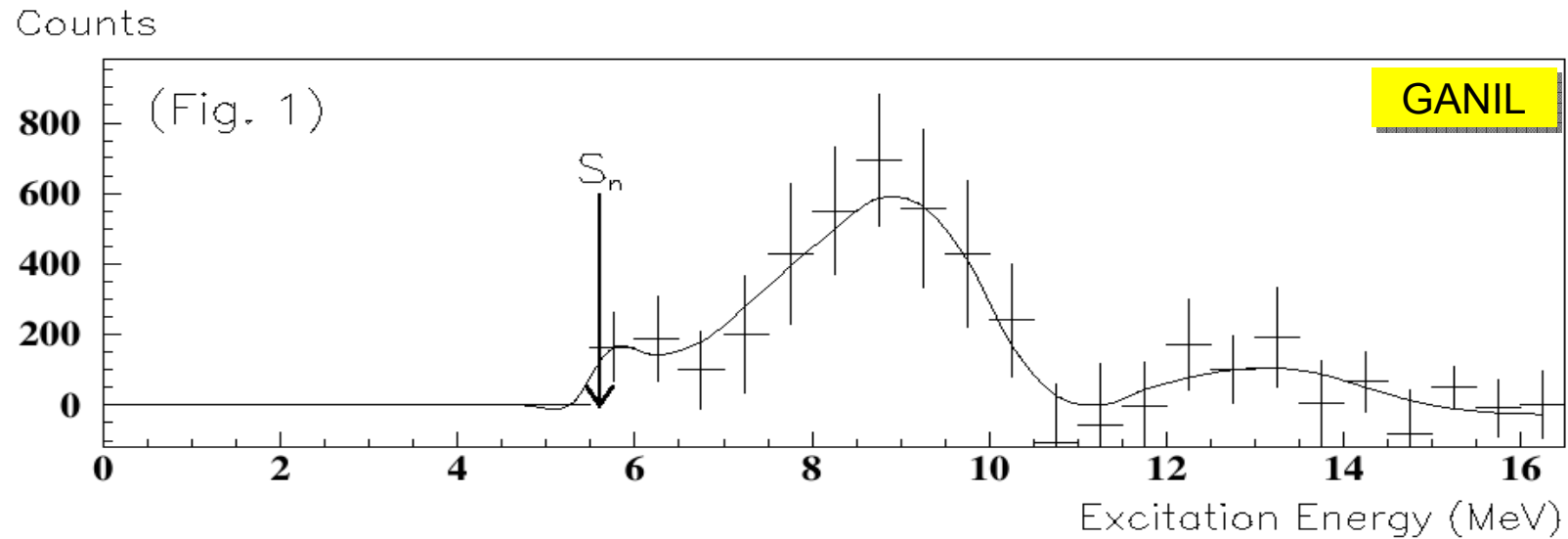
IV-dipole in ^{26}Ne



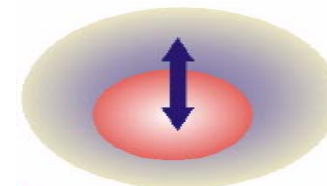
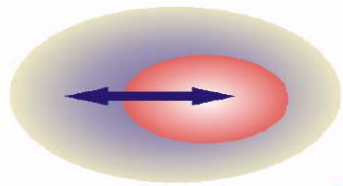
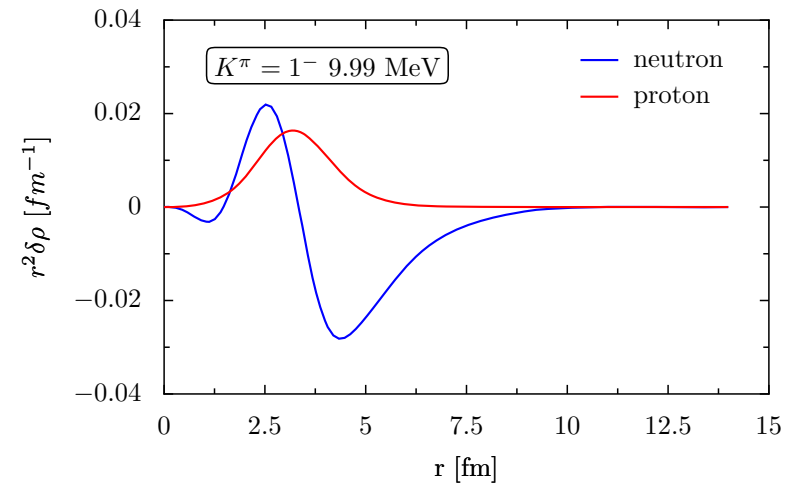
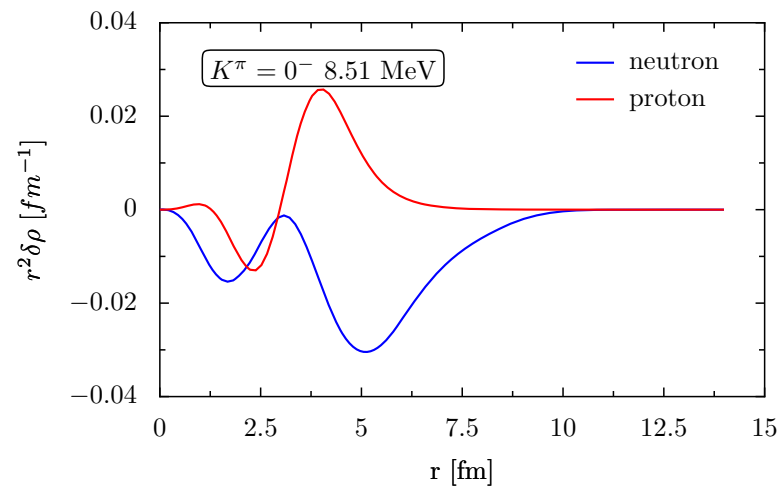
$\beta=0.29$, $\Delta_n=1.3 \text{ MeV}$, **sumrule=109 %** ($<12 \text{ MeV}:= 5 \%$)

NL3

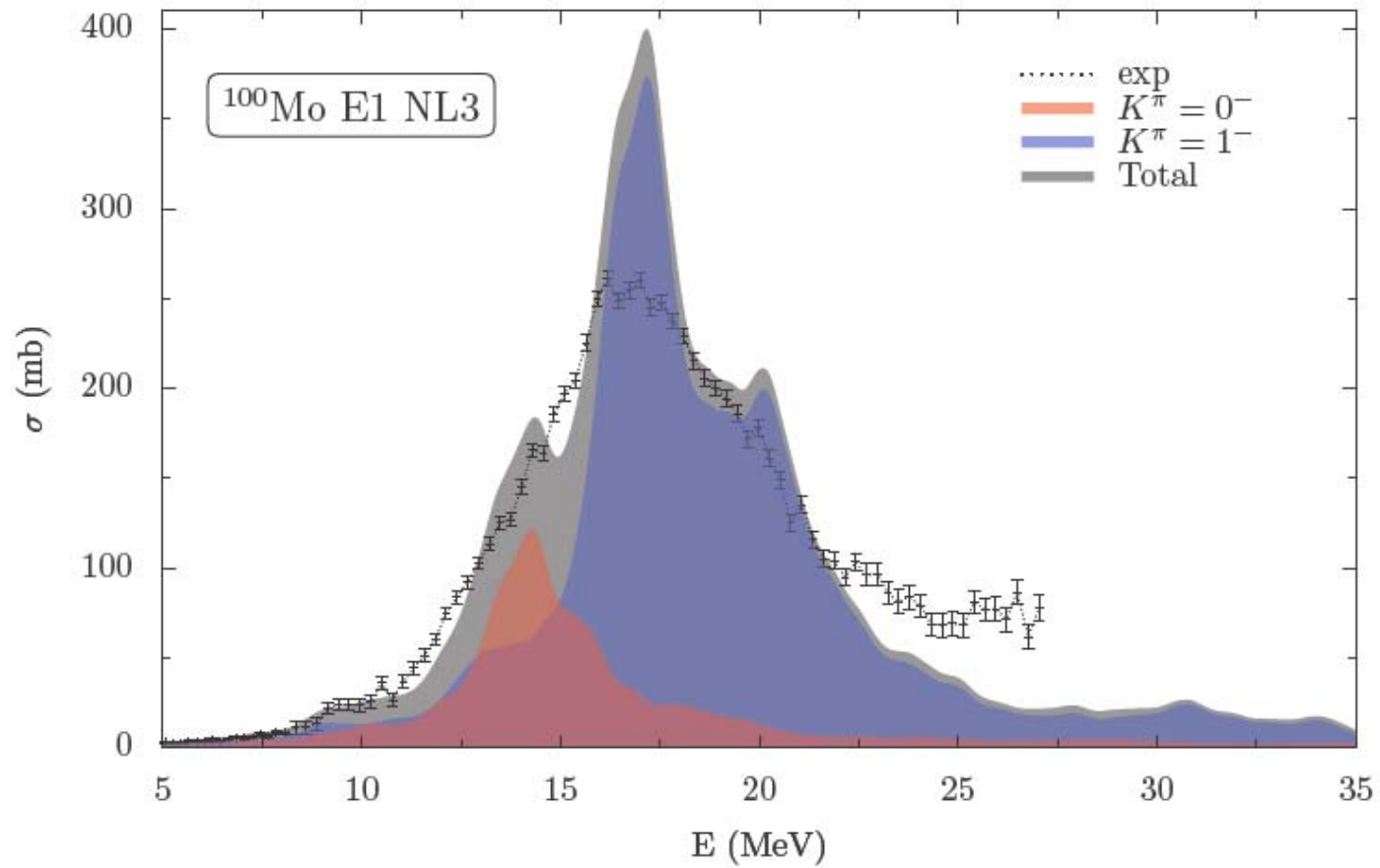
Pygmy-Resonance in deformed ^{26}Ne



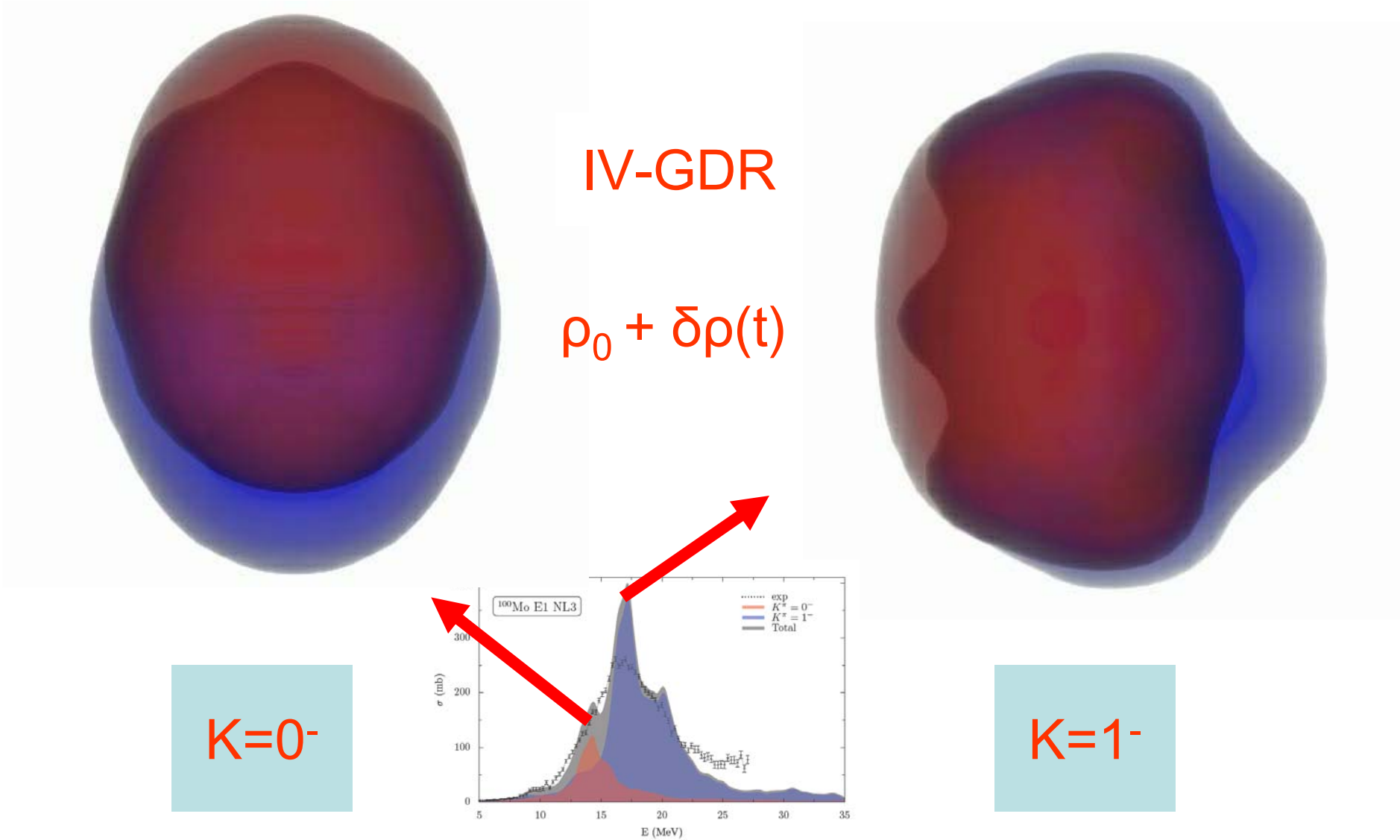
Pygmy in ^{26}Ne ?

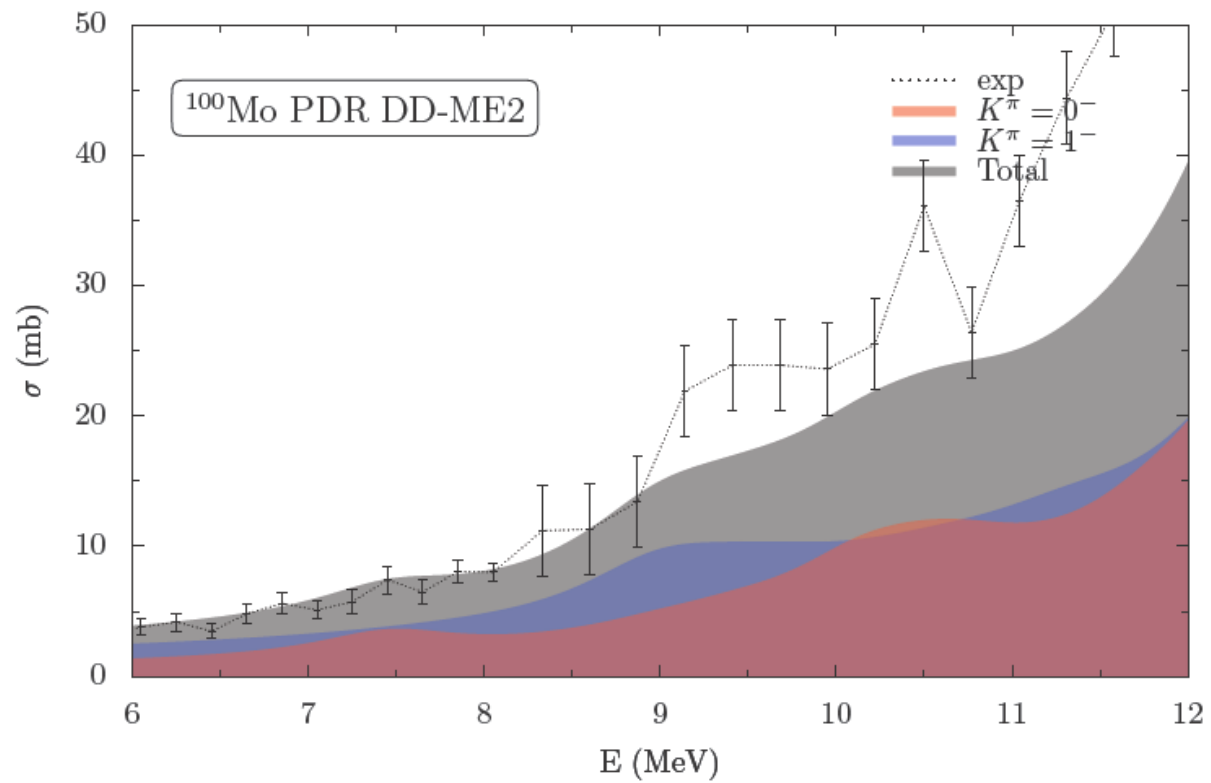


IV-GDR in ^{100}Mo



IV-GDR in ^{100}Mo





Isoscalar dipole compression -- toroidal modes

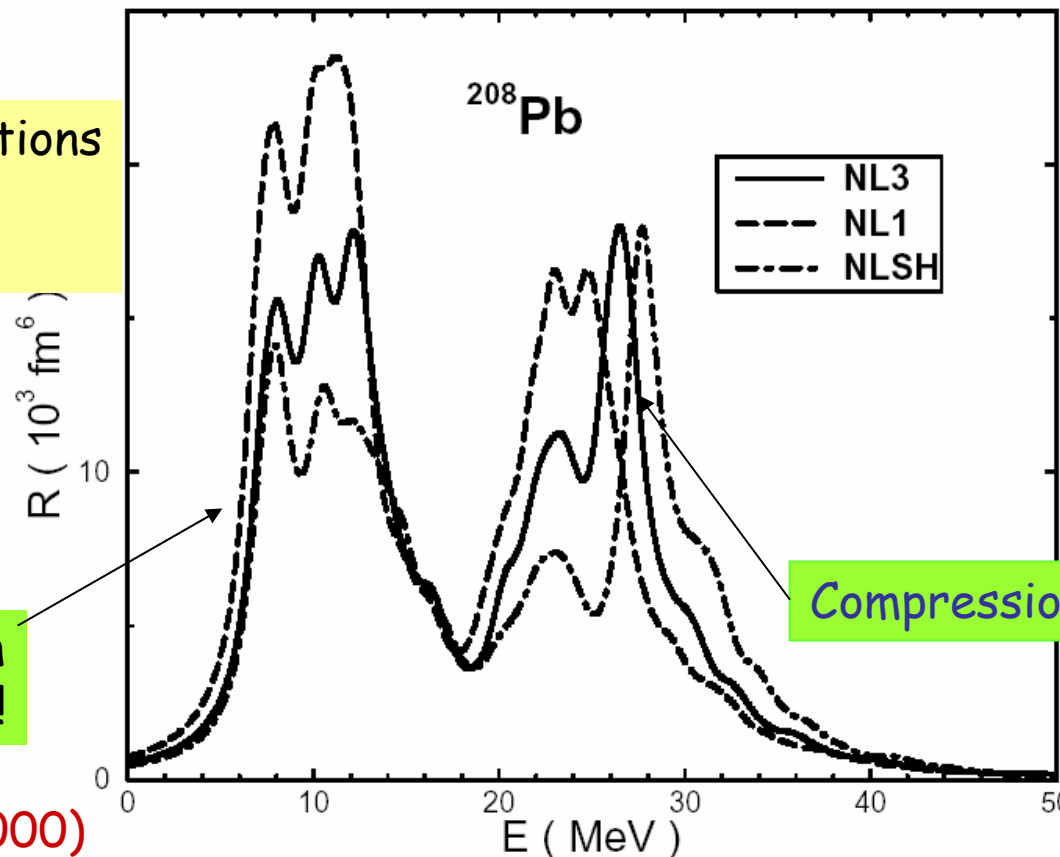
Isoscalar GMR in spherical nuclei \rightarrow nuclear matter compression modulus K_{nm} .

Giant isoscalar dipole oscillations \rightarrow additional information on the nuclear incompressibility.

$$\hat{Q}_{1\mu}^{T=0} = \sum_{i=1}^A \gamma_0 (r^3 - \eta r) Y_{1\mu}(\theta_i, \varphi_i)$$

ISGDR strength distributions
Effective interactions
with different K_{nm} .

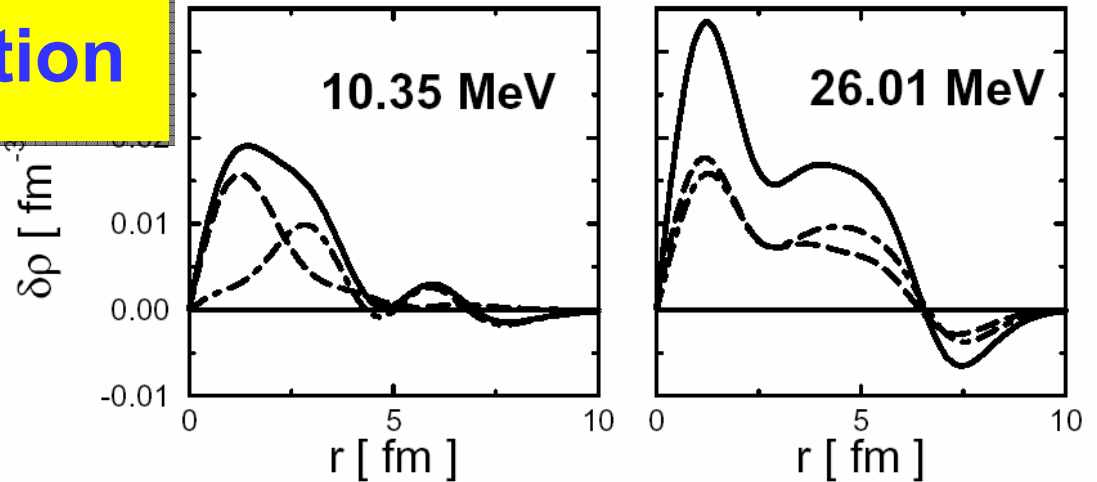
The low-energy strength
does not depend on K_{nm} !



Phys. Lett. B487, 334 (2000)

Toroidal motion

ISGDR transition densities for ^{208}Pb (NL3 interaction)



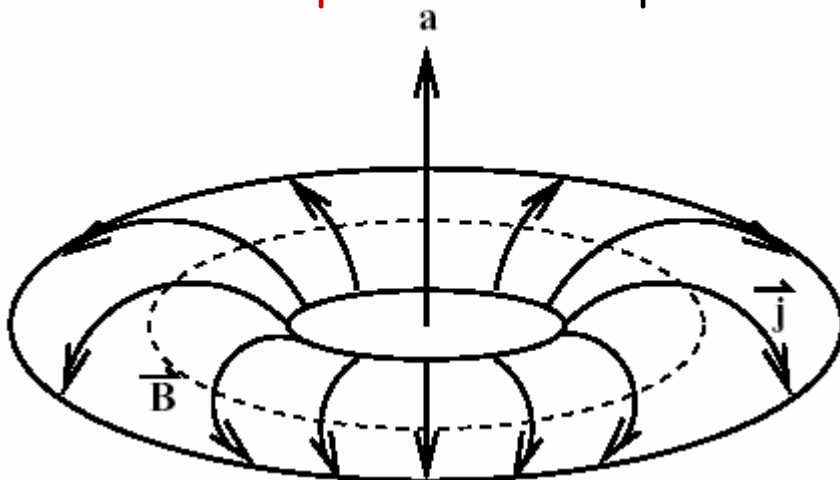
multipole expansion of a four-current distribution:

charge moments

magnetic moments

electric transverse moments \rightarrow toroidal moments

toroidal dipole moment: poloidal currents on a torus

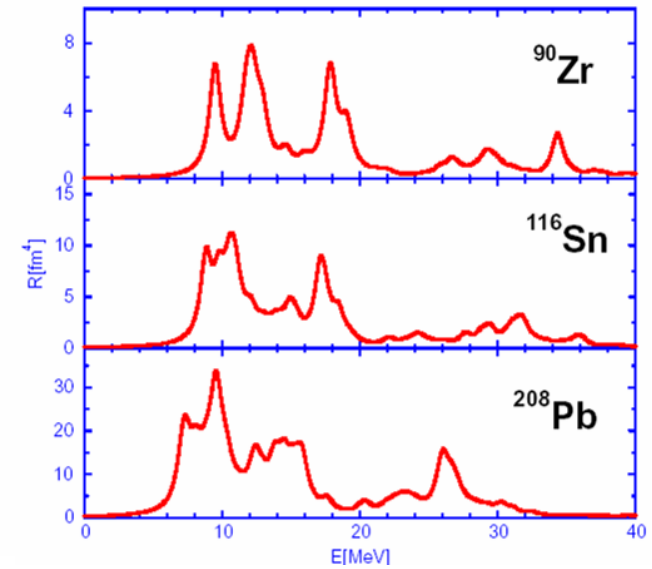
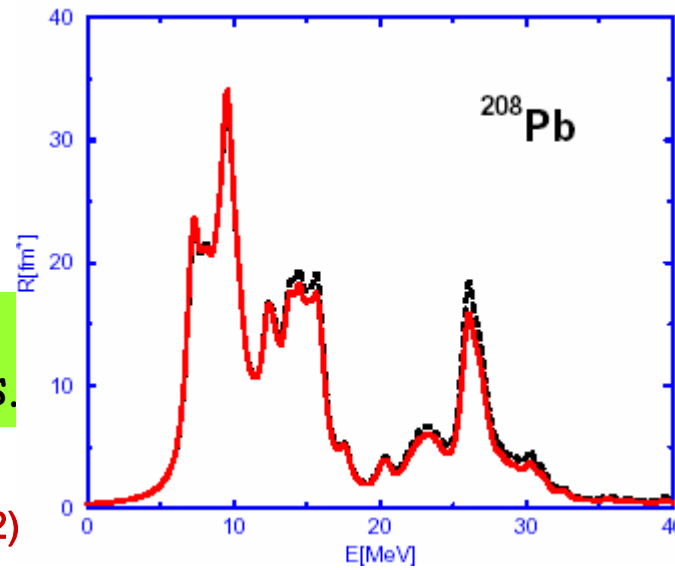


isoscalar toroidal dipole operator:

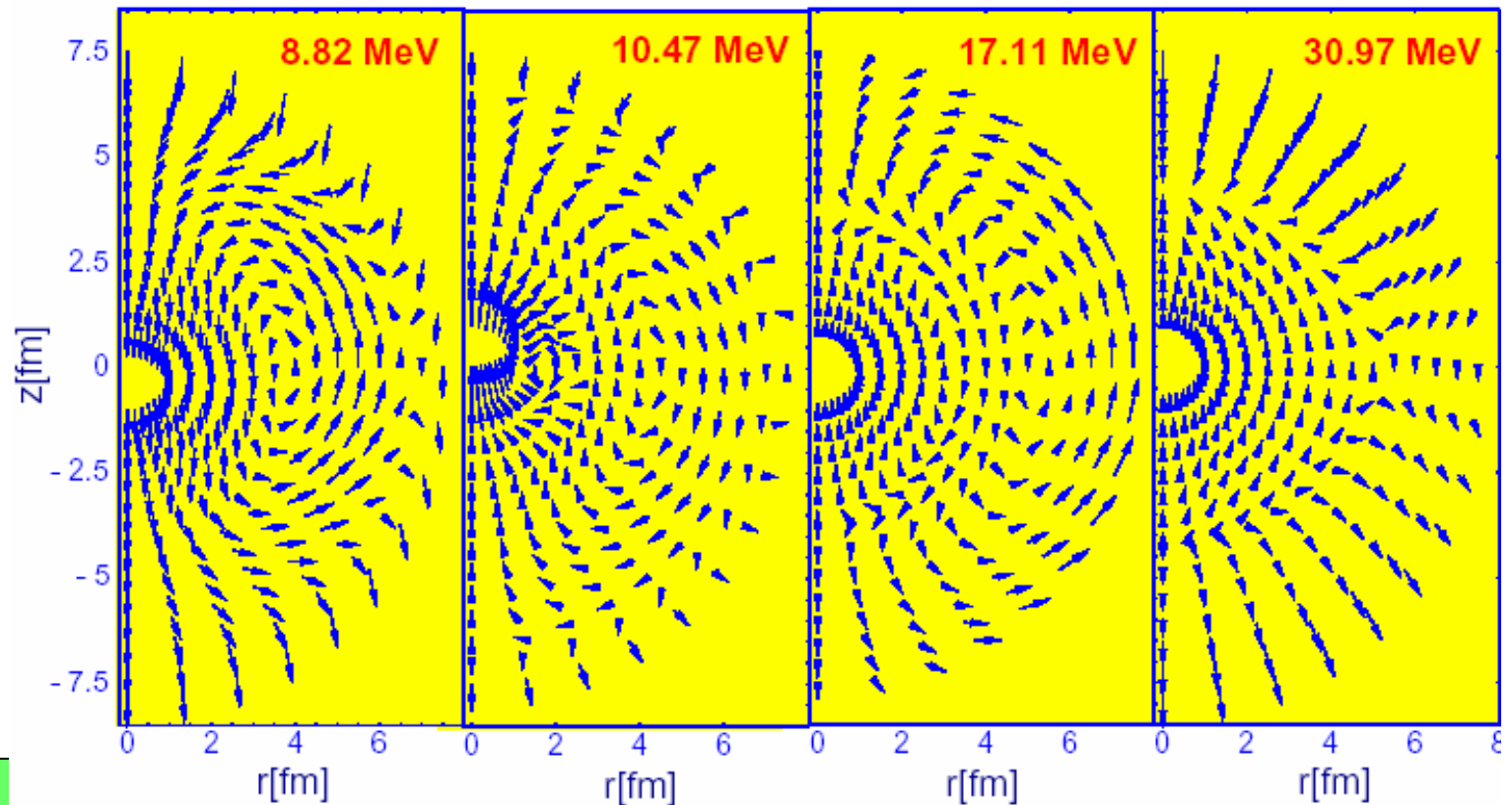
$$\hat{T}_{1\mu}^{T=0} \sim \int [r^2 \left(\vec{Y}_{10\mu}^* + \frac{\sqrt{2}}{5} \vec{Y}_{12\mu}^* \right) - \langle r^2 \rangle_0 \vec{Y}_{10\mu}^*] \cdot \vec{J}(\vec{r}) d^3r$$

Toroidal dipole strength distributions.

Vretenar, Paar, Niksic, Ring,
Phys. Rev. C65, 021301 (2002)



Velocity distributions in ^{116}Sn

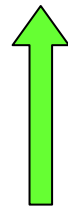


Spin-Isospin Resonances: IAR - GTR

Z, N

$Z+1, N-1$

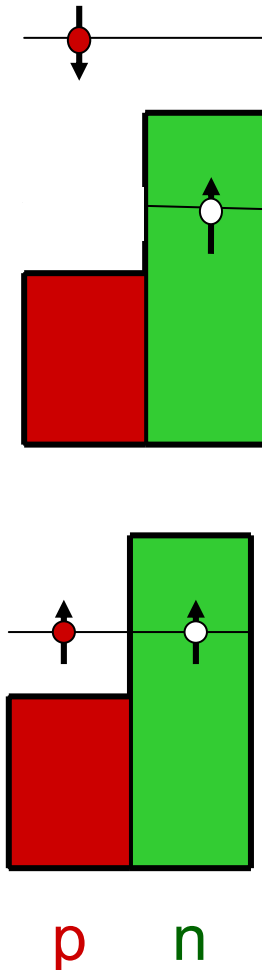
$$|\text{GTR}\rangle = S_- T_+ |Z, N\rangle$$



spin flip σ

$$|Z, N\rangle \longrightarrow |\text{IAR}\rangle = T_+ |Z, N\rangle$$

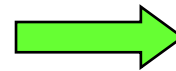
isospin flip τ



$$E_{\text{GTR}} - E_{\text{IAR}} \sim \Delta(l \cdot s) \sim \frac{dV}{dr} \sim \text{neutron skin} = r_n - r_p$$

Spin-Isospin Resonances: IAS and GTR

charge-exchange excitations



proton-neutron
relativistic QRPA

π and ρ -meson exchange
generate the spin-isospin
dependent interaction terms

$$\mathcal{L}_{\pi N} = -\frac{f_{\pi}}{m_{\pi}} \bar{\psi} \gamma_5 \gamma_{\mu} \partial^{\mu} \vec{\pi} \vec{\tau} \psi$$

the Landau-Migdal zero-range
force in the spin-isospin channel

$$V(1, 2) = g'_0 \left(\frac{f_{\pi}}{m_{\pi}} \right)^2 \vec{\tau}_1 \cdot \vec{\tau}_2 \Sigma_1 \cdot \Sigma_2 \delta(r_1 - r_2) \quad (g'_0=0.55)$$

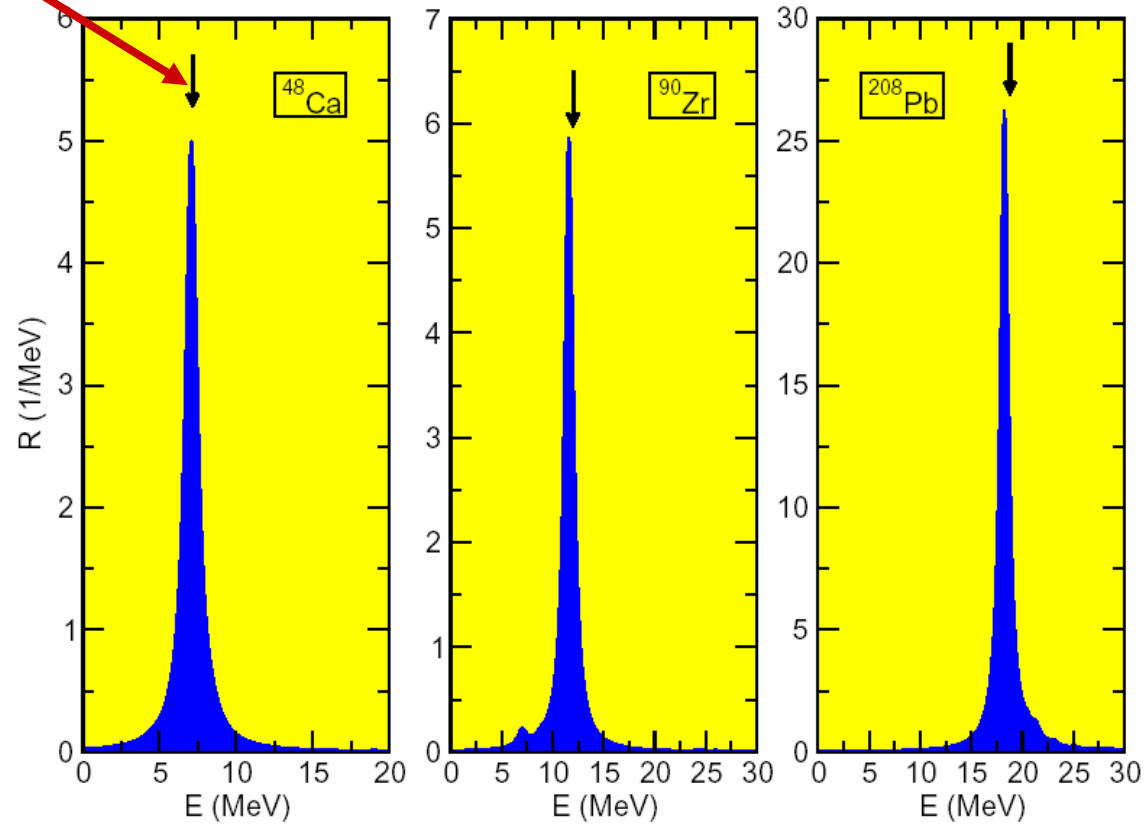
GAMOW-TELLER RESONANCE: $S=1 \quad T=1 \quad J^{\pi} = 1^{+}$

ISOBARIC ANALOG STATE: $S=0 \quad T=1 \quad J^{\pi} = 0^{+}$

Isobaric Analog Resonance: IAR

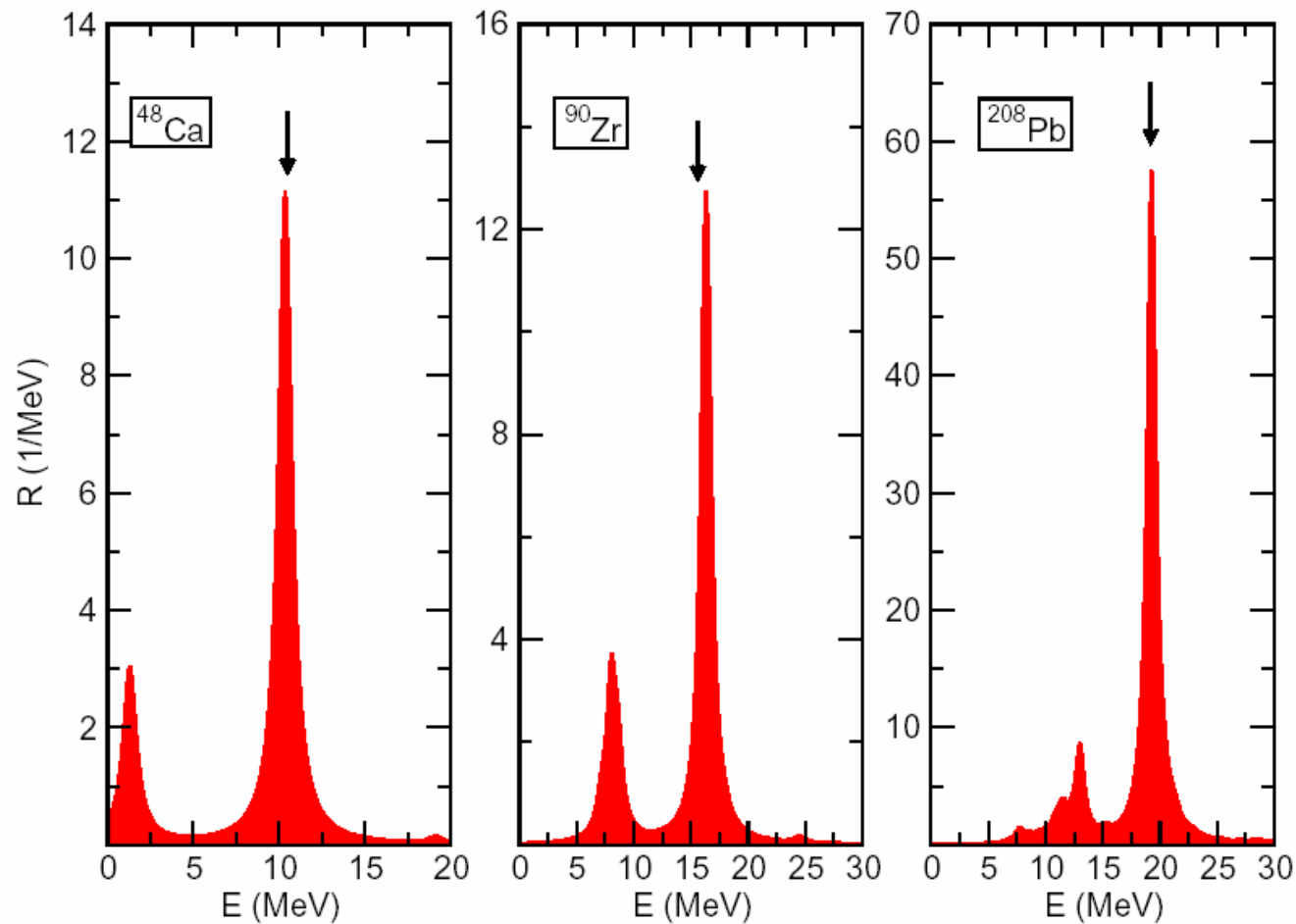
N. Paar, T. Nikšić, D. Vretenar, P. Ring, PR C69, 054303 (2004)

experiment

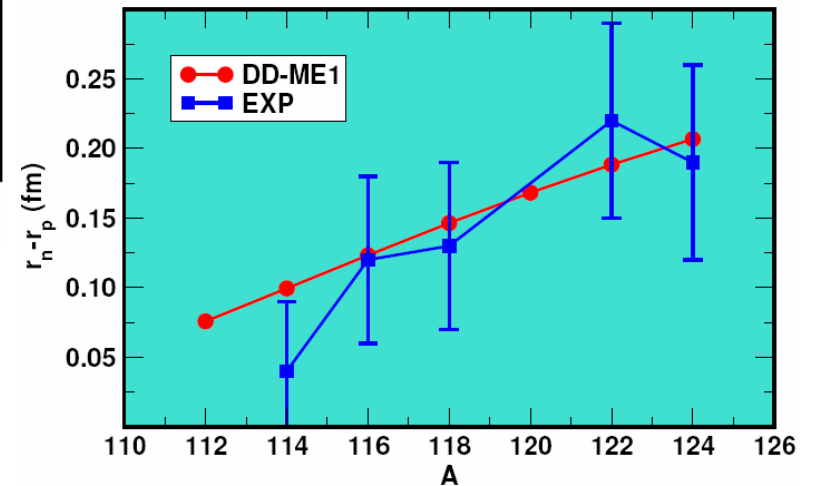
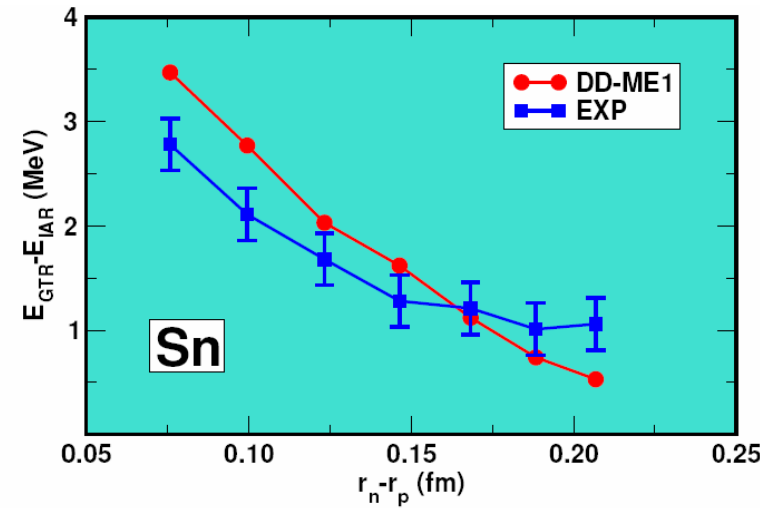
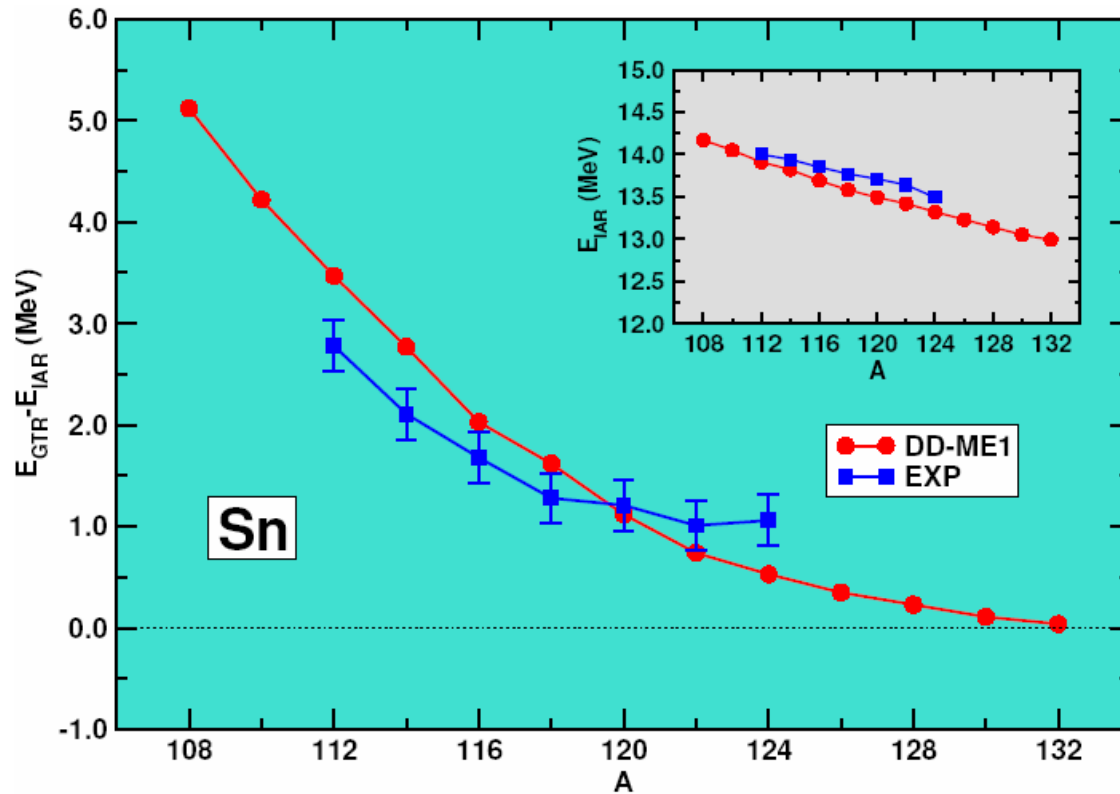


GT-Resonances

N. Paar, T. Niksic, D. Vretenar, P. Ring, PR C69, 054303 (2004)

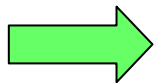


Neutron skin and IAR/GRT

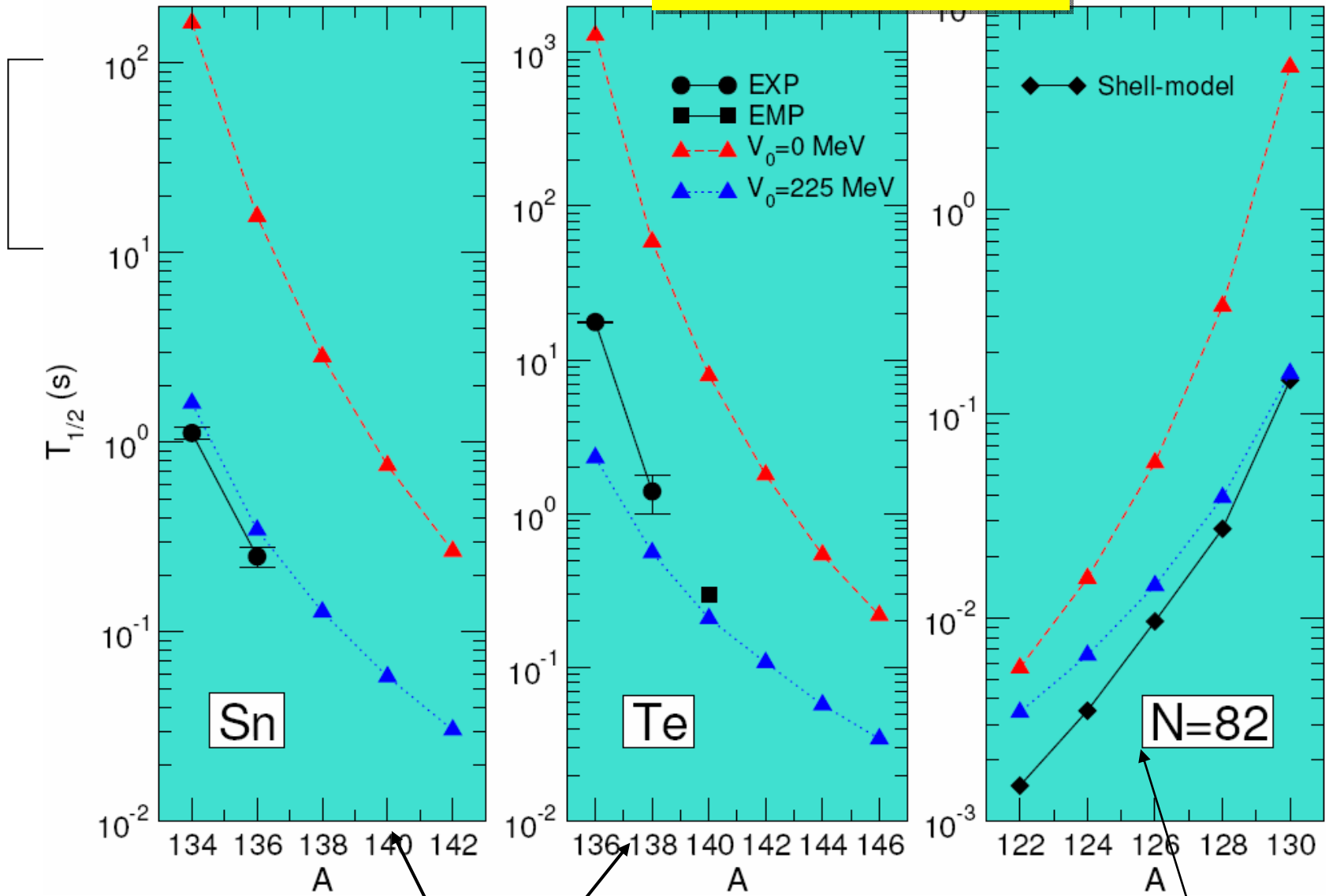


The isotopic dependence of the energy spacings between the GTR and IAS

direct information on the evolution of the neutron skin along the Sn isotopic chain



β-decay



$\nu h_{9/2}^- \rightarrow \pi h_{11/2}$

G. Martinez-Pinedo and K. Langanke, PRL 83, 4502 (1999)

Content

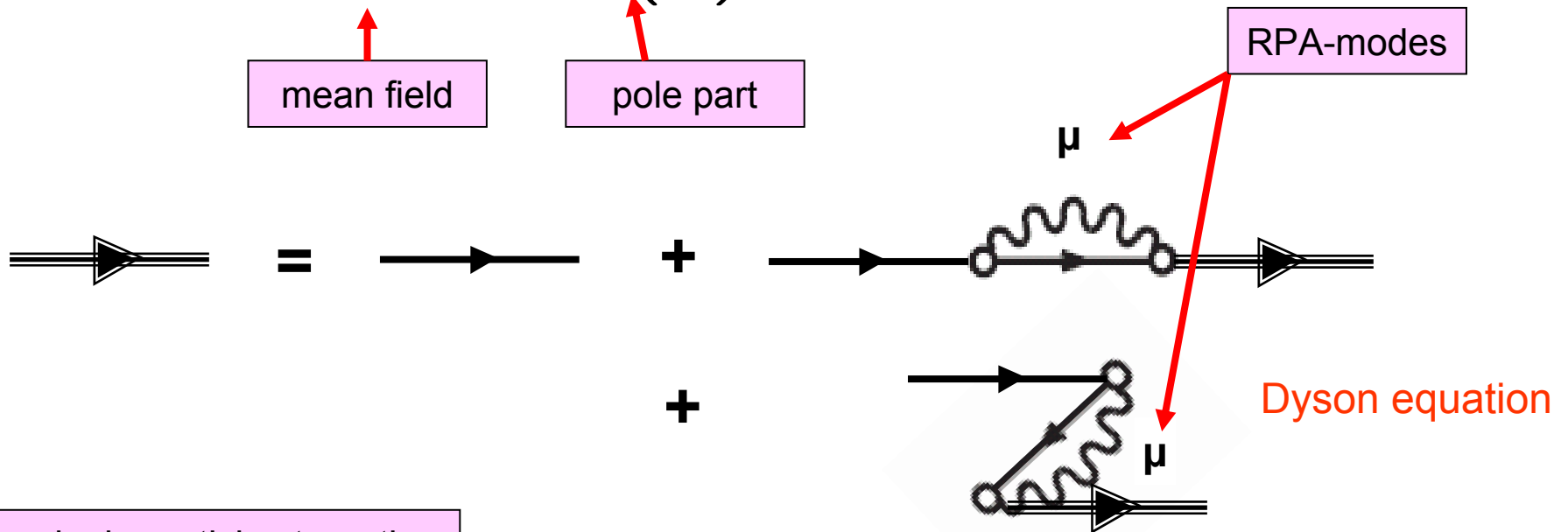
- Density functional theory in nuclei
- Ground state properties
- Nuclear dynamics and excitations
- **Methods beyond mean field**
- Conclusions

Particle-Vibrational Coupling (PVC): energy dependent self-energy

$$\Sigma = S + V + \Sigma(\omega)$$

mean field

pole part



single particle strength:

$$z_\nu = \left[1 - \frac{d\Sigma_{\nu\nu}}{d\omega} \Big|_{\omega=\epsilon_\nu} \right]^{-1}$$

non-relativistic investigations:
 Ring, Werner (1973)
 Hamamoto, Siemens (1976)
 Perazzo, Reich, Sofia (1980)
 Bortignon et al (1980)
 Bernard, Giai (1980)
 Platonov (1981)
 Kamerzhiev, Tselyaev (1986)

Contributions to $\Sigma(\omega)$ in the relativistic case:

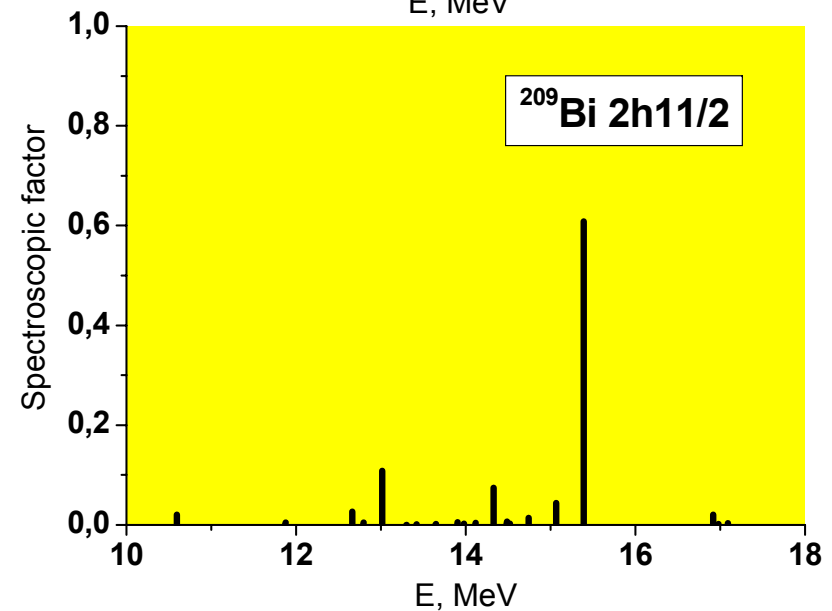
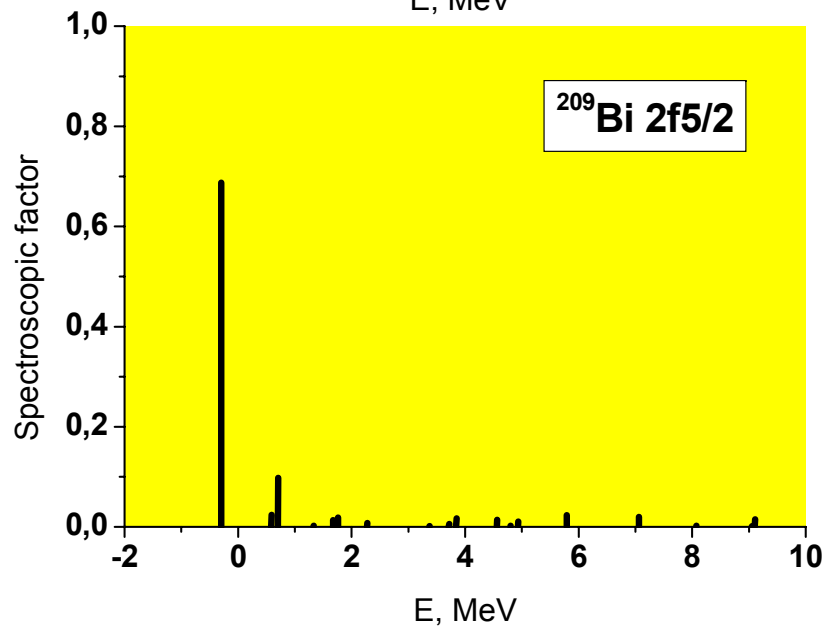
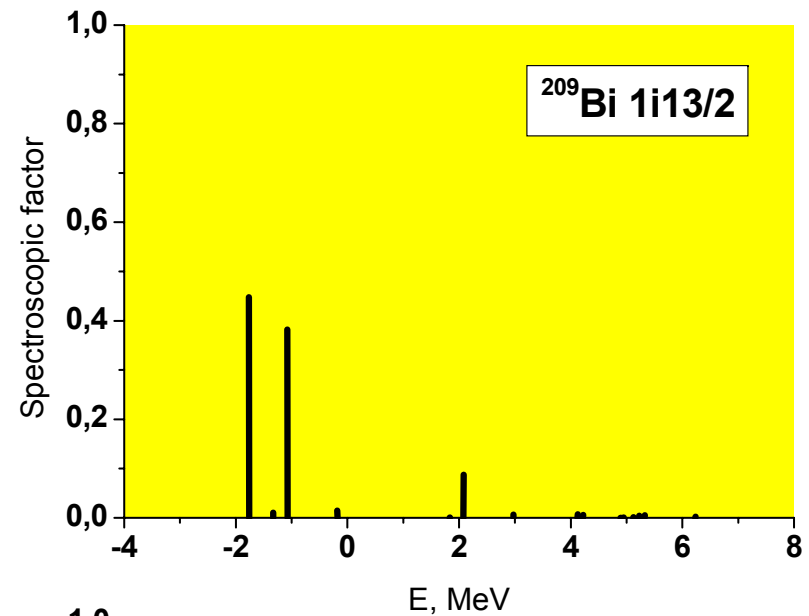
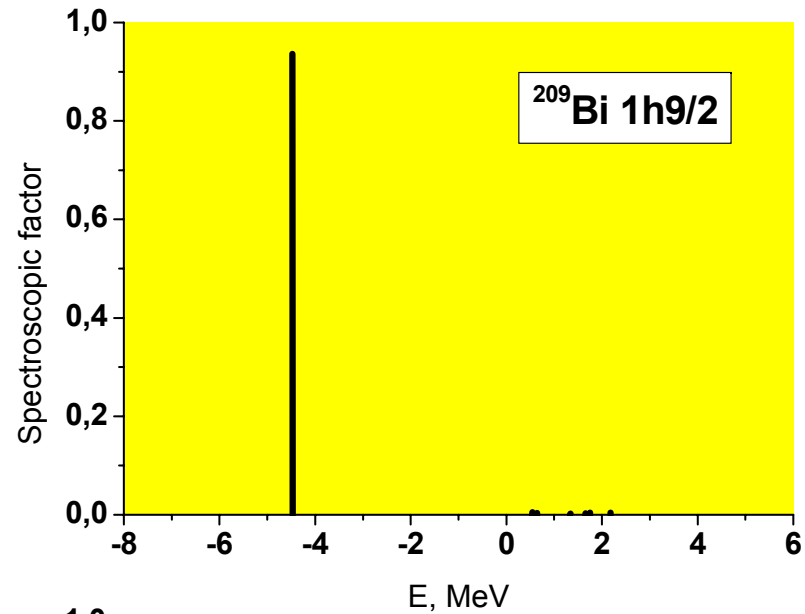
$$\Sigma_{p'p''}^e = \text{Diagram 1} + \text{Diagram 2} + \text{Diagram 3}$$

$$\Sigma_{h'h''}^e = \text{Diagram 4} + \text{Diagram 5} + \text{Diagram 6}$$

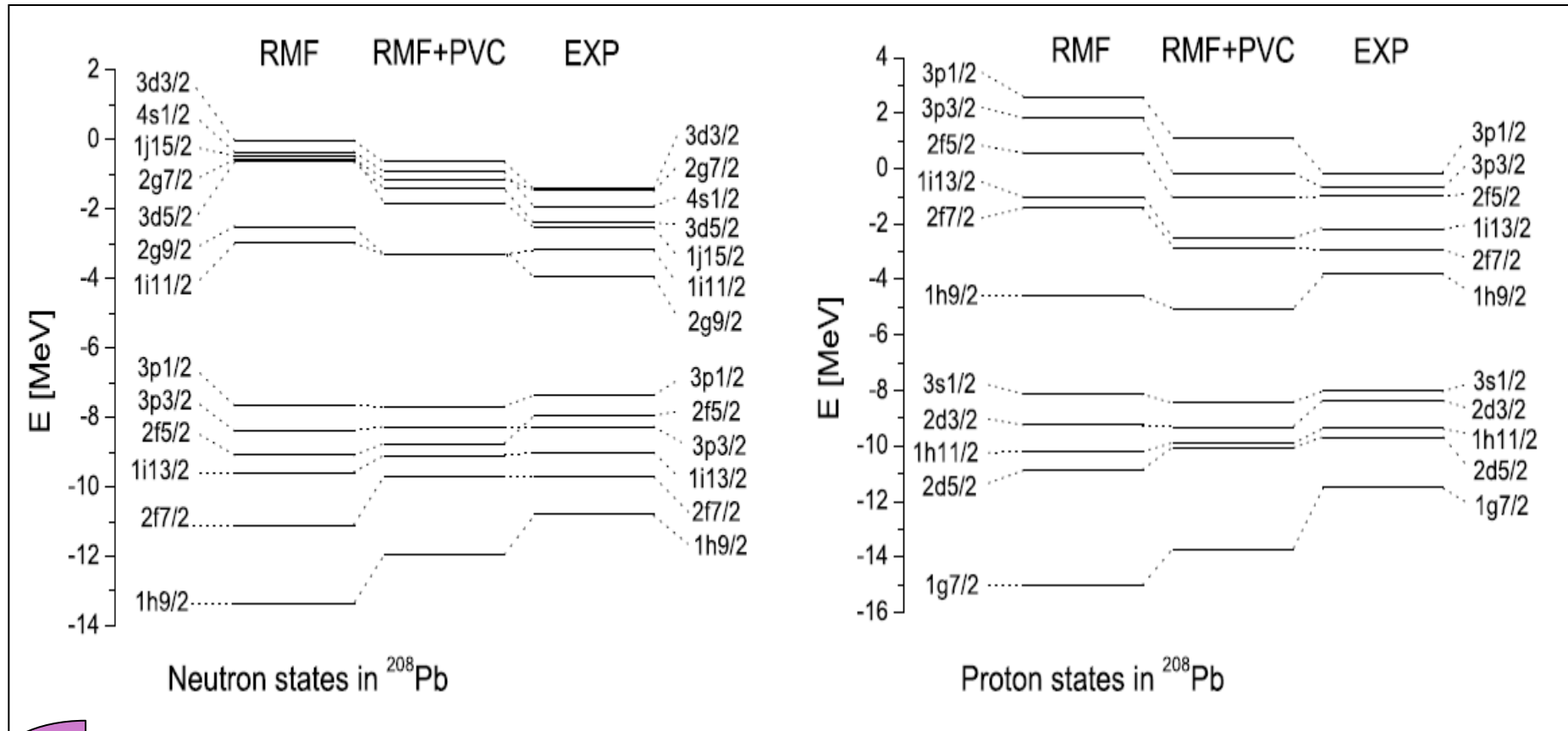
The diagrams represent the following contributions:

- Diagram 1:** A fermion loop with incoming momentum p' and outgoing momentum p'' . The loop contains a fermion line with momentum p and a wavy boson line with index μ .
- Diagram 2:** Similar to Diagram 1, but the fermion line between the vertices is dashed and labeled α .
- Diagram 3:** A fermion loop with incoming momentum p'' and outgoing momentum p' . The loop contains a fermion line with momentum h and a wavy boson line with index μ .
- Diagram 4:** A fermion loop with incoming momentum h'' and outgoing momentum h' . The loop contains a fermion line with momentum p and a wavy boson line with index μ .
- Diagram 5:** Similar to Diagram 4, but the fermion line between the vertices is dashed and labeled α .
- Diagram 6:** A fermion loop with incoming momentum h'' and outgoing momentum h' . The loop contains a fermion line with momentum h and a wavy boson line with index μ .

Distribution of single-particle strength in ^{209}Bi



Single particle spectrum in the Pb region



m_{eff}

0.76

0.92

1.0

0.71

0.85

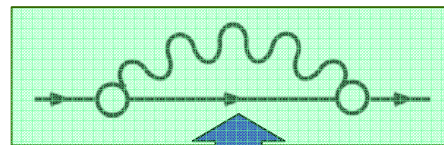
1.0

E. Litvinova and P. Ring, PRC 73, 44328 (2006)

Width of Giant Resonances

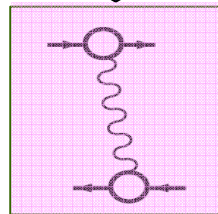
The full response contains energy dependent parts coming from vibrational couplings.

$$V(\omega) = \frac{\delta\Sigma(\omega)}{\delta\rho}$$

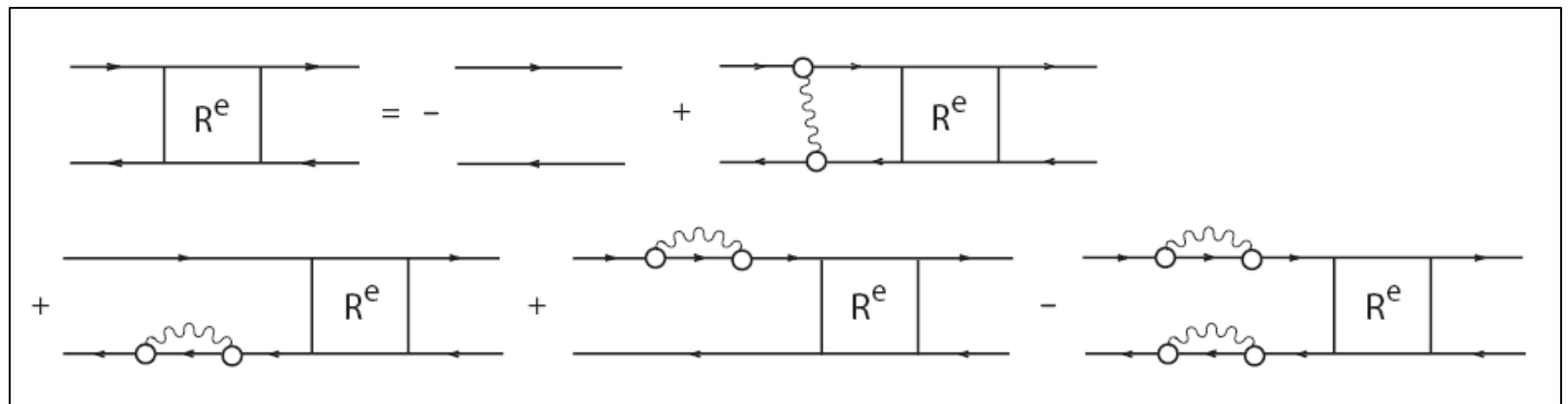


Self energy

ph-phonon amplitudes(QRPA)



ph interaction amplitude



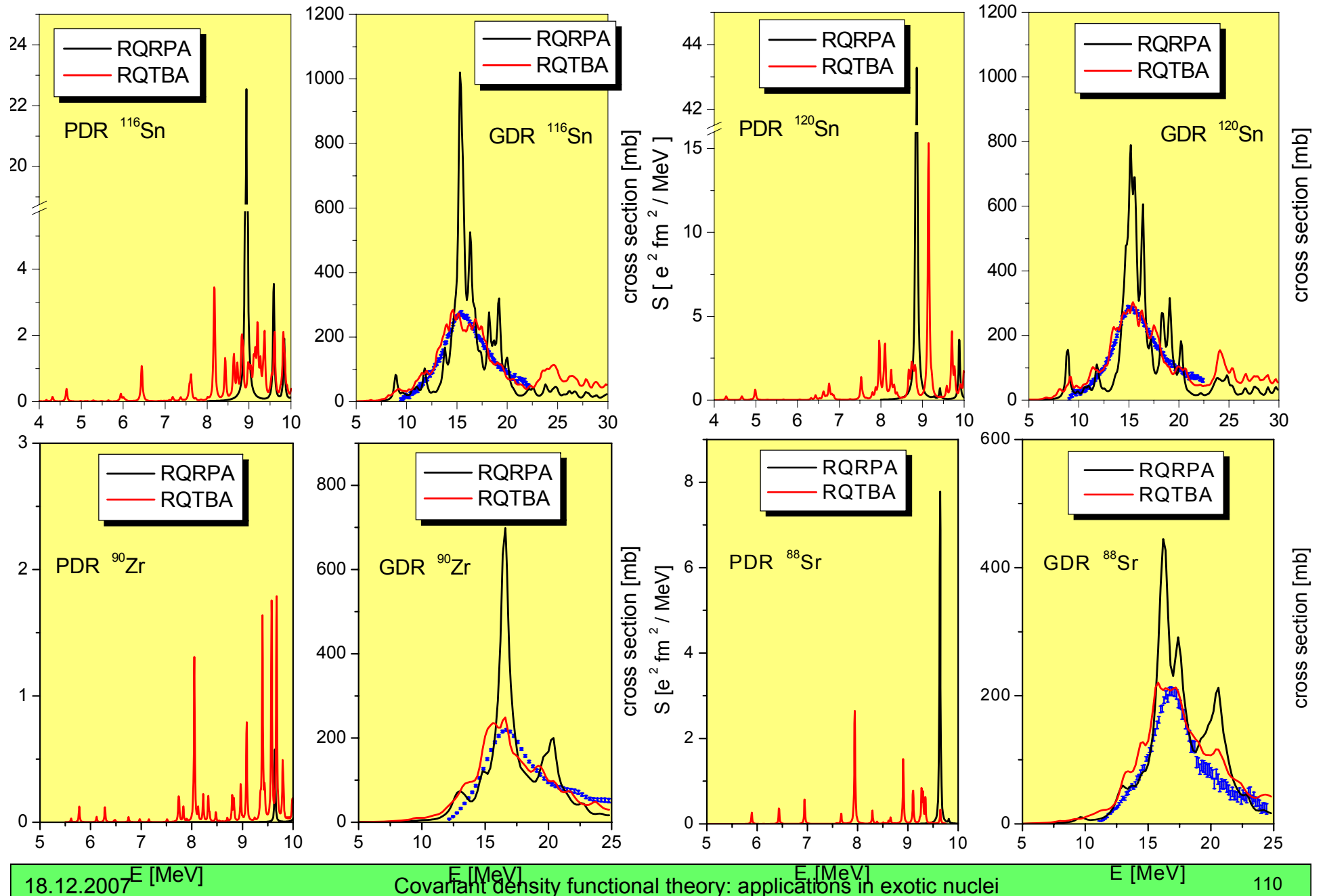
photoabsorption cross section

$$S(E) = -\frac{1}{\pi} \text{Im} \Pi(E + i \Delta)$$

**E1 photoabsorption
cross section**

$$\sigma_{\text{E1}}(E) = \frac{16\pi^3 e^2}{9\hbar c} E S_{\text{E1}}(E)$$

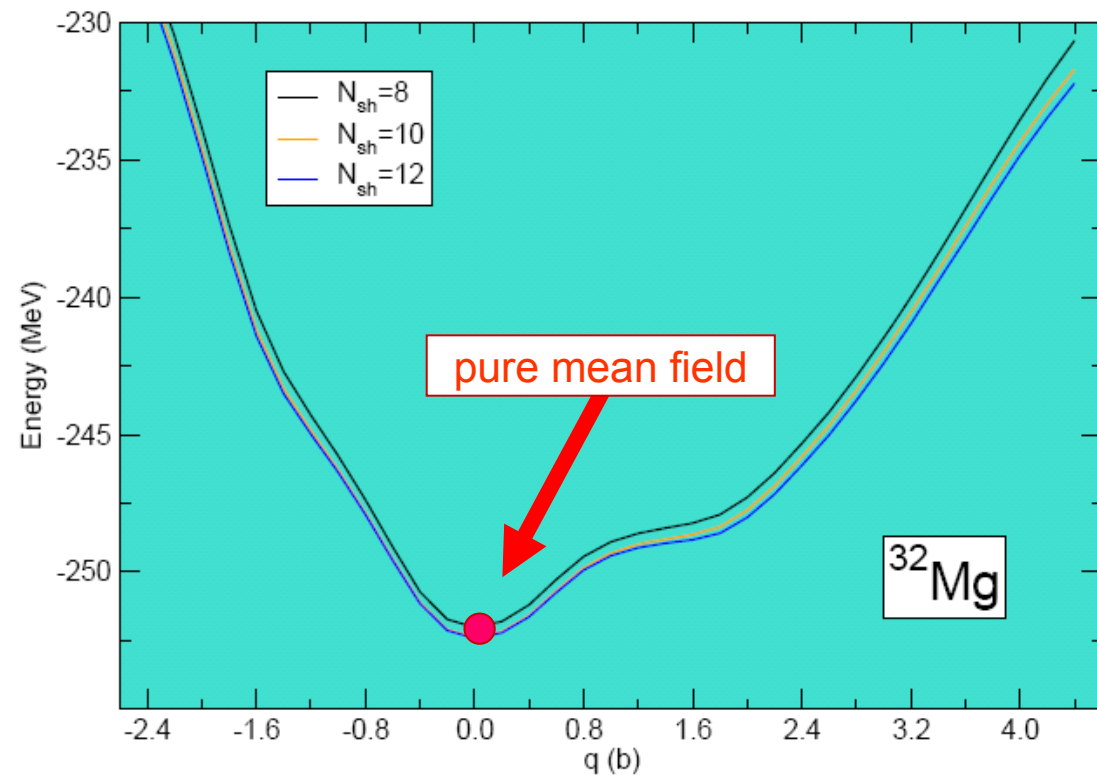
Electric dipole excitations in stable nuclei



Beyond Mean Field:

Energy surface in ^{32}Mg

$$\langle \delta\Phi | \hat{H} - q\hat{Q} | \Phi \rangle = 0$$



Generator Coordinate Method (GCM)

$$\langle \delta\Phi | \hat{H} - q\hat{Q} | \Phi \rangle = 0$$

Constraint Hartree Fock produces wave functions depending on a generator coordinate q

$$|q\rangle = |\Phi(q)\rangle$$

GCM wave function is a superposition of Slaterdeterminants

$$|\Psi\rangle = \int dq f(q) |q\rangle$$

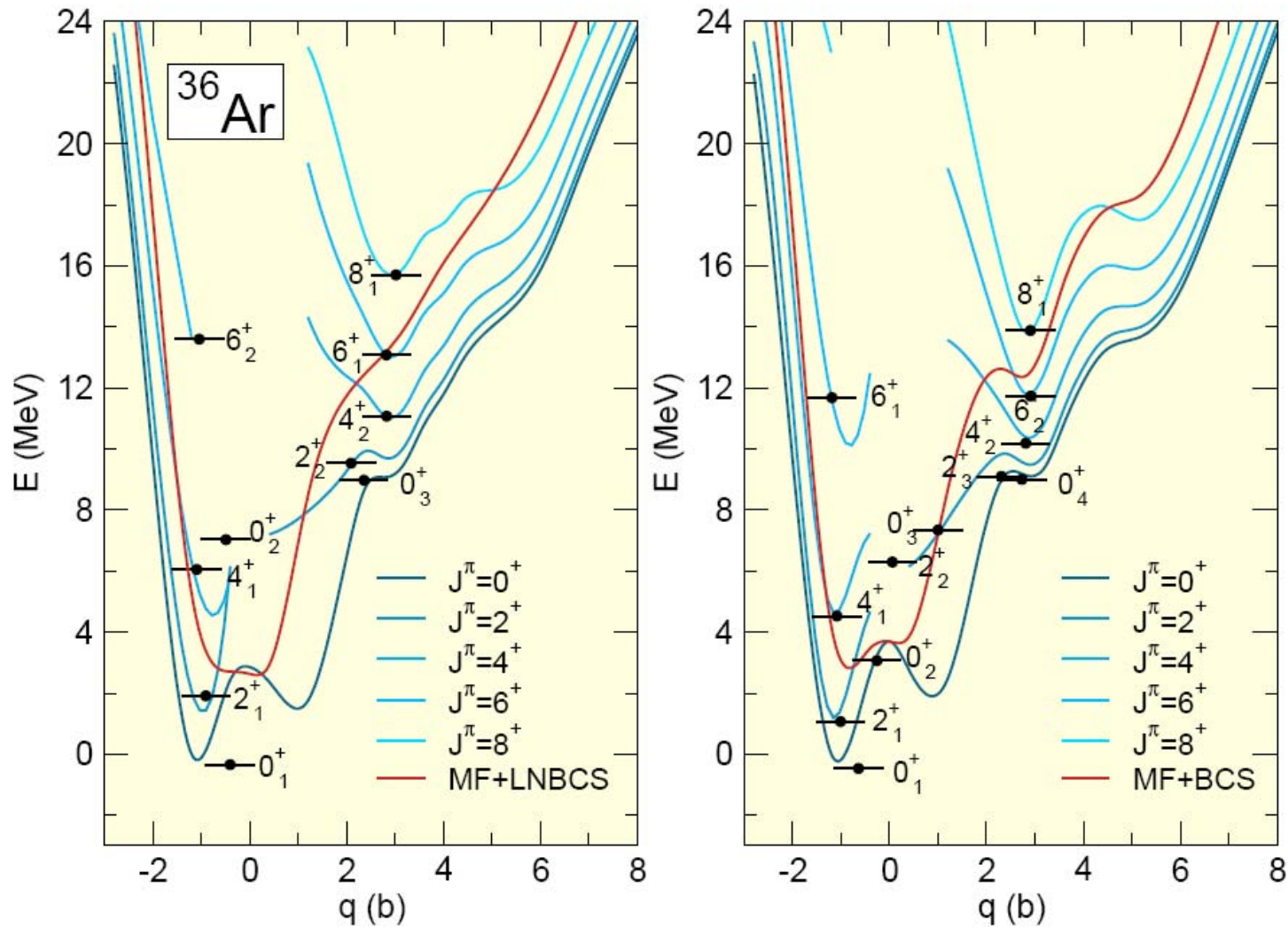
Hill-Wheeler equation:

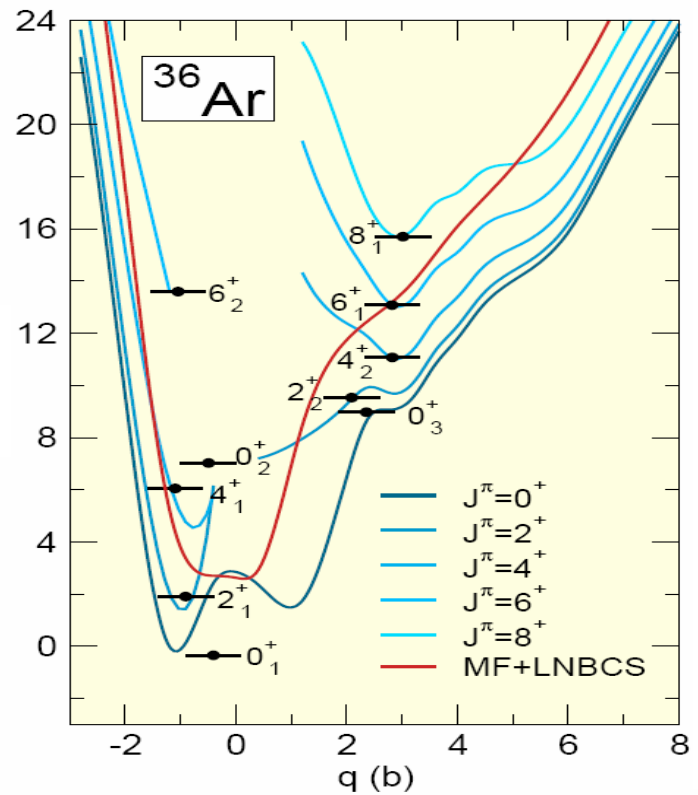
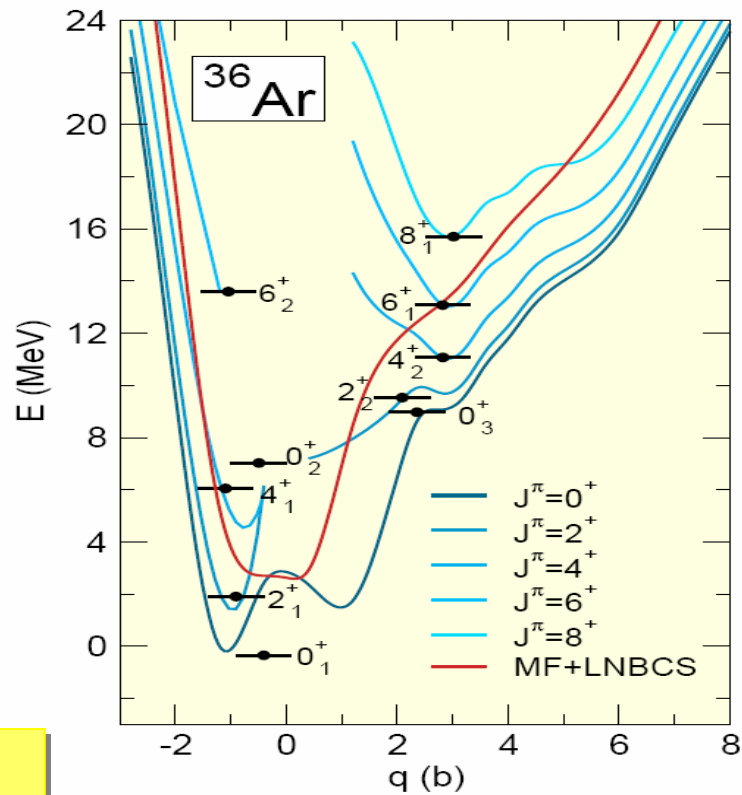
$$\int dq' [\langle q | H | q' \rangle - E \langle q | q' \rangle] f(q') = 0$$

with projection:

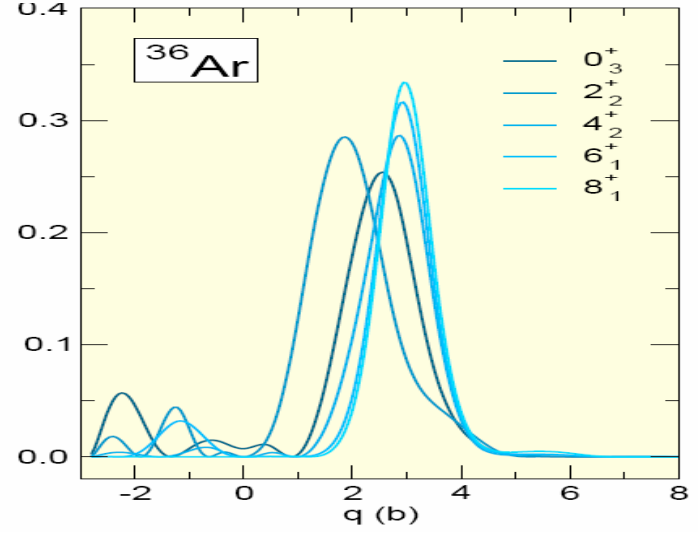
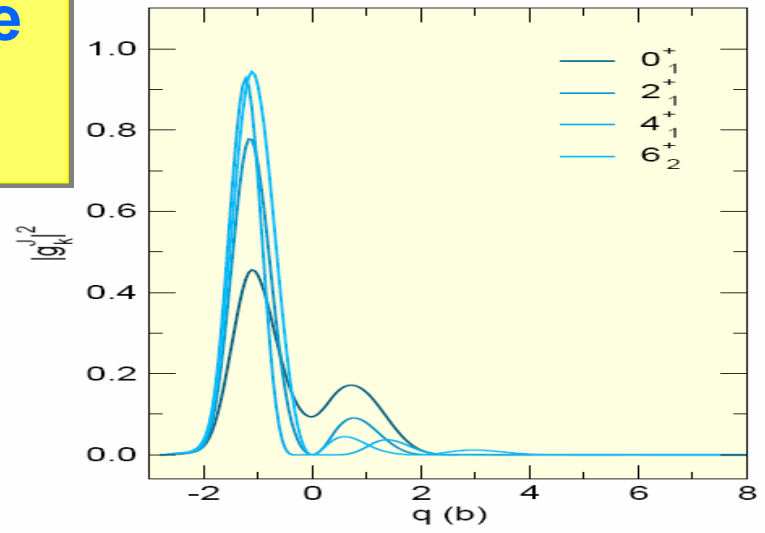
$$|\Psi\rangle = \int dq f(q) \hat{P}^N \hat{P}^I |q\rangle$$

^{36}Ar : GCM: N+J projection vs. J-projection

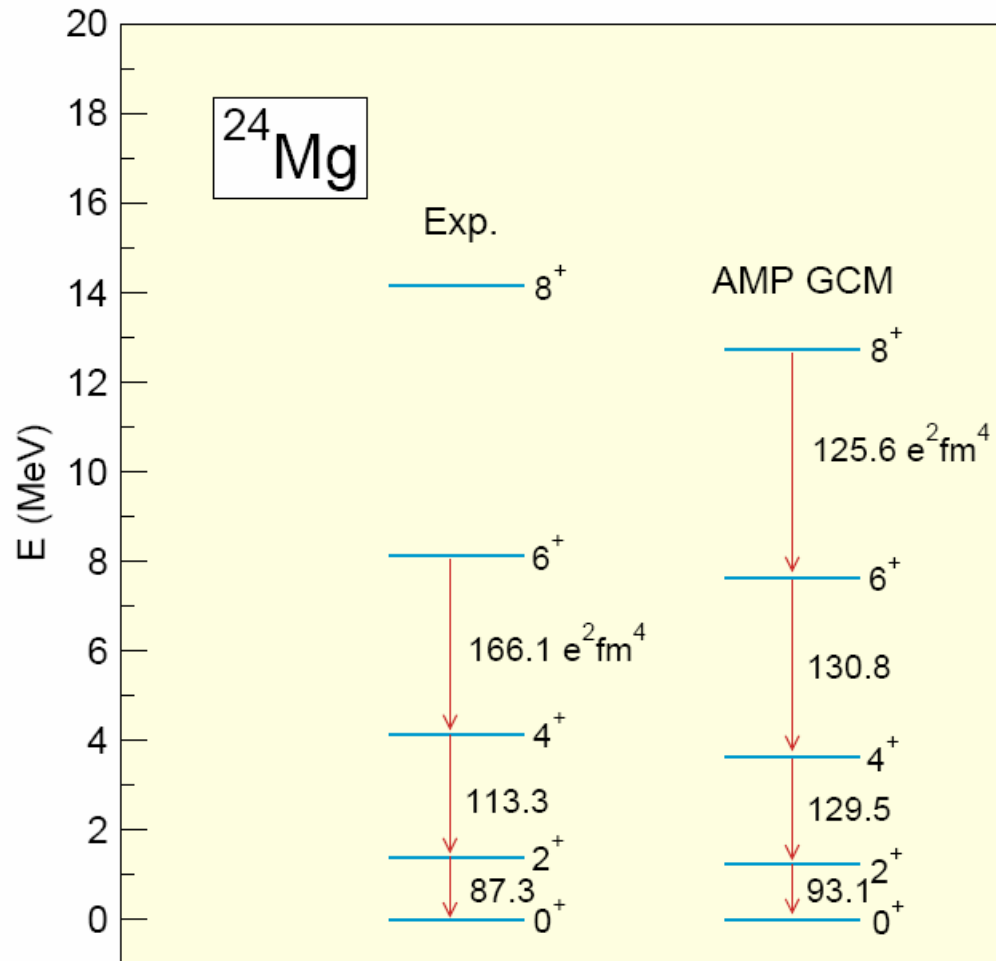




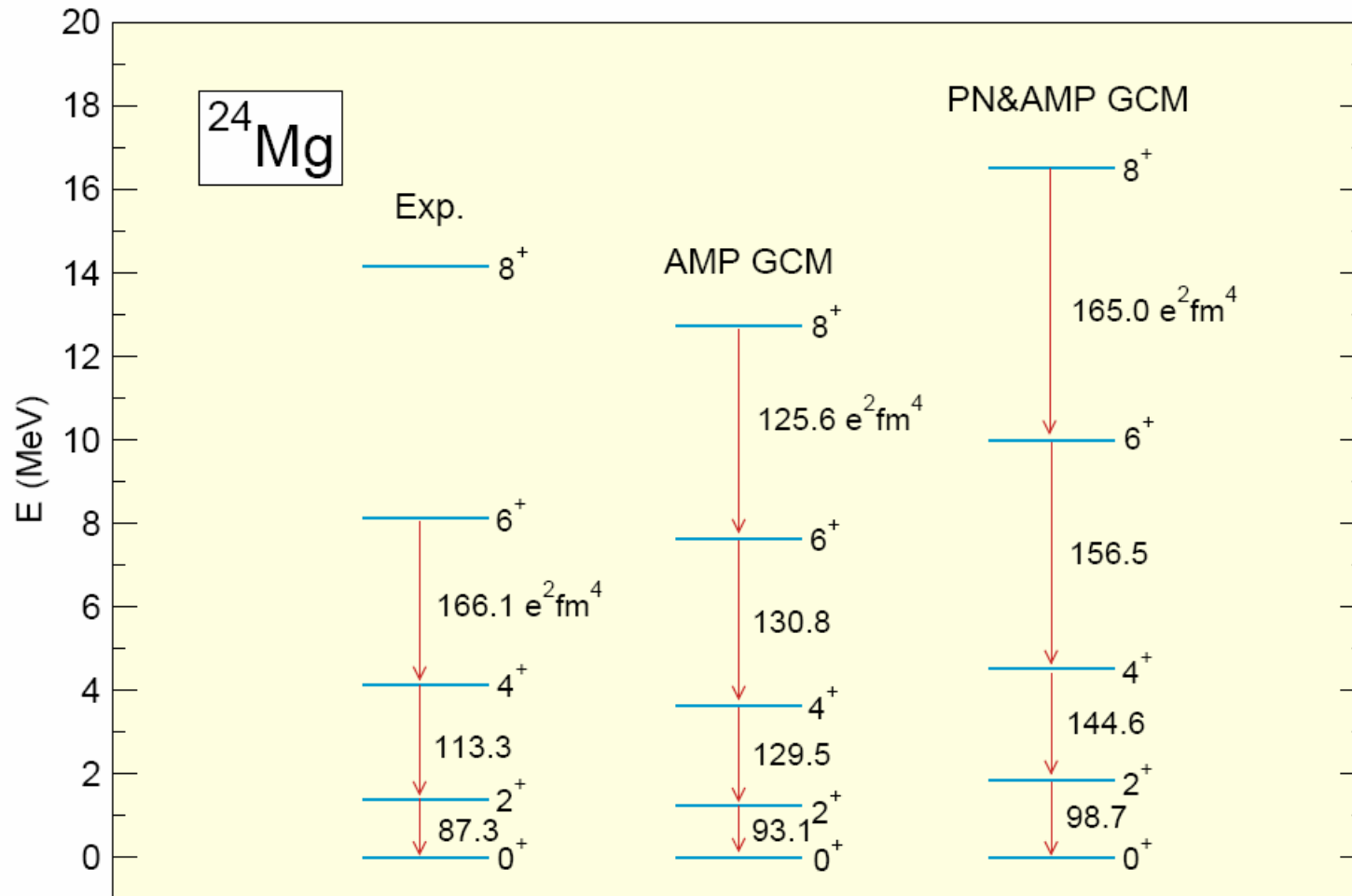
GCM-wave functions



Spectra in ^{24}Mg



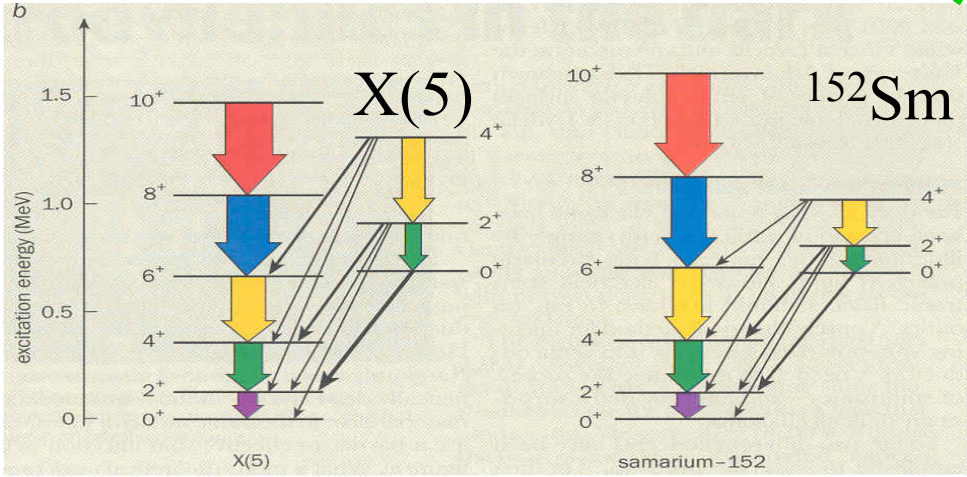
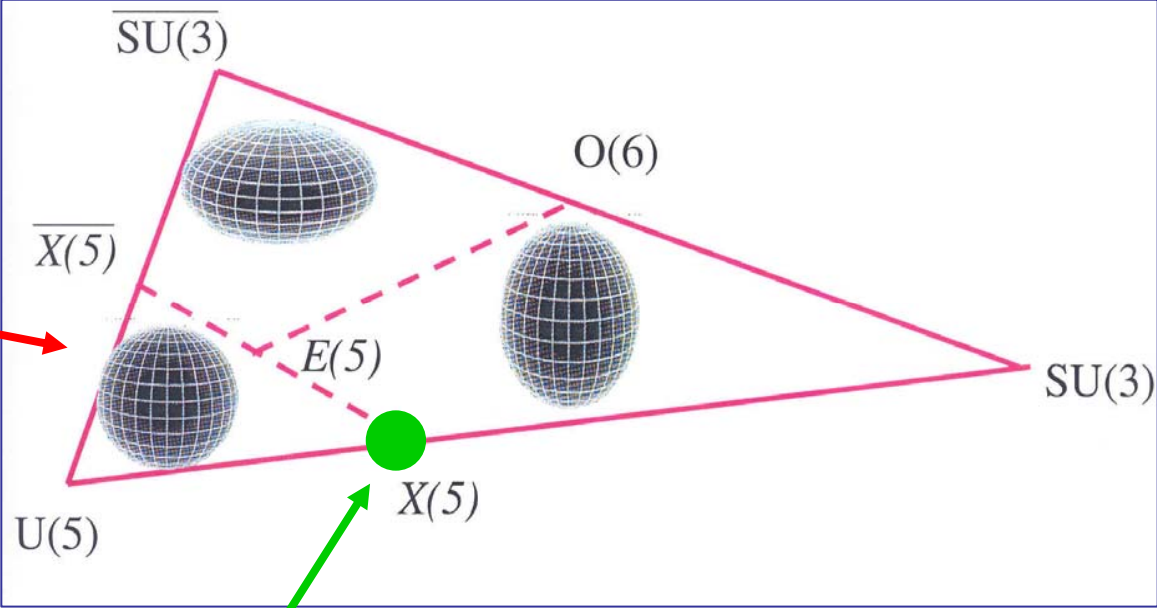
Spectra in ^{24}Mg



Quantum phase transitions and critical symmetries

Interacting Boson Model

Casten Triangle

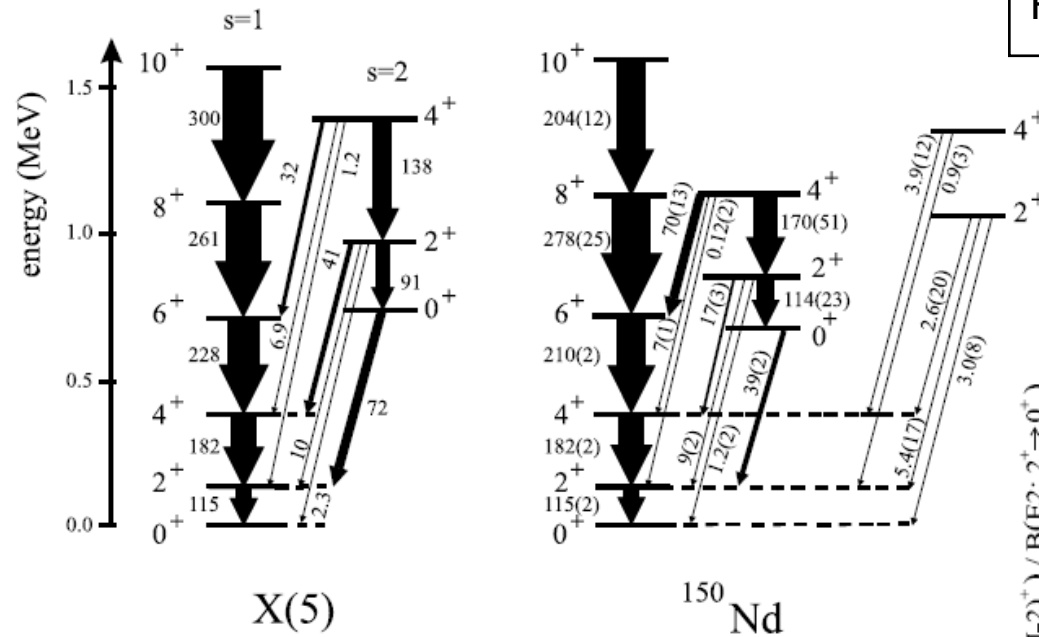


E(5): F. Iachello, PRL 85, 3580 (2000)
 X(5): F. Iachello, PRL 87, 52502 (2001)

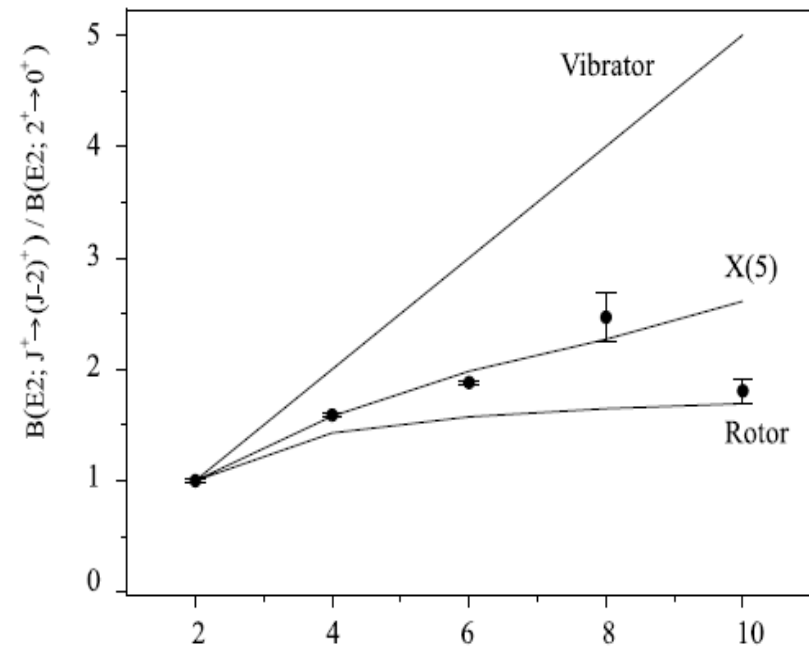
R.F. Casten, V. Zamfir, PRL 85 3584, (2000)

Transition U(5) \rightarrow SU(3) in Ne-isotopes

R. Krücken *et al*, PRL 88, 232501 (2002)



$$R = BE2(J \rightarrow J-2) / BE2(2 \rightarrow 0)$$



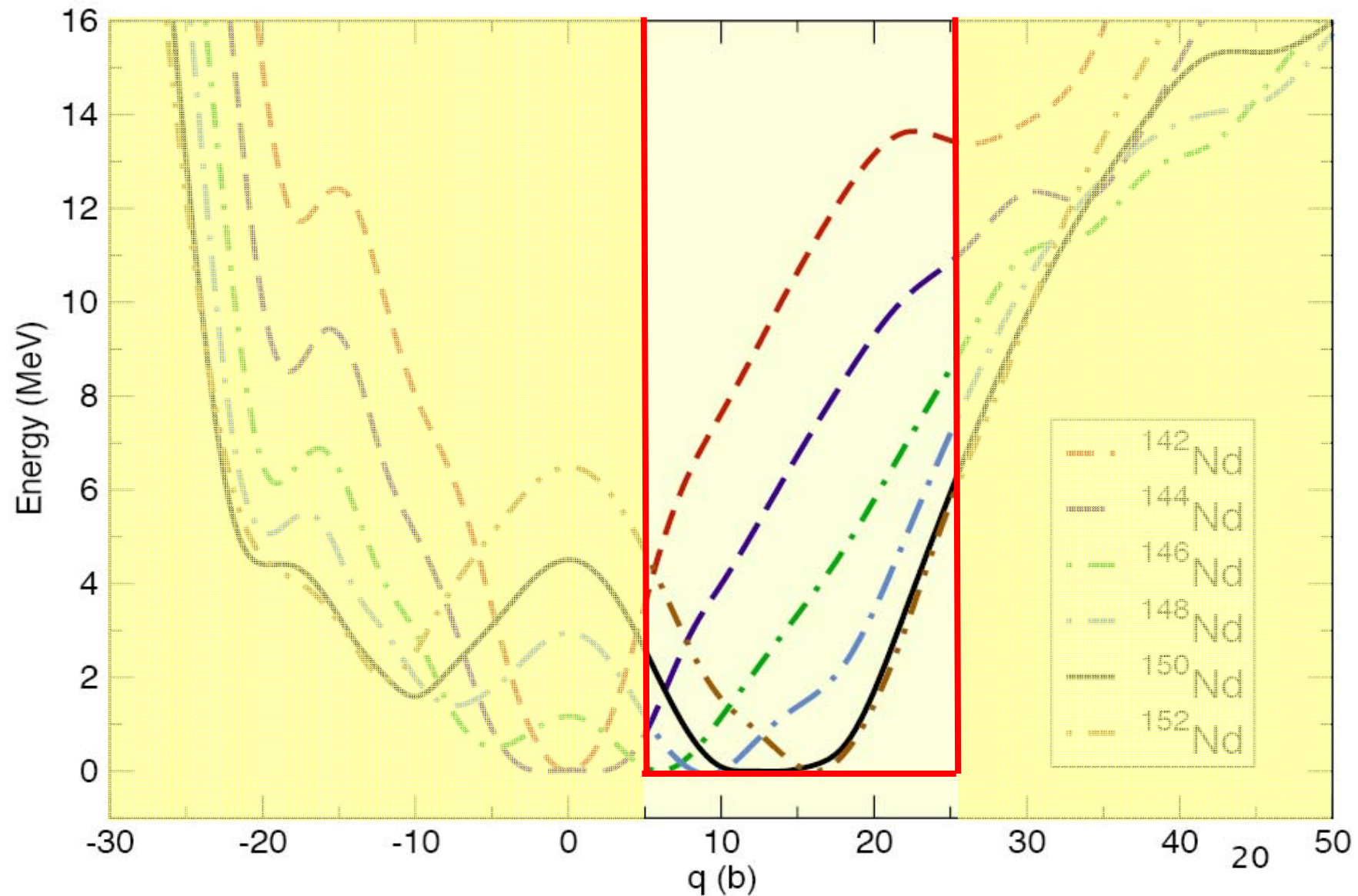
Microscopic description of nuclear quantum phase transitions

Can a **universal density functional**, with parameters adjusted to global ground-state properties (masses, radii), at the same time reproduce the singular behavior of excitation spectra at the **critical point of shape phase transition**?

Transitions between spherical (**U(5)**) and axially deformed (**SU(3)**) shapes in the chain of **Nd isotopes**.

Experimental evidence for a first-order shape phase transition in **¹⁵⁰Nd**: associated with the **X(5) critical symmetry**.

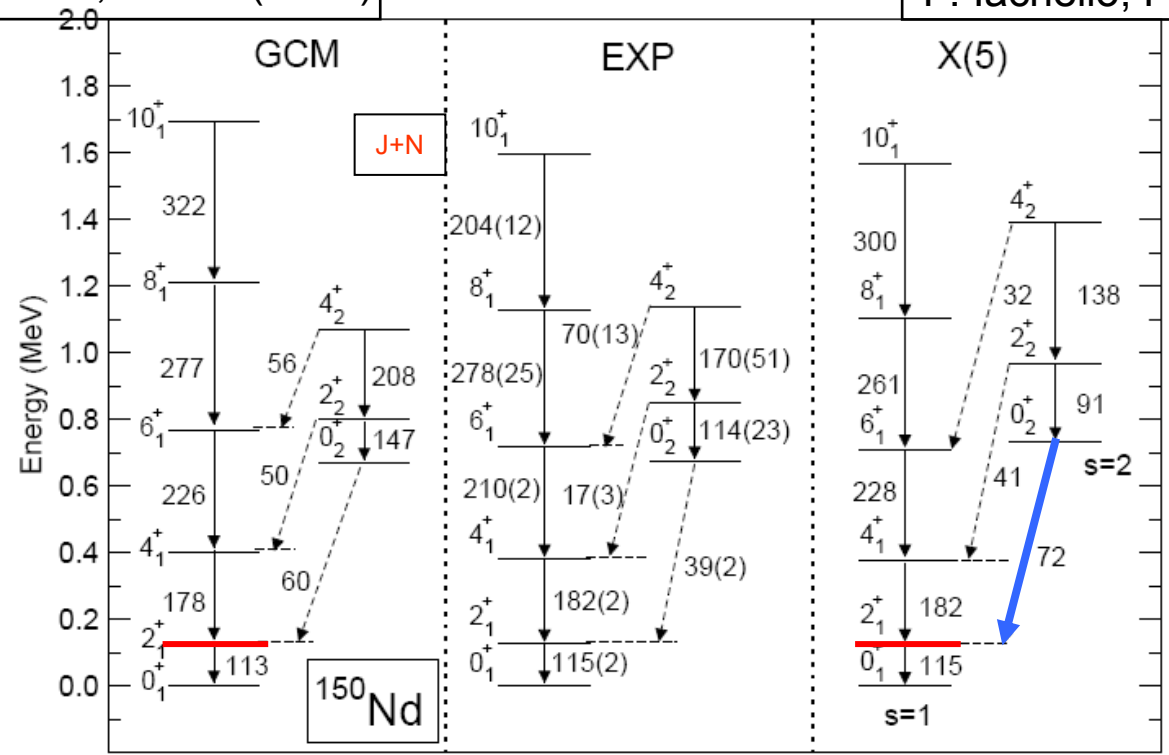
Self-consistent RMF plus Lipkin-Nogami BCS binding energy curves of $^{142-152}\text{Nd}$, as functions of the mass quadrupole moment.



R. Krücken *et al*, PRL 88, 232501 (2002)

Niksic *et al* PRL 99, 92502 (2007)

F. Iachello, PRL 87, 52502 (2001)

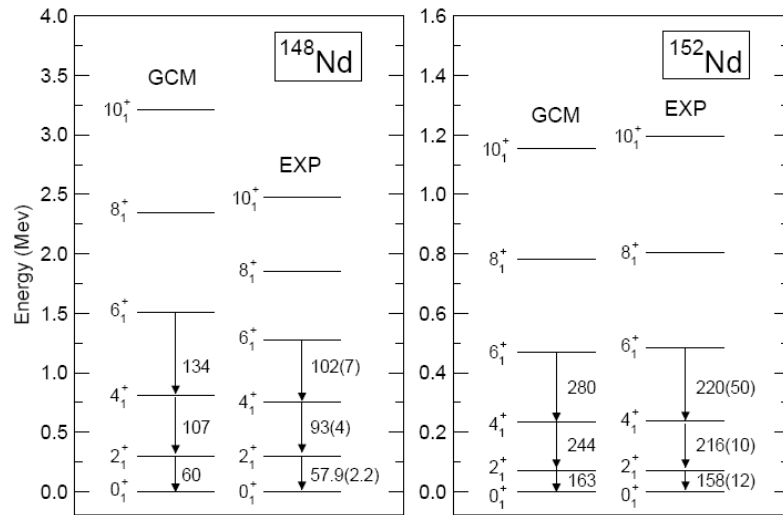
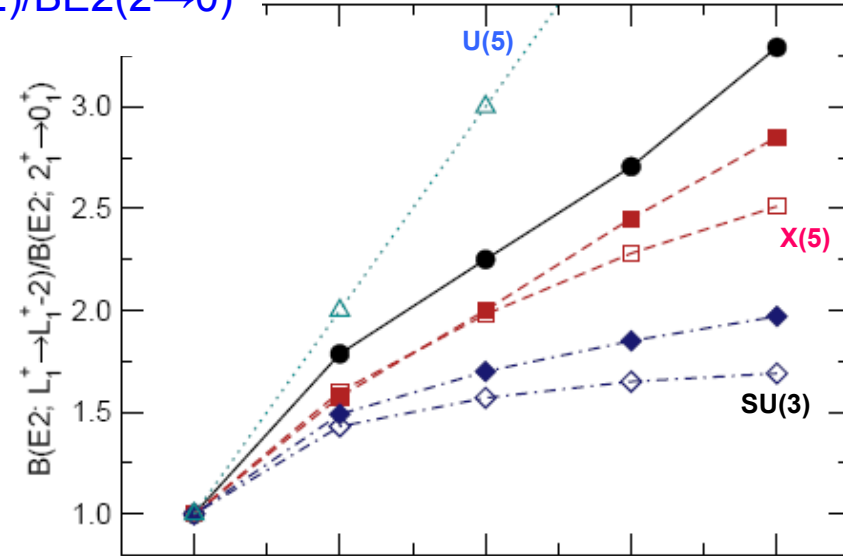


GCM: only one scale parameter: $E(2_1)$
 X(5): two scale parameters: $E(2_1)$, $BE2(0_2 \rightarrow 2_1)$

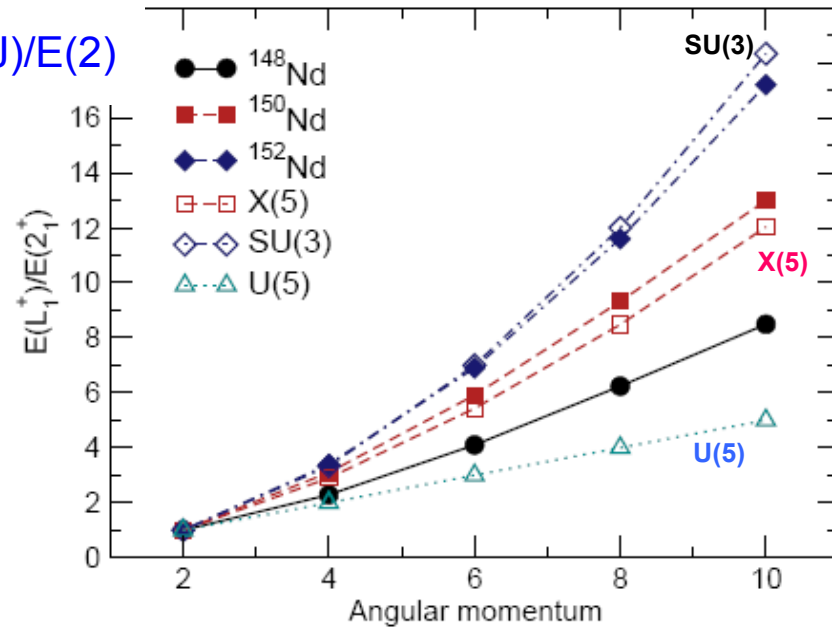
Problem in present GCM: restricted to $\gamma=0$

Neighboring nuclei:

$$BE2(J \rightarrow J-2)/BE2(2 \rightarrow 0)$$



$$E(J)/E(2)$$



Covariant Energy Density Functional Framework

- unified microscopic description of the structure of stable and nuclei far from stability, and reliable extrapolations toward the drip lines.
- when extended to take into account the most important correlations, it describes deformations and shape-coexistence phenomena associated with shell evolution.
- (Q)RPA analysis of low-energy multipole response in weakly-bound nuclei, dynamics of exotic modes of excitation, β -decay rates, and neutrino-nucleus reactions.

Colaborators:

A. Ansari (Bubaneswar)
G. A. Lalazissis (Thessaloniki)
D. Vretenar (Zagreb)

E. Litvinova (Obninsk)
T. Niksic (Zagreb)
N. Paar (Darmstadt)

D. Pena de Arteaga
E. Lopes (BMW)
A. Wandelt (Telekom)

References

Books on Nuclear Structure Theory

- A. Bohr and B. Mottelson, “*Nuclear Structure, Vol. I and II*”
- P. Ring and P. Schuck, “*The Nuclear Many-Body Problem*”
- J.-P. Blaizot and G. Ripka, “*Quantum Theory of Finite Systems*”
- V.G. Soloviev, “*Theory of Atomic Nuclei*”

Review Articles on Covariant Density Functional Theory

- B. D. Serot and J. D. Walecka, *Adv. Nucl. Phys.* **16**, 1 (1986)
- P.-G. Reinhard, *Rep. Prog. Phys.* **52**, 439 (1989)
- B. D. Serot, *Rep. Prog. Phys.* **55**, 1855 (1992)
- P. Ring, *Progr. Part. Nucl. Phys.* **37**, 193 (1996)
- B. D. Serot and J. D. Walecka, *Int. J. Mod. Phys.* **E6**, 515 (1997)
- Lecture Notes in Physics 641 (2004), “*Extended Density Functionals in Nuclear Structure*”
- D. Vretenar et al, *Phys. Rep.* **409** (2005) 101

Computer Programs

- H. Berghammer et al, Comp. Phys. Comm. 88, 293 (1995),
“*Computer Program for the Time-Evolution of Nuclear Systems in Relativistic Mean Field Theory.*”
- W. Pöschl et al, Comp. Phys. Comm. **99**, 128 (1996), “*Application of the Finite Element Method in self-consistent RMF calculations.*”
- W. Pöschl et al, Comp. Phys. Comm. **101**, 295 (1997), “*Application of the Finite Element Method in RMF theory: the spherical Nucleus.*”
- W. Pöschl et al, Comp. Phys. Comm. **103**, 217 (1997), “*Relativistic Hartree-Bogoliubov Theory in Coordinate Space: Finite Element Solution in a Nuclear System with Spherical Symmetry.*”
- P. Ring, Y.K. Gambhir and G.A. Lalazissis, **105**, 77 (1997),
“*Computer Program for the RMF Description of Ground State Properties of Even-Even Axially Deformed Nuclei .*”